NASA Contractor Report 172318

Nimbus-Earth Radiation Budget Instrument Analysis

R.M. Maschhoff

Gulton Industries, Data Systems Division

P.O. Box 3027

Albuquerque, NM 87190

Contract NAS1-16468

May 1984

National Aeronautics and
Space Administration

Langley Research Center
Hampton, Virginia 23665

TABLE OF CONTENTS

		Page
Summary/Overview		1
Sensor Characterizations		4
1.0	Introduction	4
2.0	FOV Characteristics	7
3.0	Long Wave Sensitivity of Short Wavelength Detectors	9
4.0	Short Wavelength Heating and Other Thermal Effects	12
5.0	Conclusions - Applying the Corrections	16
Appendix I	WFOV/NFOV Intercomparison Report; G.G. Campbell, T.H. Vonder Haar	I-1
Appendix II	Further Analysis of G.G. Campbell and T.H. Vonder Haar Report - The Stutter Temperature Connnection	II-1
Appendix III	NET Meeting Presentation, February 14, 1984	III-1

Summary/Overview

This final report to Contract NAS1-16468 presents our present understanding of the Earth Flux Sensors aboard the Nimbus ERB instrument. The summary of most of the findings of the study are shown in the main body of the report which closely parallels an article accepted for publication in the Journal of Geophysical Research (Special Nimbus Issue). This deals very effectively with several important instrument characteristics useful for a more accurate understanding of the orbital measurements. The most difficult to qualify effect, that of direct and reflected solar radiation impinging on the instrument housing (and other parts such as the shutter), has continued to receive study. The results of this most recent effort is summarized below and reported in detail in Appendices I, II, and III of this report. Appendix I is mainly the result of effort performed by Campbell/Vonder Haar incorporated under subcontract. Apendix III reflects the most recent thinking and has led directly to construction of a model which uses key instrument temperatures to predict offsets in the most troublesome earth flux channel. It is expected that very similar models can be constructed for the other channels. The other two appendices are included for historical purposes.

The modeling procedure is being carried out by RDS Lanham Md. under the direction of Dr. Lee Kyle of GSFC and this author and uses a multiple linear regression statistical analysis computer which maximizes the explained variance program. The program determines appropriate coefficients for the key temperatures and temperature differences to predict offsets of the wide field of view (WFOV) Channel 13 at night. The coefficients are optimized to minimize the difference between the actual observed offsets and the model. Any signal other than zero is erroneous for short wave sensors at night and is known not to be of an electronic origin

from a large body of test data. The model as of this date derived from all nightime data for one day per month over a full year is as follows:

$$I = 24.8 - 1.642xT - 1.12\Delta T + 0.197|\Delta T|$$

Where I = Irradiance W/M^2
T = Earth Flux Assy Temp in C°
T = Chan 13 Module Temp-Chan 12 FOV Stop Temp

It has been found that the Chan 12 FOV Stop temperature is an even better indicator than the Chan 12 shutter temperature which is mentioned in Appendix 3. The former is physically closest to Chan 13. The above model derived using day 2 of the ERB 3 day cycle explains greater than 90% of the variance with an rms error of 0.86 W/M^2. Some problems are encountered when this model is applied directly to day 1 of the cycle. Additional warm-up type terms will most likely be needed based on temperatures deep inside the instrument.

Using this model at the seasonal extremes yields an offset difference of about 6 W/M^2 for most of orbital day. This is in the sense that in southern hemisphere winter the flux is underestimated and in summer it is overestimated unless the offset correction is made. This greatly improves agreement between the WFOV Channel 13 data and independent data used for truth such as the Pacific Ocean CAT.

Although there is little reason to doubt that the model derived at night is not applicable in the daytime, a special test is being planned to increase confidence in the model (NASA GSFC Contract #NAS528146). This test is planned as a partial orbit simulation using a solar simulator impinging on a spare Earth Flux Assembly.

The Assembly is to be rotated at an orbital rate so the solar insolation and earth short wave scene signatures can be duplicated. An essential aspect of the test is the ability to shutter the simulator at any time to establish offset. It is expected that since the sensors are basically thermal devices, offsets should be related to temperatures and temperature gradients regardless of what drives them. The test differs from any discussed in this report in that the assembly is in near flight configuration with all shutters in place. The tests reported here were all done on individual sensors. J. Hickey of Eppley Laboratory is responsible for performing the tests on the entire assembly.

SENSOR CHARACTERIZATIONS

ABSTRACT

Detailed characterizations of flight spare earth flux sensors from the Nimbus Earth Radiation Budget (ERB) program have been performed which, when coupled with a more careful accounting of the orbital instrument environment, provide the potential for improved accuracy in the final data products. The characterizations included detailed FOV mappings, responses to transient long and short wavelength radiation, and response to sensor temperature changes. These sensor and environment characterizations, along with the outstanding low noise and stability properties of the ERB instrument signal processing system, promise improvement of the data accuracy to levels sufficient for long term budget and climatological purposes. The combined data sets from Nimbus 6 and 7 are expected to span a period in excess of 10 years. The improvements in data accuracy are particularly significant over zonal latitude bands because the corrections are strongly latitude-dependent.

1.0 INTRODUCTION

Characterization studies of residual wide field of view (WFOV) earth flux sensors built for the ERB Nimbus program have recently been performed. As a result of these studies and a critical re-examination of raw flight data, a much more complete understanding of Nimbus ERB earth flux data has been developed. Prior to these studies no satisfactory mechanisms were available to explain anomalous transients around satellite sunrise and sunset times nor could the non-zero outputy of the shortwave channels during satellite

night be totally explained. The purpose of this paper is to report the necessary correction approaches, and how they relate to the physical situation, and how they were derived.

The ERB instrument is described by Jacobowitz (1983) in the Journal of Geophysical Research Special Nimbus, special issue. Two nearly identical ERB radiometers were placed in orbit, one on Nimbus 6 and one on Nimbus 7. This paper deals only with the four WFOV earth flux sensors designated Channels 11 through 14 (See Figure 1). These sensors all employ identical flatplate thermopile detectors baffeled to limit their unencumbered field of view to 121 degrees. Channels 11 and 12 are called total or long wavelength channels since they have no limiting spectral filters. Channels 11 and 12 are identical channels on Nimbus 6, with channel 11 used as a reference and kept shuttered for protection. On Nimbus 7, channel 11's baffels are painted black to reduce internal reflections and spurious reponse wings. Channels 13 and 14 use the same type of thermopile detectors but they employ filters to limit the sensor spectral response. Channel 13 has two quartz dome filters and Channel 14 has an added RG 695 red glass dome filter. These are referred to as the short wavelength channels.

The Nimbus ERB Science Team and Project Scientists spent considerable effort in interpreting and validating the WFOV Earth Flux data. While most aspects of the data and sensors submitted to reasonable explanations there remained some questions and apparent contradictions at the time this work was performed. The most significant are summarized on the following pages:

1. It was concluded on the basis of nightime intercomparisons between the integrated long wavelength scanner data and Channel 12 data that an offset existed in the Channel 12 data caused by radiative losses to deep space. The magnitude was such that it could not be explained by the small ring of deep space falling within the prescribed FOV. Tests performed at Eppley showed that there were leaks beyond that prescribed by the FOB limiter geometry. This led to the painting of the baffles of Channel 11 of the Nimbus 7 ERB which, when in orbit produced data which showed that the leak was largely eliminated. Channel 12, which is the working sensor on both Nimbus 6 and 7, was left unpainted on Nimbus 7 so that Nimbus 6 data could be compared directly. The details of the FOV for the unpainted sensor were still required for best understanding of the data.

2. The behavior of the signals from the short wavelength channels, in particular Channel 13, after sunset was not consistent with known facts. Simple geometry showed that the sun entered the FOV for brief periods at satellite sunrise and sunset causing the so called "sun blips." However, recovery from this disturbance appeared to take too long to be explained by the filter domes cooling off. In addition, the component of the solar irradiance known to be absorbed by the quartz could not account for the necessary dome temperature increase to cause the $10W/M^2$ offset observed. Tests performed at Eppley Laboratories showed that there was no evidence of bulk absorption by the domes of short wavelength solar flux. A quantitative response of the sensor module to dynamic scenes was also lacking.

3. The large negative bias (-20 to -30W/M^2) of channel 13 at night required inner dome temperatures to be 5 degrees C or more below that of the thermopile sensor receiver. No such gradients or offsets were ever produced during pre-launch thermal vacuum testing. From electrical calibrations performed on the sensor amplifier the source of the offset was known not to be electronic. The possibility of temperature gradients as a cause was considered but the basic resolution of the measurement system of 0.1 degree C seemed inadequate to be of any help. An explanation of the mechanism was clearly needed.

Based on the questions raised in attempting to explain the above problems, a series of tests were performed using sensors identical to the sensors in ERB. The objectives were to determine the mechanisms responsible for their unexpected behavior and to eliminate conflicting theories. The tests were, in general, performed in vacuum. They included measurements of the field of view, response to long (greater than 2.7 micrometers) and short (less than 2.7 micrometers) wavelength radiation. After the tests were completed, orbital data averaged over selected time intervals became available. This provided the data base necessary to verify that the laboratory tests adequately described the sensor behavior in space and to corroborate the test results.

2.0 FOV CHARACTERISTICS

All the WFOV sensors were designed with a field of view such that the earth, as seen from the Nimbus orbit, would

just underfill it. A small ring of deep space is therefore included in the sensor FOV. This adds a negative offset to the output of Channels 11 and 12. At spacecraft sunrise and sunset, when the sun is in that narrow ring, it causes large outputs (which have been named "sun blips") from WFOV sensors. If the sensors had ideal FOVs these two effects might be the only sources of error. Unfortunately, like most instruments, these depart from ideal. The ideal FOV is a cosine response over the unencumbered field and no response outside the field. The laboratory measurements of FOV indicate that the only channel approaching ideal is the Nimbus 7 Channel 11 with its black painted baffles. Fig. 2 shows the results of the lab FOV tests plotted as deviation from ideal and normalized to the on axis response. In the unencumbered field the response of all channels except Channel 11 is 2% to 4% below cosine. At 70 degrees, out of the FOV, all other channels show a response of about 3% which decreases to zero at 90 degrees. One other anomaly is also apparent. Channel 12 has an enhanced response which reaches a maximum of about 6% greater than cosine at 55 degrees. This enhancement, plus response beyond 70 degrees is due to reflections from the baffles. This increased view of space over that expected largely explains the negative bias on Channel 12.

The total wavelength channels require two corrections to remove the errors introduced by the FOV problems. The most important one is to remove the solar contribution to signal when the sun is in the region between 60 degrees and 90 degrees from the normal to the detector. Removal of the "sun blips" themselves, while possible in principle is probably of little value because the signal is near zero anyway. The offset introduced by the ring of deep space is

a constant correction whose magnitude can be established by comparison with the painted channel 11 on Nimbus 7. This, of course, also corrects for the departure from ideal response. Such an inflight correction technique is not possible with the short wavelength channels since they have no comparable reference channel. Fortunately the out of field responses described above have no effect on the data from the short wavelength channels except near spacecraft sunrise and sunset when the sun can contaminate the sensor output. Thus two corrections need to be made to the short wavelength channel data. The first is the removal of the solar contamination, both the out-of-field response and the in-field or "sun blips." The second is the correction of the measured earth flux required by the departure from the ideal cosine response. The negative offset of the short wavelength chaannels is discussed in sections 3.0 and 4.0.

3.0 LONG WAVELENGTH SENSITIVITY OF SHORT WAVELENGTH DETECTORS

The ERB short wavelength sensors, Channels 13 and 14, were intended to be insensitive to long wavelength radiation. Fig. 3 shows a drawing of the Channel 13 module. The two quartz domes were intended to filter out all long wavelength radiation with the inner dome shielding the thermopile from heating of the outer dome caused by long wave absorption.

3.1 Short Wavelength Data Anomalies

Raw orbital data showed several anomalies which appeared to be related to long wavelength radiative interchange. The first was a nightime dc offset. The second was a fluctuation in this offset during nightime which appeared to be

coupled to the long wavelenght radiation from the earth. The third was an exponential decay in the offset level from the beginning of night to a more or less constant level equivalent to a change of flux of 10 W/M^2.

3.2 Laboratory Tests Of Long Wavelength Sensitivity

The sensitivity of the short wavelength channels to long wavelength radiation was obtained in the laboratory tests using an impulse forcing function and observing the response. Once the impulse response is known the response to an arbitrary forcing function can be determined. In this test a heated shutter was rapidly placed in front of the module for short periods of time. The shape of the response for a single dome was found to fit a simple exponential quite well. The double and triple domes of Channels 13 and 14 were then shown to be convolutions of their respective single dome responsee. The outer dome absorbs the long wavelength radiation and heats up. It then reradiates to the inner dome, heating it up. Figure 4 shows the measured thermal impulse response of Channel 13 and a calculated response which is simply the convolution of two exponentials with amplitude normalized to the measured response. A similar results was obtained for the three domes of Channel 14. The nightime dc offset was partly caused by the radiative interchange between the domes and deep space which cooled the domes below the temperature of the thermopile. An additional cause of the dc offset is discussed in section 4.0.

3.3 Corroboration Of Long Wavelength Sensitivity From Orbital Data

With the long wavelength impulse response known, orbital data was re-examined to verify that the flight sensor was not significantly different from the sensor module tested in the laboratory. It was also hoped that a simple correction algorithm could be verified to ease data reduction computational burdens. For this verification, the variation in Channel 13 output due to long wavelength radiation from the earth had to be isolated from all other factors which effect Channel 13, such as spacecraft temperature excursions and exposure to sunlight. Since the spacecraft environment is reasonably stable with time and the long wavelength earth radiation varies with the season, the difference between data taken several months apart emphasises the long wavelength contribution and supresses others.

In selecting a data set to minimize changes in spacecraft environment, days were chosen in which the spacecraft temperature was nearly equal. The day chosen also had to have full earth coverage for the entire day since the data had to be averaged for a full day to remove local variations in the earth long wavelength signature. The data chosen for reduction was from 18, June and 29, September 1979. Figure 5 shows the results of this verification in which all data are the difference between the June daily average and the September daily average. The upper curve shows the Channel 13 output for the nightime portion of the actual difference over the two days. The forcing function curve is the long wavelength scene for those two days. The simulated response is the convolution of the laboratory

determined impulse response with the forcing function. The shapes of the actual and simulated responses agree very well.

3.4 Data Correction Algorithm For Long Wavelength Sensitivity

These results suggest a simple correction to Channel 13 data. Figure 6 shows the result of multiplying the long wavelength scene variations by 4%. A shift equivalent to 20 degrees in earth latitude makes the curves almost coincide. Thus a simple correction to Channel 13 and Channel 14 consists of scaling the long wavelength data, delaying it in time and subtracting it from the short wavelength channel. Kyle (1983) has subsequently shown that this procedure produces good results over a wide range of scenes and conditions. A set of regressions over 8 three-day data sets yielded a delay of 336 seconds and an amplitude coefficient of 0.04 for maximum correlation of the long wavelength scene to anomalous Channel 13 responses at night.

4.0 SHORT WAVELENGTH HEATING AND OTHER THERMAL EFFECTS

Sensitivity to long wavelength radiation alone is not adequate to explain the amplitude of exponential decay observed in the data from Channels 13 and 14 immediately after satellite sunset. The presence of a delayed response to short wavelength irradiance was observed during laboratory testing. A typical result shown in Figure 7 shows a response immediately after removal of short wavelength irradiance which decays to zero in about 8 to 10 minutes. The laboratory tests do not directly reveal the physical cause of the response, however the changes in the thermo-

pile base temperature suggested that the cause was related to the change in temperature of the base structure.

4.1 Orbital Temperature Data

A detailed investigation of sensor temperatures versus time was undertaken. The temperature monitoring points available relative to WFOV sensor performance included thermistors in the thermopile body of each channel and in the module floors of Channels 13 and 14. The module floors of Channels 11 and 12 contain platinum resistance thermometers. In addition there are two thermistors on the berylium block which forms the mount and heatsink for all channels. As shown in Figure 8 one of these is on the earth or scene side, the other is on the inside or instrument side. The absolute accuracy of thermistor temperature sensors is only about 1 degree but their repeatability appears to be good to the millidegree level. The measurement resolution of the bulk of the ERB temperature monitoring system is about 0.1 degree C. It was therefore necessary to average data from sucessive orbits to reveal differences at the millidegree level. The temperature data was averaged over all orbits for 10 nearly consecutive days. The results are given in figure 9. Over this average orbit, the peak to peak variation is less than 2 degrees for all sensing points. However, the difference between the thermopile and module go from near zero to 0.1 degrees depending on orbit position.

Heating Results

Cleary, the gross orbital variations of temperature are caused by the day-night differences in short wavelength radiation environment. One of the main results of the detailed temperature studies was to show that contrary to early suppositions, the earth flux assembly and sensors are driven significantly by the short wavelength radiation impinging on the earth side of the instrument. Proof of this comes from two pieces of information from the curves in Figure 9. First, the orbital peak to peak variation on the "instrument" side of the earth flux block assembly is less than the "scene" side by about 0.2 degrees. Second, the detailed signatures around satellite sunrise show that the "scene" side sensors, which include the modules themselves, reverse trend earlier than the "instrument" side assembly temperatures. What is claimed here is that, although the short wavelength flux obviously affects the instrument as a whole, the effect on the earth flux assembly dominates.

The source of this heating relates to the delayed short wavelength response mentioned earlier and shown in Figure 7. This test was performed with collimated light which showed that this type of response occurred well beyond 60 degrees off normal. At angles beyond 60 degrees light does not strike the detector patch directly, therefore the structure of the modules including the FOV baffles must be the absorbers. Mylar spacers used to cushion the filter domes under the dome hold-down rings were eliminated as the potential absorbers. When removed, the results of Figure 7 were duplicated.

All other surfaces of the sensor other than the domes that are illuminated are polished aluminum including the baffles. The exact absorptivity of this polished aluminum is not known but is estimated to be in the range of 2% to 5%, therefore significant heating of the module must be expected, especially the exposed front (earth) side of when hit by direct sunlight. This type of surface extends beyond the FOV aperture producing a heating effect correspondingly greater. Superimposed on the gross orbital temperature variations is fine detail of significant amplitude caused by periods of direct sunlight hitting the sensors around sunrise and sunset.

The result of these detailed temperature and temperature gradient disturbances is a temporary decrease in the large negative offset for a large portion of the first half of satellite night. A good argument can then be made that the amplitude of the disturbance at sunrise should be similar to that at sunset and of similar duration. From the channel 13 output following sunset this is seen to be a quasi-exponential decaying disturbance of 10 W/M^2 peak and a 10 minute 1/e time. Figure 10 depicts daily average long and short wavelength records for day 334, 1978 and shows the applicable regions. Support for the contention that sunrise and sunset effects are equal is derived from observing the minima in the short wavelength responses. The one associated with sunrise is about 10 W/M^2 higher than the sunset one. Maximum solar heating preceeds the one at sunrise and follows the minimums at sunset.

4.3 ERB On-Off Duty Cycle Temperature Variations

An additional significant effect relating to module temperatures and offsets is the primary ERB duty cycle of three days on and one day off. This has the effect of varying the flow, of heat through the earth flux assembly and modules to space (and to a lesser extent the earth since it is at about the temperature of the instrument). Heat flow is always out of the modules as demonstrated by the fact that they are the coldest part of the instrument. The amount of flow varies with the amount of heat internally generated by the electronics and also with the amount of radiant heat absorbed by the module. These varying inputs cause a large variation in the output offsets of Channels 13 and 14. The offset is negative when the instrument is off and becomes more negative when the instrument warms. Examination of offsets at night, after long wavelength scene corrections have been made, reveal offsets ranging from -20 W/M^2 to -35W/M^2 over the time period from the first orbit after turn-on till the end of the second day. Figure 11 shows a typical three-day temperature signal for Channel 13 beginning at 15.5 degrees C, coming to a peak at the end of the second day at 22.5 degrees C; note that on the third day the ERB scanner is typically turned off. The short wavelength heating disturbances can be seen to follow this temperature curve. These instrument effects are in concert with an early recommendation by the author which has been made part of the data processing routine. The correction consists of forcing the offset in the channel output data to zero at satellite midnight, which along with a linear interpolation between these points drives the duty cycle effects to a very small level. This constitutes a significant improvement over the initial data correction approach which used a constant offset correction of 22 W/M^2.

5.0 CONCLUSION - APPLYING THE CORRECTIONS

The test results and the data corrections produced by this instrument characterization effort have been input to the orbital data reduction team as the results became available. This is reflected in the paper by Kyle et. al. (1983) which describes in detail the data processing algorithms that have or will be applied to specific raw data sets.

It should be noted that the errors in the raw data are orbital position and therefore latitude dependent. Without correction this could lead to especially serious errors regarding global circulation studies. The effort reported in this report has provided a substantial improvement of understanding and implementing corrections to the raw orbital data. Figure 12 summarizes the various corrections that need to be made and over which latitudes they are most important. The figure shows a daily average of the short and long wavelength WFOV data for day 176, 1979 (which is typical) as produced by the early Nimbus 7 algorithms. It can be noted that the high latitude regions require the most correction since these regions suffer the most contamination.

This record is taken from the initial processing of the first 19 months of ERB Nimbus 7 data. The offset correction applied to the short wavelength raw data, namely a constant -22 W/M2, does not result in a zero nightime offset. The deviation from zero is caused by a combination of long wavelength heating effects and instrument warmup or duty cycle effects. When these corrections are applied, the offsets from satellite midnight to sunrise come very

close to zero. The non-zero output during the first half of the night record is due to the sunset short wavelength heating transient. The data is of no value during this period (except for understanding the instrument) so does not need to be corrected. Additional corrections for the FOV effects need to be applied at high latitudes especially when the output is a zonal product. The short wavelength signal itself becomes smaller as the dark earth fills more and more of the FOV. The quantity which must be removed from the data is the product of solar irradiance and the angle response functions as shown in Figure 2 and the basic sensitivity. In addition, another factor discussed in detail by Kyle et. al., that of dome contamination, also becomes more of a factor at these latitudes. Nevertheless, seasonal and longitudinal variations can be more effectively studied when the FOV effects are either removed directly or are in effect removed by assuming them constant from orbit to orbit except for Earth-Sun distance corrections.

6.0 REFERENCES

Kyle, H. E., F. B. House, P. E. Ardanuy and H. Jacobowitz. "New Inflight Calibration Adjustment of Nimbus 6 and 7 Earth Radiation Budget Wide Field of View Radiometers, The Journal of Geophysical Research, Vol., No., Date, pp. or 1984 (to be published).

Jacobowitz, H., H. V. Soule, F. B. House, H. L. Kyle, and the Nimbus-7 ERB Experiment Team, "The Earth Radiation Budget (ERB) Experiment, An Overview, The Journal of Geophysical Research, Vol., No., Date, pp., or 1984 (to be published).

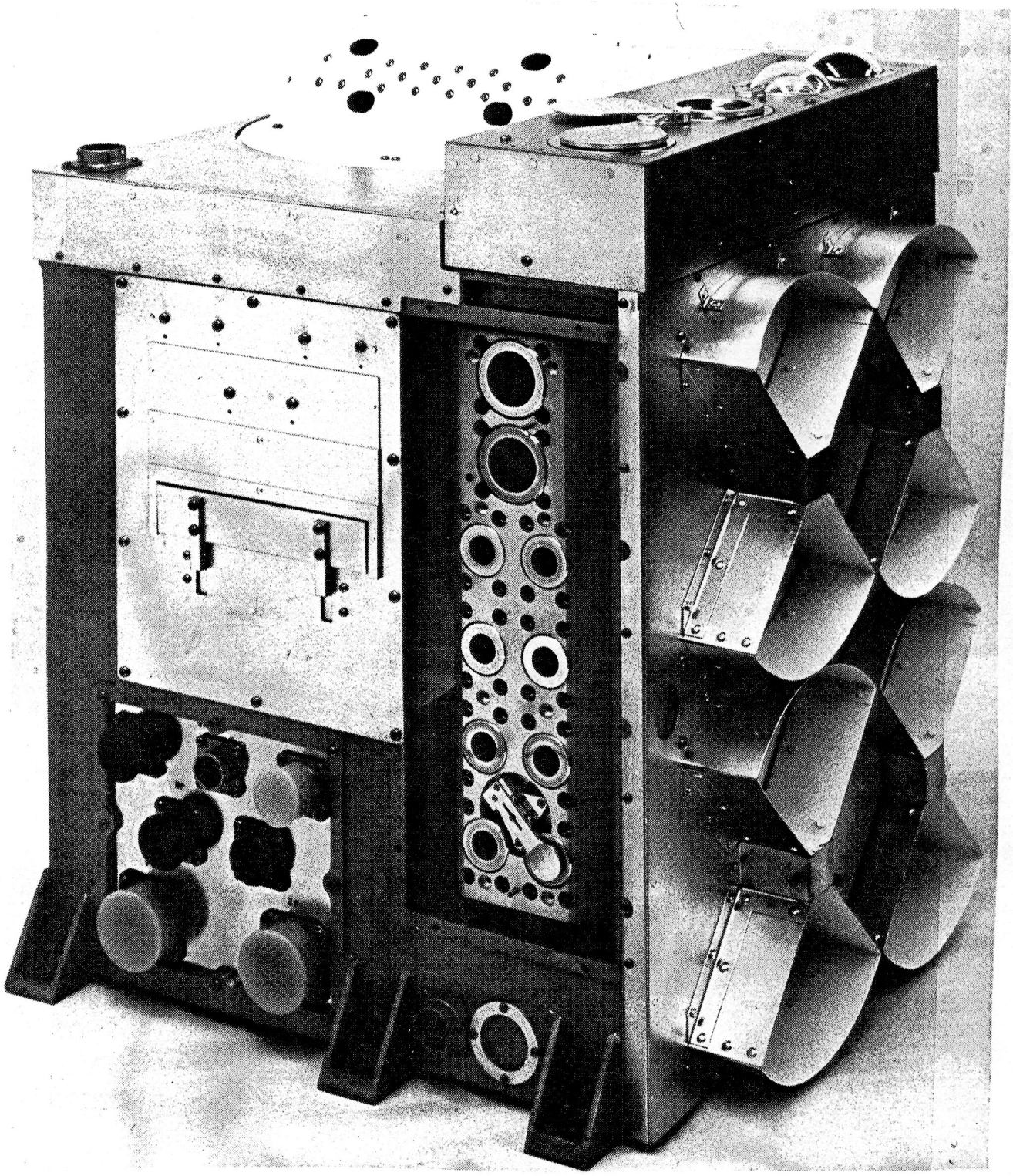

Figure 1
The Nimbus ERB subsystem. The wide field of view earth flux channels are at top right. Channel 11 is shown as in normal operations.

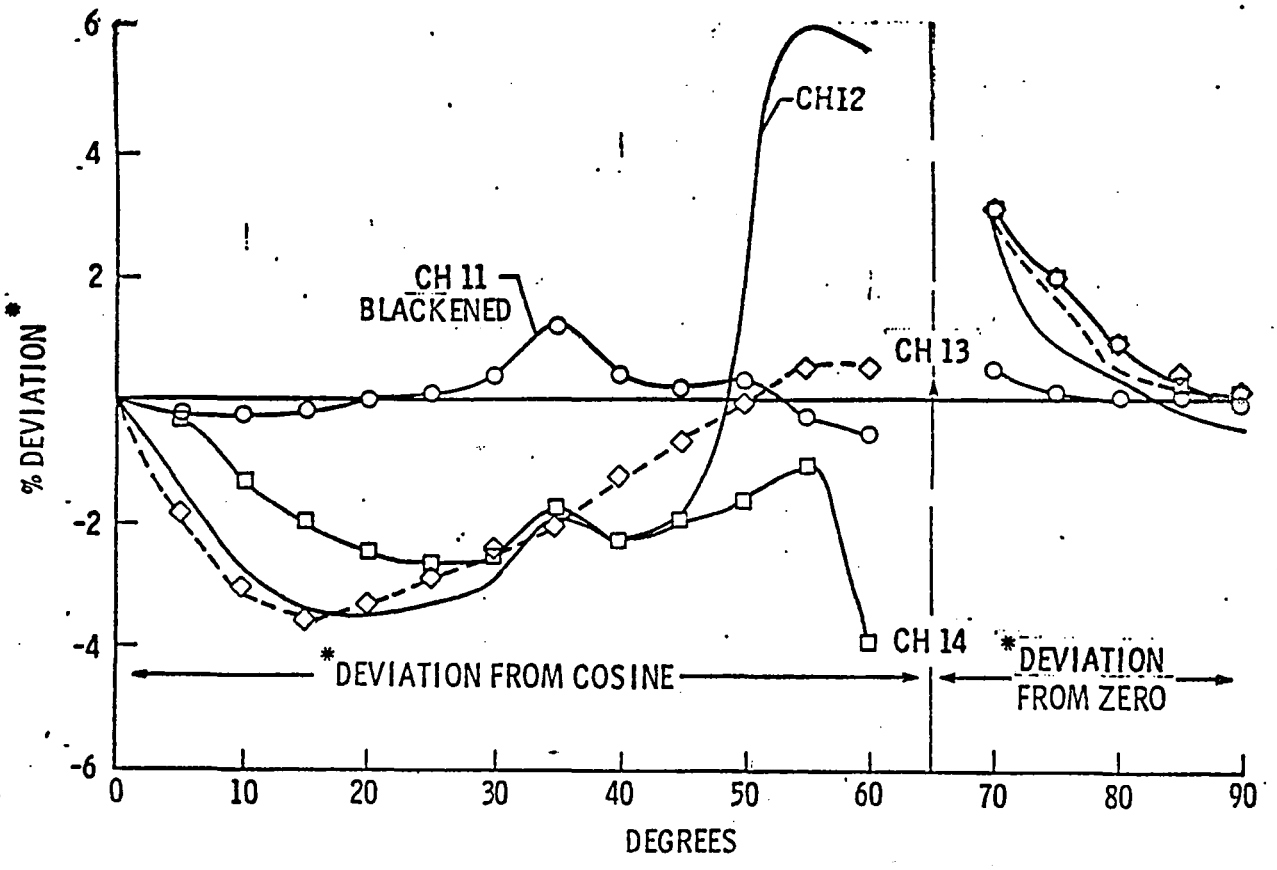

Figure 2

Results of detailed FOV measurements of the wide angle earth flux sensors. Multiple bounces off the baffles cause the out of field responses indicated as a percentage of normal incidence full scale.

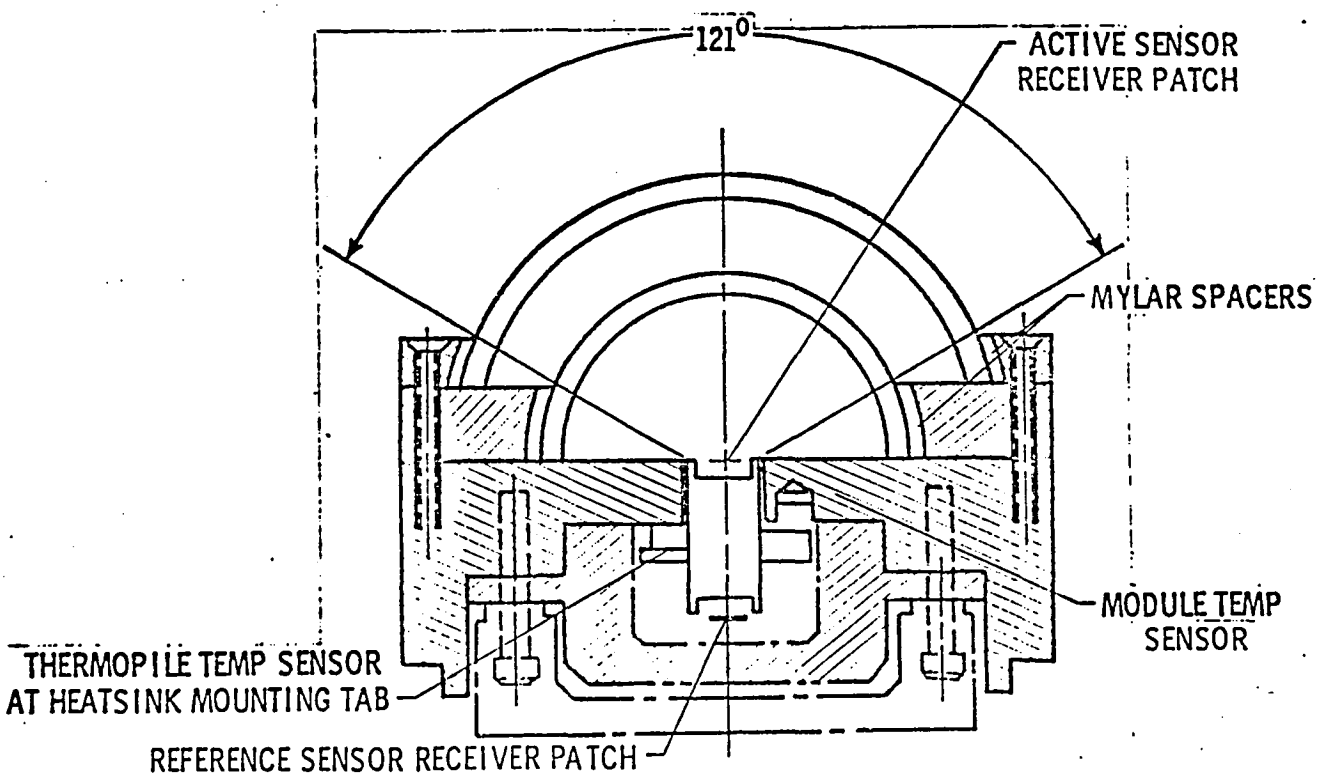

Figure 3

Geometry of short wavelength sensor Channel 13 with its quartz filter domes. Channel 14 has an additional dome of RG 695 Shott glass between the two shown.

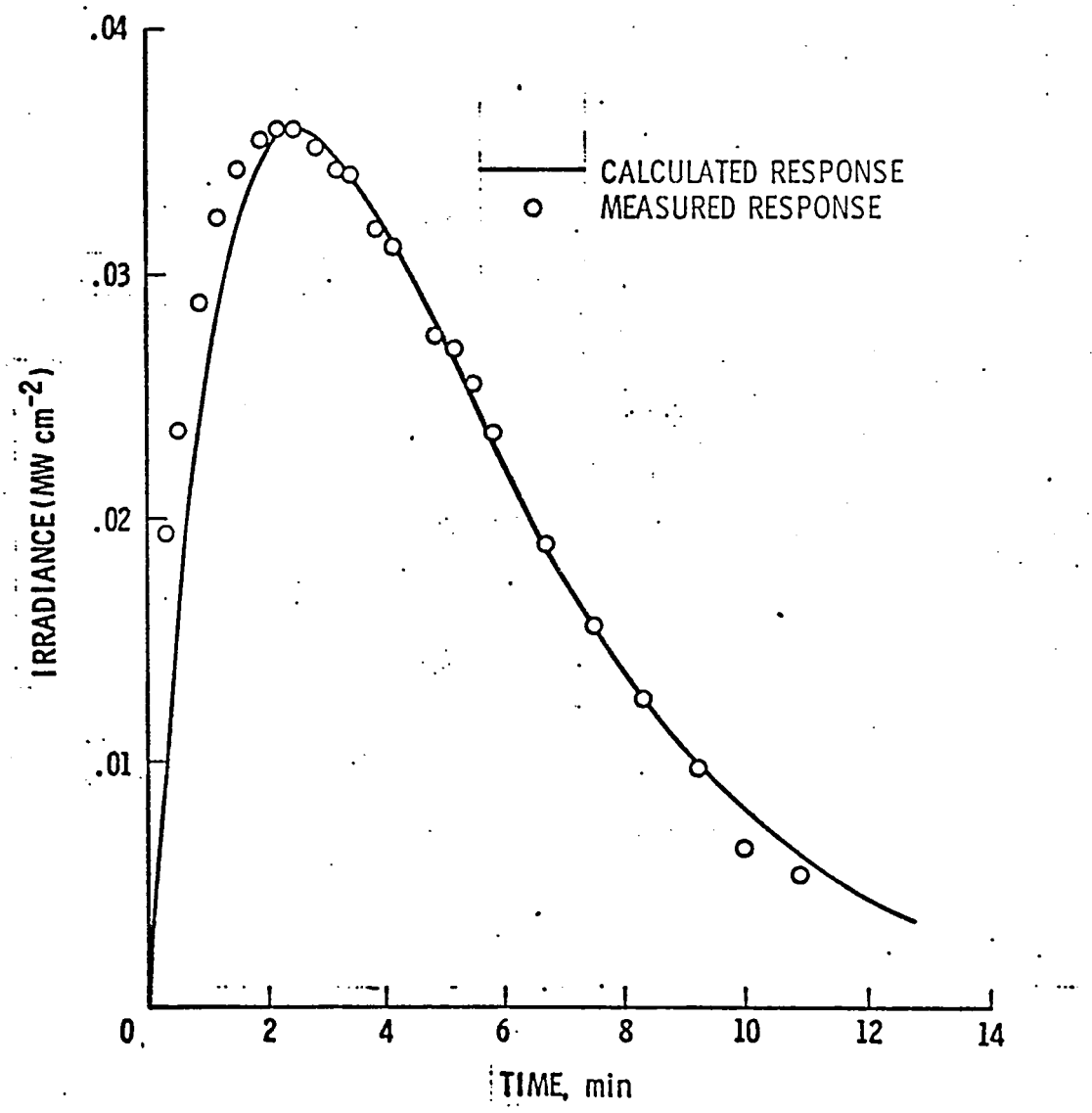

Figure 4

Response of short wavelength sensor Channel 13 to an impulse of long wavelength radiation. The outer dome first absorbs the radiation which reradiates to the inner dome causing a second-order effect.

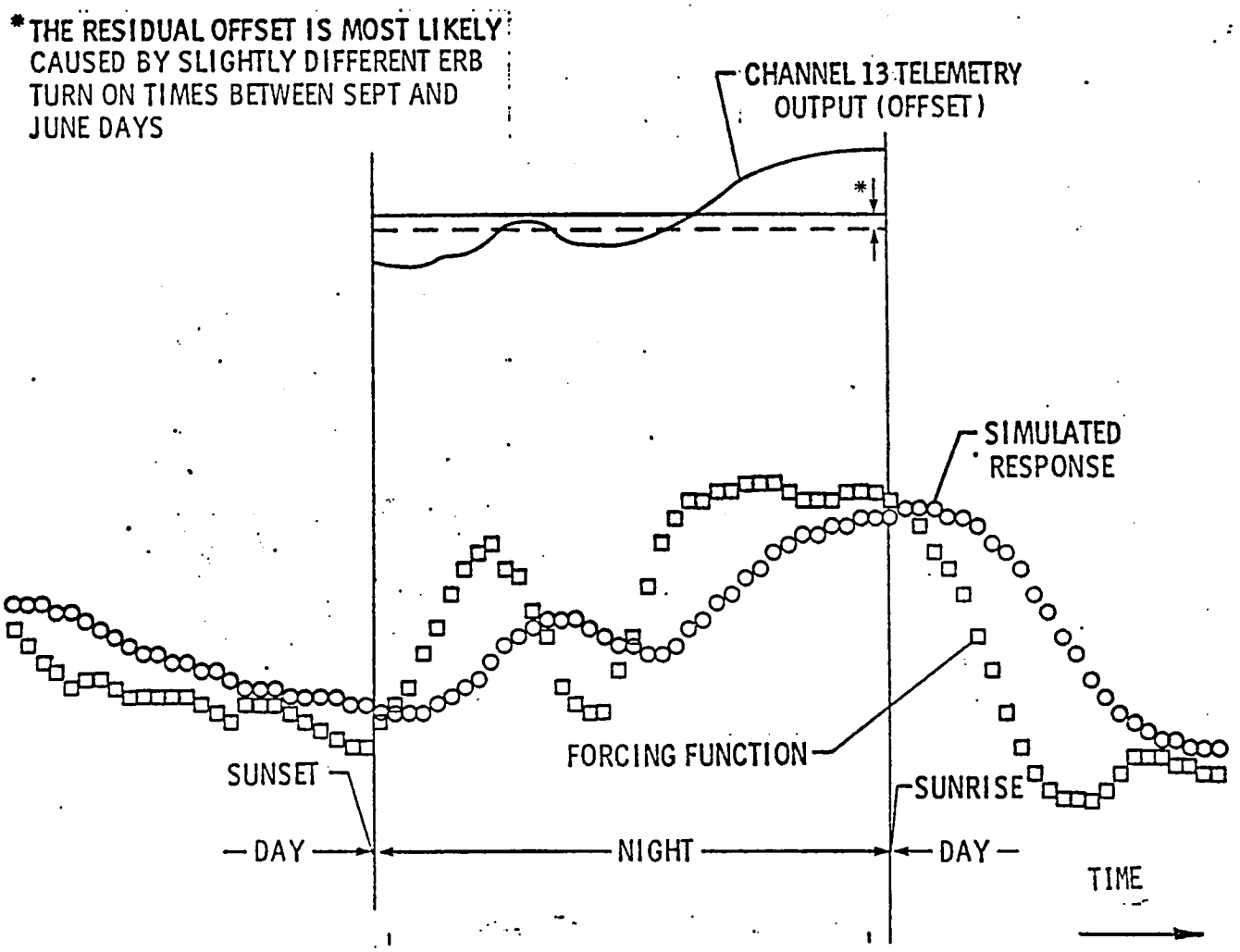

Figure 5
Differences in the longwave scene between September and June produce a difference in Channel 13's nighttime signature. The simulated responses is the convolution of the impulse response shown in Figure 4 with the longwave scene. It has a shape very similar to the nighttime offset differences shown in the upper curve.

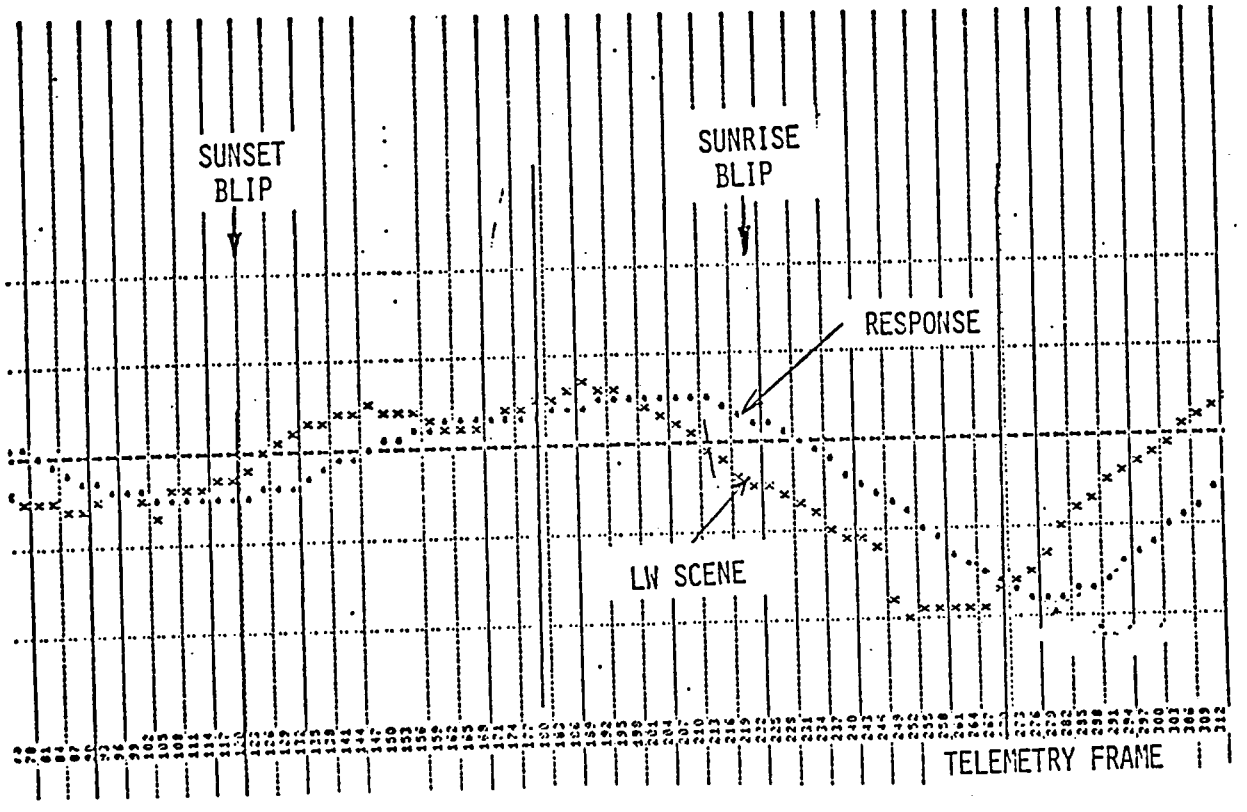

Figure 6
Raw computer output, which shows that the response generated by convolution of the long wave scene with the Figure 4 impulse response can be well approximated by a simple shift in time.

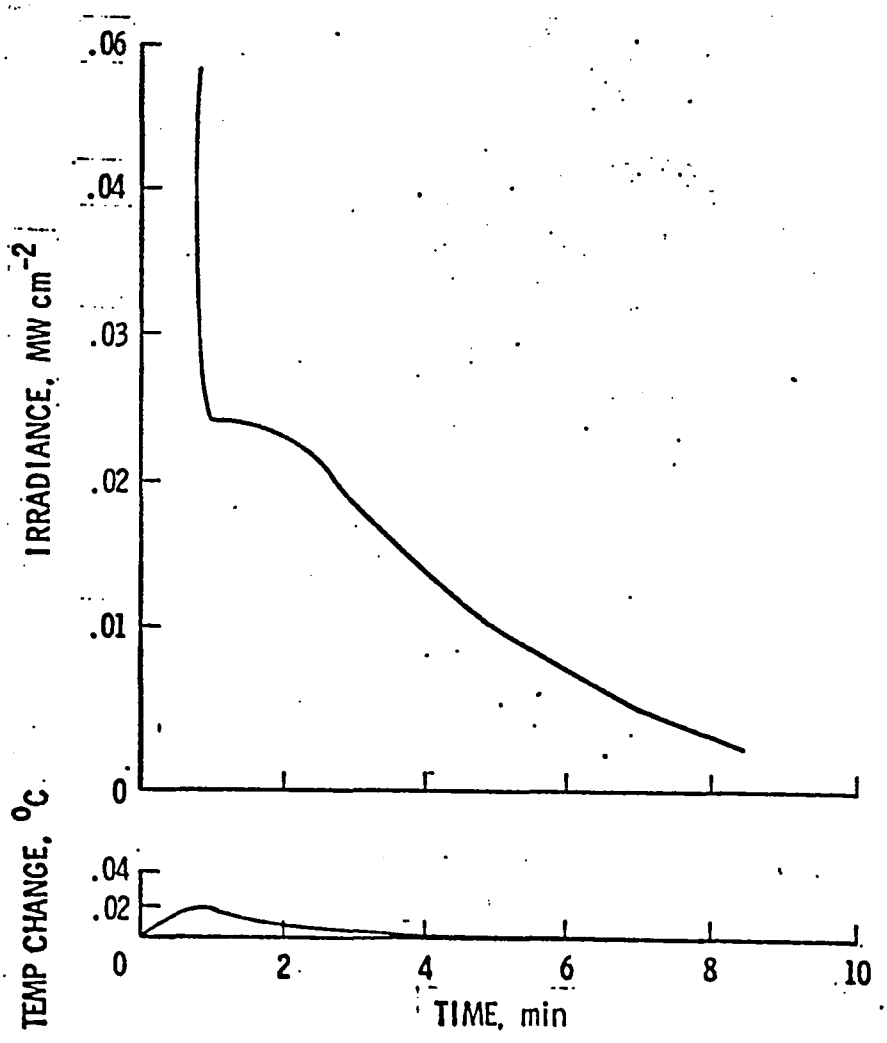

Figure 7
A spurious delayed response is clearly indicated for Channel 13 after a burst of short wavelength radiation. Evidently, front to back receiver gradients occur during the cooling process.

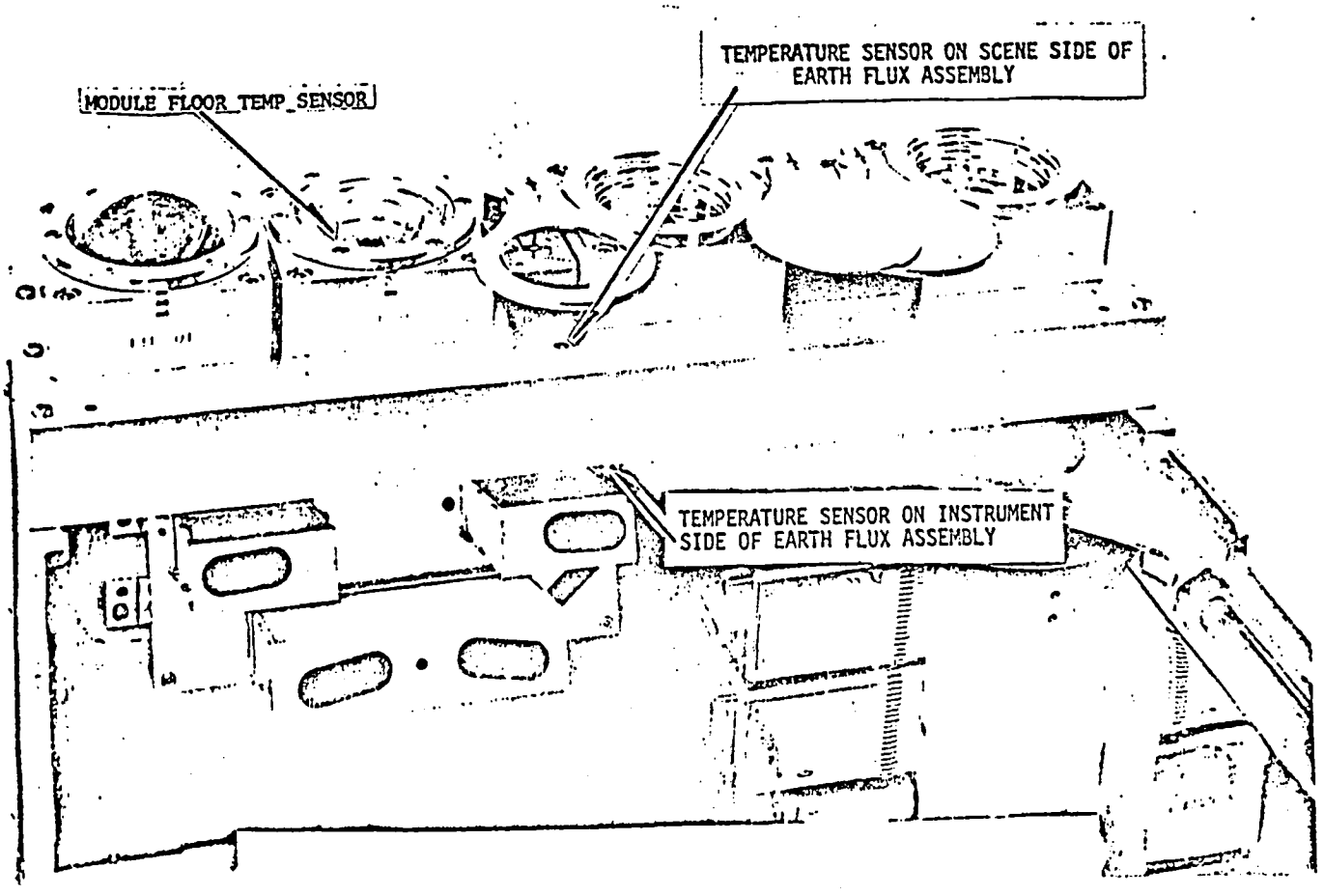

Figure 8
Earth flux channel assembly with insulating shroud removed showing location of temperature sensors. The channels are numbered 11-14, right to left.

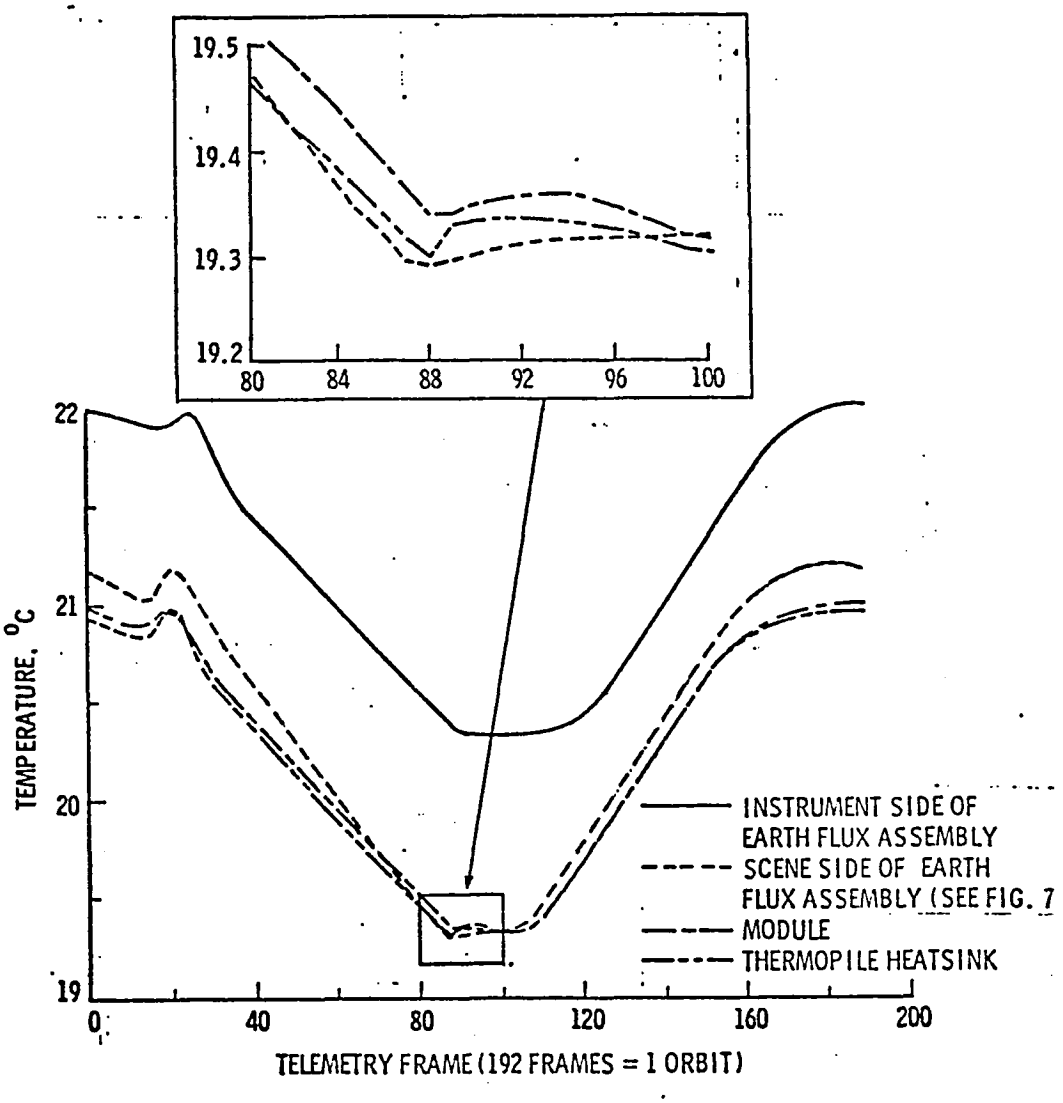

Figure 9
Typical orbital temperature signatures for the sensors identified in Figure 8. Note differences in the short-term transients near the sunset and sunrise sun blip periods.

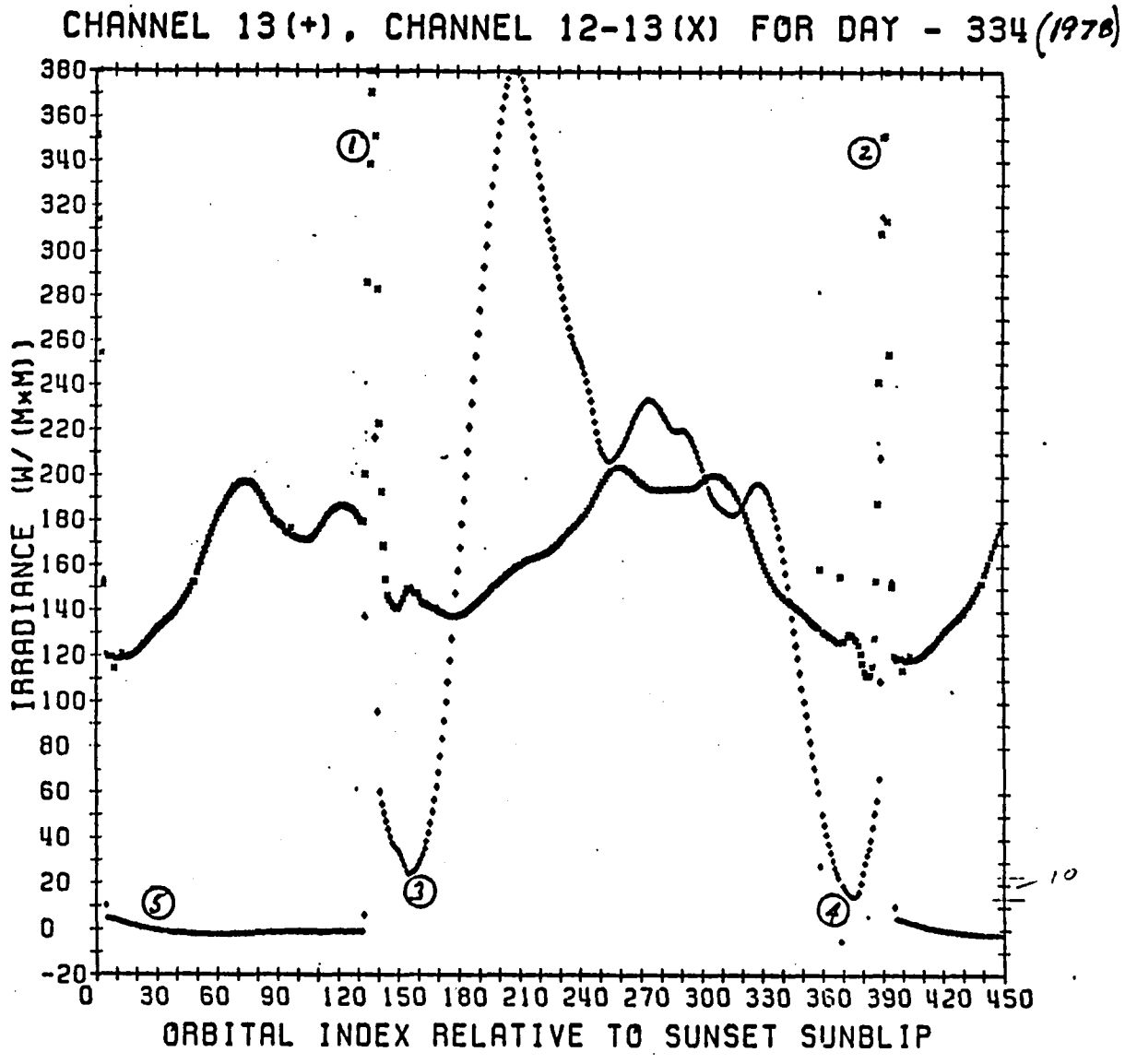

Figure 10
Shortwave (Channel 13, plus) and longwave (Channels 12 and 13, cross) outputs averaged over the orbits of day 334 (1978). No corrections have been made to Channel 13 for out of field response of longwave heating. The maximum potential useful daytime data falls between the polar minima (Points 3 and 4). 1, Sunrise sun blip; 2, Sunset sun blip; 3, Minimum after sunrise; 4, Minimum before sunset; 5, Transient decay after sunset.

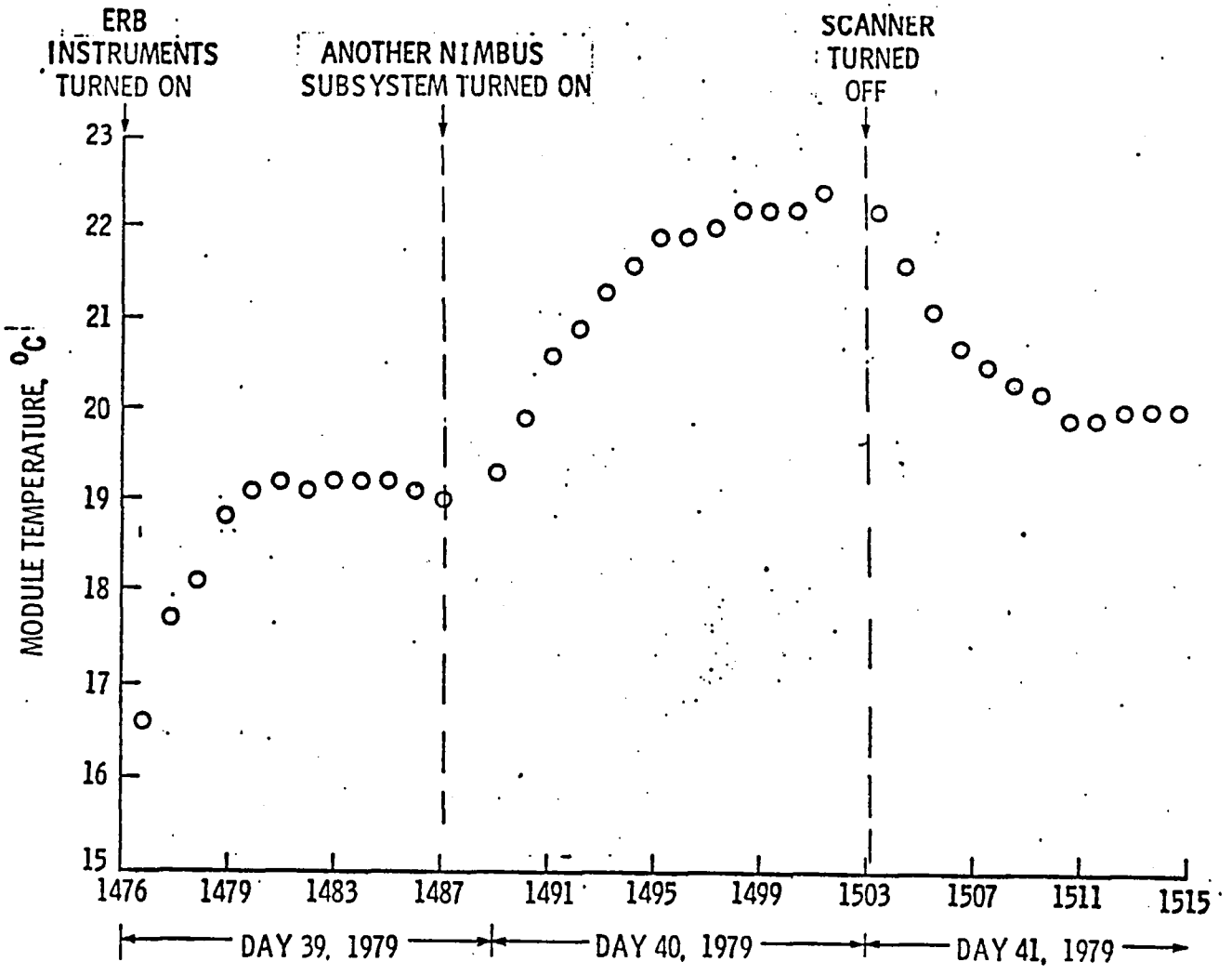

Figure 11
A long stabilizing period is indicated when the operational configuration of the NIMBUS observatory is changed. Channel 13's offset is lowest when the instrument is losing the smallest amount of heat.

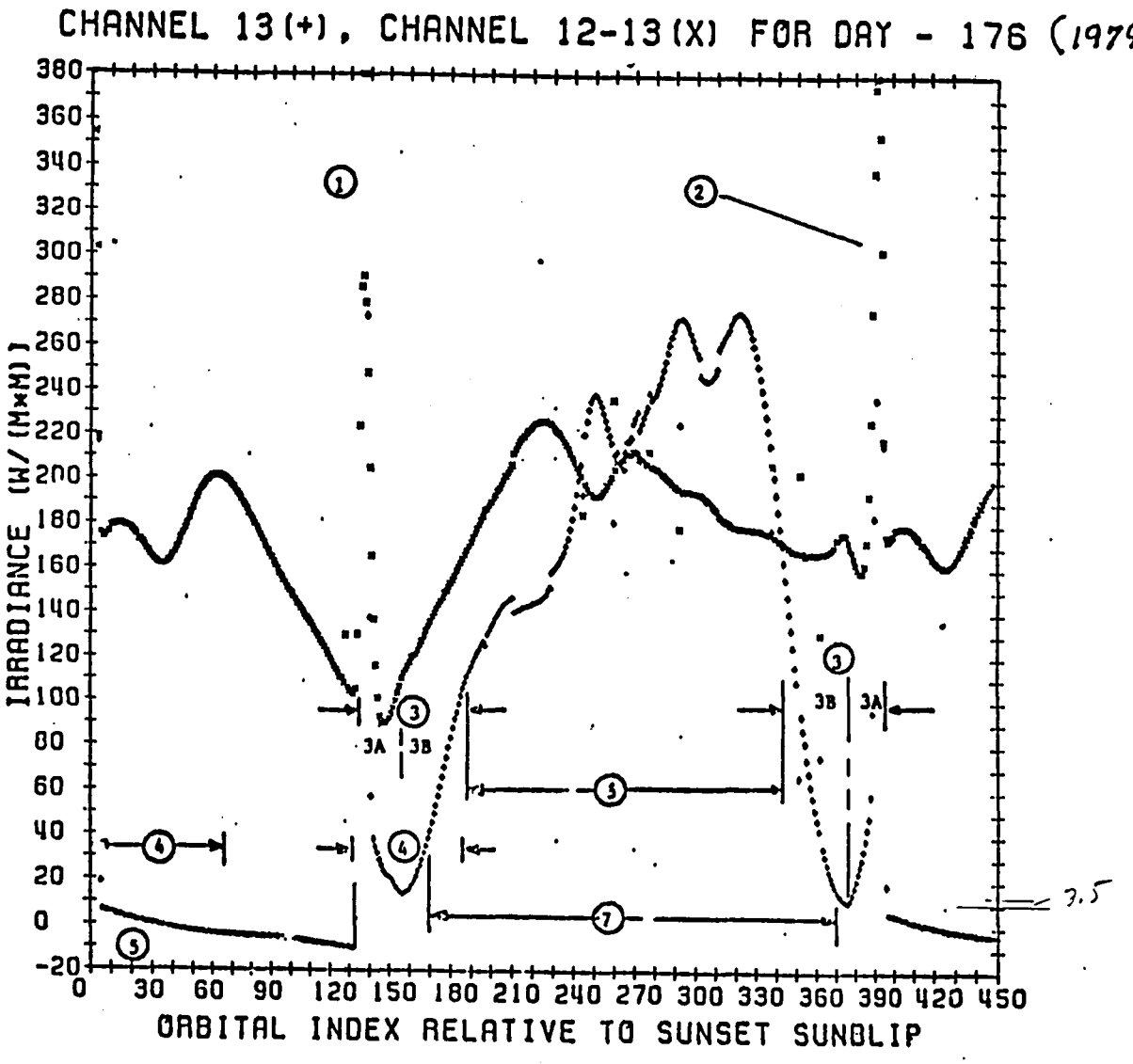

Figure 12

Outputs for day 176 (1979) showing what types of disturbances are applicable as a function of satellite orbital position. The need for corrections is greatest at high latitudes. Note the differences in the nighttime signature here with day 334 in Figure 10. The continuing decrease throughout the night here is caused by wintertime Antarctica cooling the dome. Channel 13, plus; Channel 12-13, cross. 1, Sunrise sun blip; 2, Sunset sun blip; 3, Regions contaminated by sun in FOV (A, severe; B, mild); 4, Regions contaminated by shortwave heating due to direct sun; 5, Transient decay after sunset; 6, Range or usable data when only longwave heating corrections are applied, 140°; 7, Range of usable data when all corrections are made, 180° latitude.

APPENDIX I
WIDE FIELD OF VIEW
NARROW FIELD OF VIEW INTERCOMPARISONS

by

G.G. Campbell
T.H. Vonder Haar

December 15, 1983

BACKGROUND

From the time of launch of the Nimbus-6 instrument in June, 1975, and continuing with the Nimbus-7 instrument, it was apparent that the wide field-of-view (WFOV) instruments were not responding to the incident radiation precisely as expected. This is most obvious in the large negative radiance analyzed from the reflected solar energy Channel 13 readouts during the night. This report is a contribution to the effort to review this and other instrumental features by detailed comparisons between an integration of the scan channels data and the WFOV data. We were looking particularly for estimates of offsets and apparent sensitivity differences from the preflight predictions of the response. Our approach is designed to be combined with the work by Gulton and others to better characterize the instrument in orbit. Together this should improve the scientific value of the Nimbus data and identify improvements for future earth radiation budget sensors.

$$\text{Wide} = \int r(\theta,\phi)\,\frac{d\cos^2\theta}{2}\,d\phi \qquad (1)$$

r = radiance from scanner

included the small scale variations in angular response measured by Maschhoff (1983). For numerical purposes the $\frac{d\cos^2\theta}{2}$ term was broken into twenty bins. All scanner data irrespective of ϕ were collected into these bins for sixteen second intervals or a major frame, 32 radiances from each sensor. The WFOV data was averaged into 16 second major frames, 4 radiances from each sensor.

Finally, for comparing to any individual WFOV observation, the scanner binned data was averaged from 112 seconds before and 96 seconds after the WFOV. This period is the time required to complete one scan mode 5 sweep of the earth. Each WFOV observation in time is not statistically independent of its neighbors because there is a very large overlap in the earth region they look at. Similarly, the integrated scan data has this large overlap because the integration is approximately a running mean for 208 seconds.

DATA SOURCE

We have used data from the Master Archive Tapes (MAT) from the NIMBUS project. Only days with scan mode 5 were used because it provides the widest angular sampling. We have depended upon the NIMBUS Project ephemeris for deriving satellite position and viewing geometry. Days 320 of 1978 and 159, 217 and 245 of 1979 were examined. Ideally, data in early 1979 would have been used, but no scan mode 5 was collected for that 5-month interval.

The first order analysis scheme radiance values are used as read from the MAT. We have not gone back to the raw voltage and temperature data from which the radiances were derived. There is a general consensus of the NIMBUS-7 team that the longwave scan data is slightly low because the filter is not as wide in frequency response as ideally required to measure in the earth infrared flux. This is about a two percent effect not included in analysis. Finally, channel 18, a shortwave scan channel, was not included in the integral because of instrument noise.

The orbit to orbit variation in channel 13 midnight radiance was subtracted during our processing before analysis. This removes the gross negative offset in channel 13 data seen since 1975 and also removes the day-to-day changes in this offset identified by Maschhoff et al. (1983). In addition, to adjust for longwave heating of the channel (Maschhoff et al, 1983) we subtracted a small fraction of channel 12 lagged in time, Equation 2.

$$13(t) = 13_{MAT} - 13_{MIDNIGHT} - 0.04(12-13)_{t-320\ sec} \qquad (2)$$

ORBIT TIME SERIES AND COMPOSITES

Several qualitative results can be seen by looking at the basic data from MAT. Figure 1 shows a sample of many of the orbital data sets we have studied. First, one sees several gaps in the data because in these plots we have excluded the times when the WFOV sensors receive radiation directly from the sun. Next one sees the time variation in channel 13 at night, a transient also caused by illumination by the sun near the sunset point. One of our original goals was to measure this transient in the daytime.

INTEGRATION METHOD

Since the long wave scan channel has an internal black body for periodic calibration, it will be used as a reference for comparison with the other observations. To compare with the WFOV the scan data must be integrated numerically to simulate the angular response of the WFOV channels. If the scan data were just averaged independent of angle the average would greatly over weight the limb because of the sampling scheme used in recording the scan data.

Using the satellite-nadir line as a reference, Equation 1 represents the angular weighting response of a flat plate detector. We have not included the small scale variations in angular response measured by Maschhoff (1983).

$$\text{Wide} = \int r(\theta,\phi)\ \frac{d\cos^2}{2}\ \theta\, d\phi \qquad (1)$$

r = radiance from scanner

For numerical purposes the $\frac{d\cos^2}{2}\theta$ term was broken into twenty bins. All scanner data irrespective of ϕ were collected into these bins for sexteen second intervals or a major frame, 32 radiances from each sensor. The WFOV data was averaged into 16 second major frames, 4 radiances from each sensor.

Finally, for comparing to any individual WFOV observation, the scanner binned data was averaged from 112 seconds before and 96 seconds after the WFOV. This period is the time required to complete one scan mode 5 sweep of the earth. Each WFOV observation in time is not statistically independent of its

neighbors because there is a very large overlap in the earth region they look at. Similarly, the integrated scan data has this large overlap because the integration is approximately a running mean for 208 seconds.

DATA SOURCE

We have used data from the Master Archive Tapes (MAT) from the Nimbus Project. Only days with scan mode 5 were used because it provides the widest angular sampling. We have depended upon the Nimbus Project ephemeris for deriving satellite position and viewing geometry. Days 320 of 1978 and 159, 217 and 245 of 1979 were examined. Ideally, data in early 1979 would have been used, but no scan mode 5 was collected for that 5-month interval.

The first order analysis scheme radiance values are used as read from the MAT. We have not gone back to the raw voltage and temperature data from which the radiances were derived. There is a general consensus of the Nimbus-7 team that the longwave scan data is slightly low because the filter is not as wide in frequency response as ideally required to measure in the earth infrared flux. This is about a two percent effect not included in analysis. Finally, Channel 18, a shortwave scan channel, was not included in the integral because of instrument noise.

The orbit to orbit variation in Channel 13 midnight radiance was subtracted during our processing before analysis. This removes the gross negative offset in Channel 13 data seen since 1975 and also removes the day-to-day changes in this offset identified by Maschhoff *et al.* (1983). In addition, to adjust for longwave heating of the channel (Maschhoff *et al*, 1983) we subtracted a small fraction of Channel 12 lagged in time, Equation 2.

$$13(t) = 13_{MAT} - 13_{MIDNIGHT} - 0.04(12-13)_{t-320\ sec} \qquad (2)$$

ORBIT TIME SERIES AND COMPOSITES

Several qualitative results can be seen by looking at the basic data from MAT. Figure 1 shows a sample of many of the orbital data sets we have studied. First, one sees several gaps in the data because in these plots we have excluded the times when the WFOV sensors receive radiation directly from the sun. Next one sees the time variation in Channel 13 at night, a transient also caused by illumination by the sun near the sunset point. One of our original goals was to measure this transient in the daytime.

During the night it is difficult to distinguish in Figure 1 between Channel 12 observations and the longwave scanner (LWSC) because, in fact, they are very close together. During the day, the shortwave scan (SWSC) data shows ripples which appear to be about 200 seconds long. This is because the scanning in mode 5 is not a perfect simulation of the smoothing done by WFOV. The SWSC line is, however, substantially higher than 13.

To examine the major questions in more detail, all orbits for a day were composited using the day/night sun blip to synchronize the orbits. Figures 2 and 3 show composites for the 4 days we analyzed. The ripples remain in the SWSC because the scan period is an exact multiple of an orbital period, so a small excursion from a smooth line occurs at the same point in every orbit. All data have been composited and plotted, but as noted only part of the data are useful for comparison because of sun contamination. One still sees the large excursions which occure near the sun blip.

During the night there is an apparent offset between Channel 12 and the LWSC. This could be a scaling (sensitivity) difference or a combination of an offset and a sensitivity difference. Below we present correlation fits to estimate this quantitatively.

During the day, several pairs of lines are similar. There is a substantial shift between the SWSC and Channel 13 which should be measuring the same energy. Similarly, there is a shift between Channel 12 and (SWSC plus LWSC) both of which should be the total outgoing radiation. To add to the confusion, Channel 12-13 is very close to LWSC. One would now like to decide which of the three channels, SWSC, 12 and/or 13 need to be adjusted to match up with LWSC, which we have chosen as a reference. Recall that one of our goals is to use a corrected version of SWSC to compare the detailed daytime variations in Channel 13 offset.

CORRELATIONS

Our first attempt to quantify and understand the differences noted above was to calculate linear regressions between pairs of observations which should have been nearly the same. Table 1 shows the slopes and intercepts. First, a few words about the fit method are necessary. The standard least squares fit minimizes the standard deviation between Y and aX+b by solving for a and b. This assumes that Y has no measurement error and is "correct." One could equally justify minimizing in the X direction because we are uncertain which channel is correct and especially because of the integration will produce random error in observations from the scanner. We have chosen to present the results of a total least squares fit, which selects the line which minimizes the distance between the line and the point at (X,Y). This also produces a line between the fit lines for

minimum dX and minimum dY. Also listed are the standard deviation of the fit parameters.

The purest test should be the comparison between Channel 12 and LWSC at night. The results definitely indicate an offset exists in the data as well as a sensitivity shift from that used in the MAT processing. Some physical arguments are under study by Maschhoff to explain this offset. He believes that heat is flowing out of the instrument and produces an obvious offset in Channel 13 at night. The comparison presented here shows a similar offset in Channel 12 but about half the magnitude of the Channel 13 night offset which is about $20W/M^2$. Figure 4 shows scatter diagrams of the pairs of observations for the 4 days and a solid line representing the best fit. Even an eyeball fit indicates an offset exists but its magnitude is less certain than the table standard deviations indicate. We have performed several fits excluding different amounts of lower quality data producing several values for the slope and intercept. Before attempting a conclusion, let us discuss the other comparisons.

Comparing Channel 13 to SWSC shows substantially more scatter in the parameters (Figure 5). There is, however, a clear indication of an offset between them as well as an uncertain slope. The difference between the composite fit and the individual data orbital fit for day 245 shows in Table 1 the substantial uncertainty in the method, with the disagreement in slope.

Comparing (Channel 12-LWSC) which should be the reflected flux and Channel 13 show very close correspondence, Figure 6. This, in fact, shows the closest match of all the comparisons tried. One can interpret this in two ways: (1) Both Channels 12 and 13 readings are correct during the day as shown by this good fit.

Maybe there is a small offset in Channel 12 or 13; (2) Both Channels 12 and 13 have big offsets from reality but the magnitude of the offset is nearly the same so the difference is near zero.

Finally, we compared (Channel 12-LWSC) to SWSC which showed a large offset, Figure 7. Except for day 320, the slopes are close to 1.0, and the offset is a large negative value between 12 and 34W/M^2. This agrees to some extent with results from the NIMBUS-7 NET since we had thought SWSC returned very high readings. Based on earlier comparisons an adjustment was made to force the offset (b) to zero and made the slope (a) approximately 0.9 in converting SWSC to albedoes written onto the output (MATRIX) tapes for users. Our results indicate a need to reconsider that decision.

DIFFERENCES

To detect changes in Channel 13 behavior during the day (e.g., offset changes) one can use SWSC or Channel 12-LWSC as a proxy of reflected flux and then look at the difference. The SWSC data must be adjusted by using the fit parameters to bring the two numbers close together. Figures 8 and 9 show the result of this subtraction. The SWSC comparison shows behavior after the night to day sun blip an Channel 13 alone from after day to night sun blip, from after day to night, but this is only qualitative because the ripple from the integration masks the effect. The Channel 12-LWSC difference shows small changes in the day part of the orbit, but perhaps the changes in Channel 13 response are exactly balanced by changes in Channel 12. We do not see an obvious scene-dependent offset in Channel 13 during daytime, but scan pattern integrations add noise to our comparison.

TEMPERATURES

To get some information about the physical mechanism for the offset, we looked at composite temperature traces for various sensors on the ERB instrument. Figures 10 and 11 show a sample. Of interest is the large variation in temperature of the Channel 12 shutter. This is weakly coupled to the module and so undersoes large swings in temperature. It is very close to the Channels 13 and 13 detectors and thus could be feeding energy in and out of the detector. No quantitative results are evident in the analysis thus far.

CONCLUSIONS

Strong evidence has been found for an offset in channel 12 at night, about one-half the channel 13 night offset $20W/m^2$. (See also Jacobowitz et al, 1983.) It is not possible to separate channel 12 and 13 behavior in the day. In retrospect, we should have attempted a three parameter fit during the day (LWSC = a12 +b13 + c or LWSC = a12 + BSWSC + c). This might have allowed better consistency in the parameters, but it can not resolve the offset in channel 12 separate from the channel 13 offset during the day. Some external assumption must be applied to decide the offset information relative to the SWSC understudy. It would also have been helpful to process much more data to look for time variations in slope and offset and this to understand if their changes from day to day are real or noise.

REFERENCES

Jacobwitz, H.,H. Soule, H. Kyle, F. House and the NIMBUS-7 ERB Experiment team, 1983: The earth radiation budget experiment; and overview. J. of Geo. Res., Submitted.

Maschhoff, R., A, Jalink, J. Hickey and J. Swedberg, 1983: NIMBUS - Earth radiation sensor characterization for data reduction fidelity. J. of Geo. Res., Submitted.

Figure 2a Orbital composites of 12 and LWSC+SWSC, 320

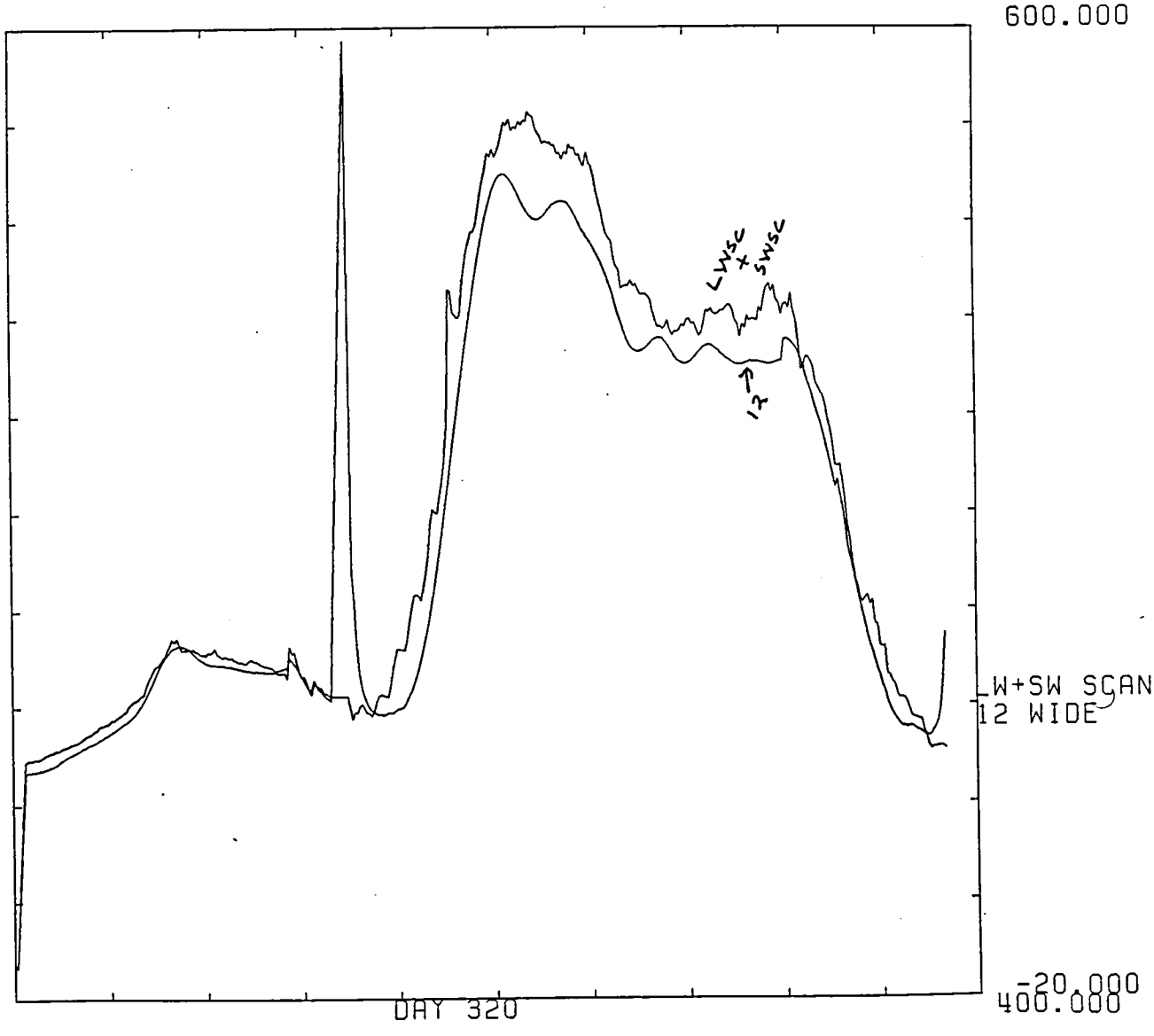

Figure 2b Orbital composites of 12 and LWSC+SWSC, 159

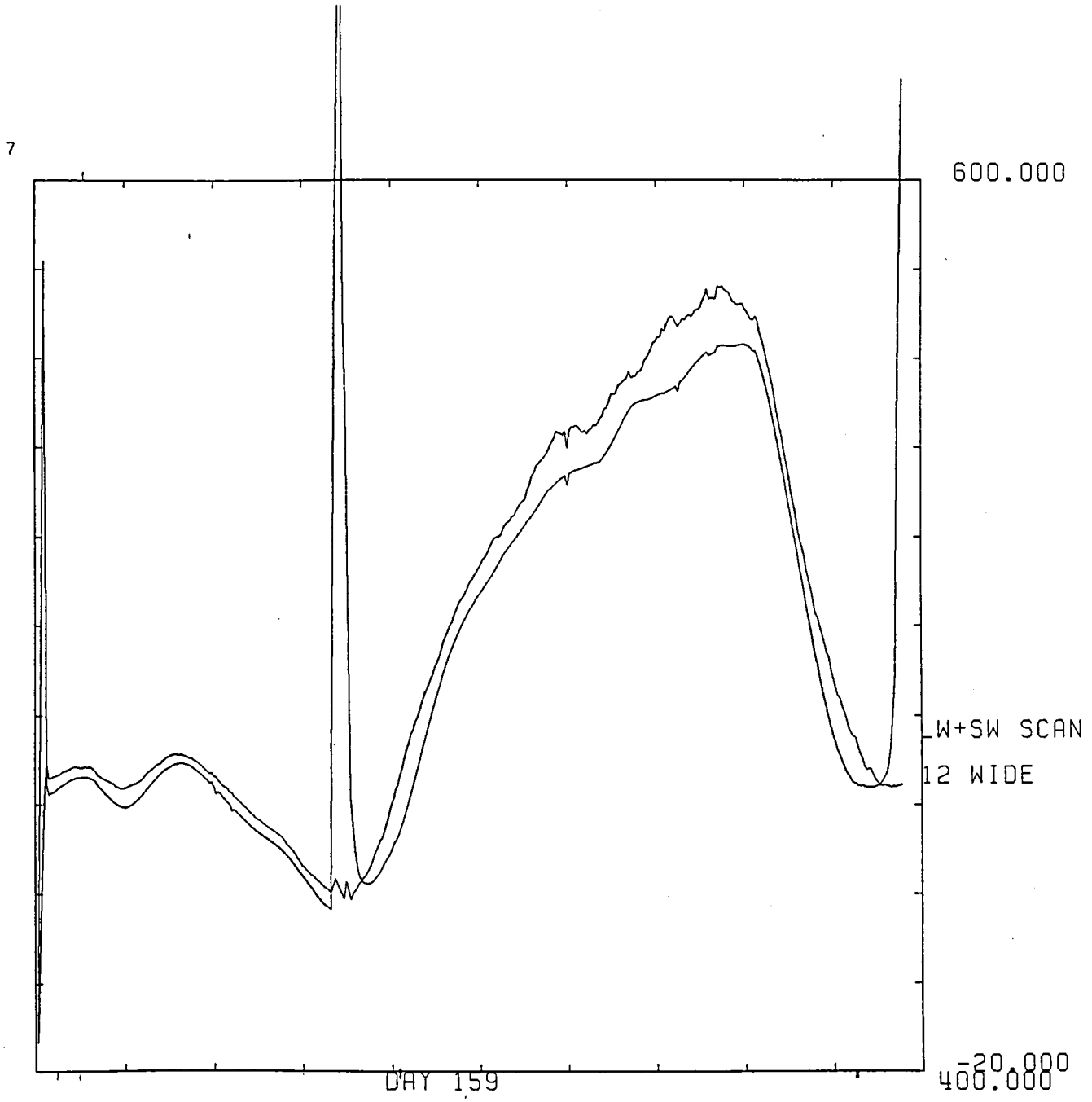

Figure 2c Orbital composites of 12 and LWSC+SWSC, 217

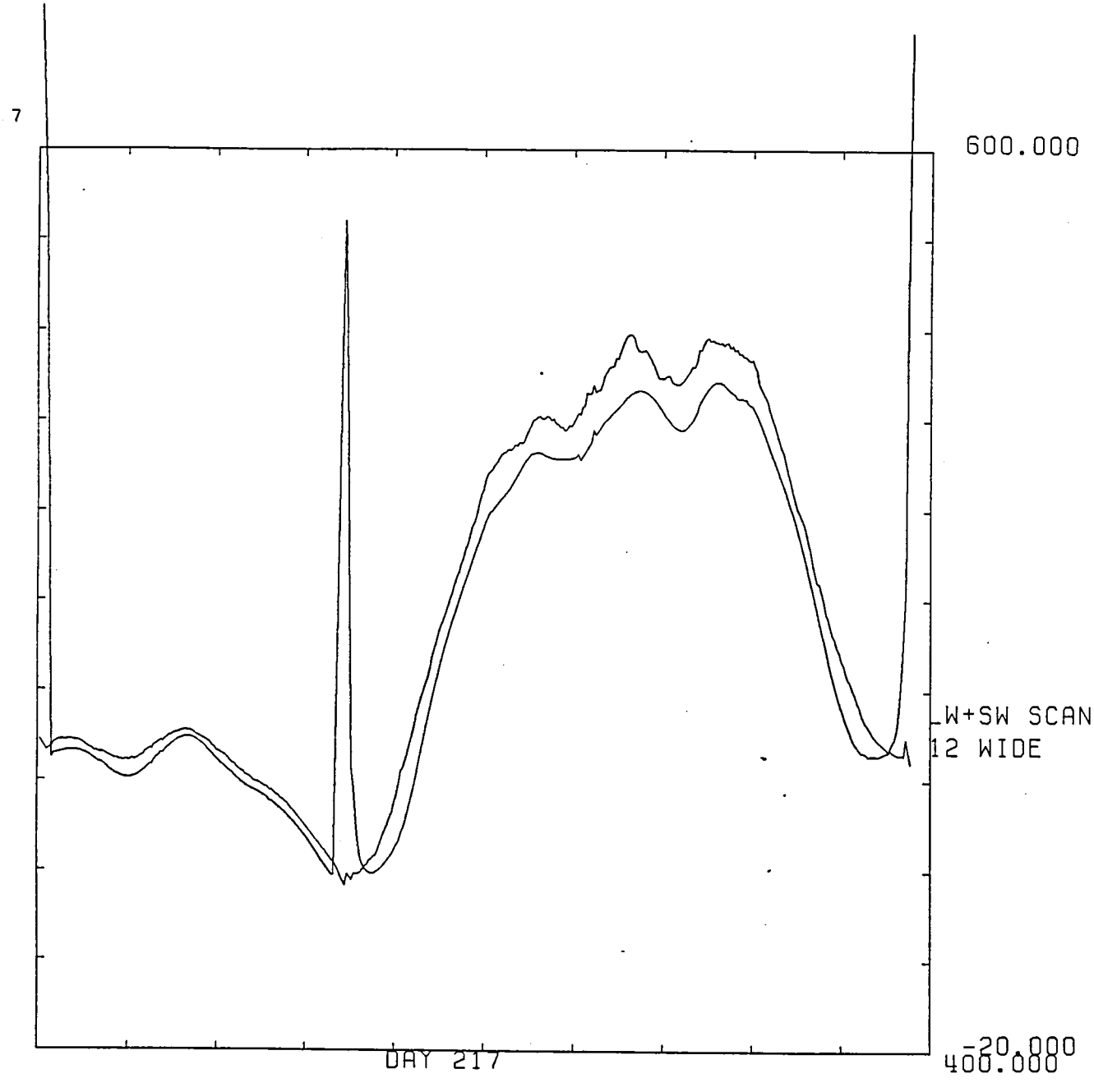

Figure 2d Orbital composites of 12 and LWSC+SWSC, 245

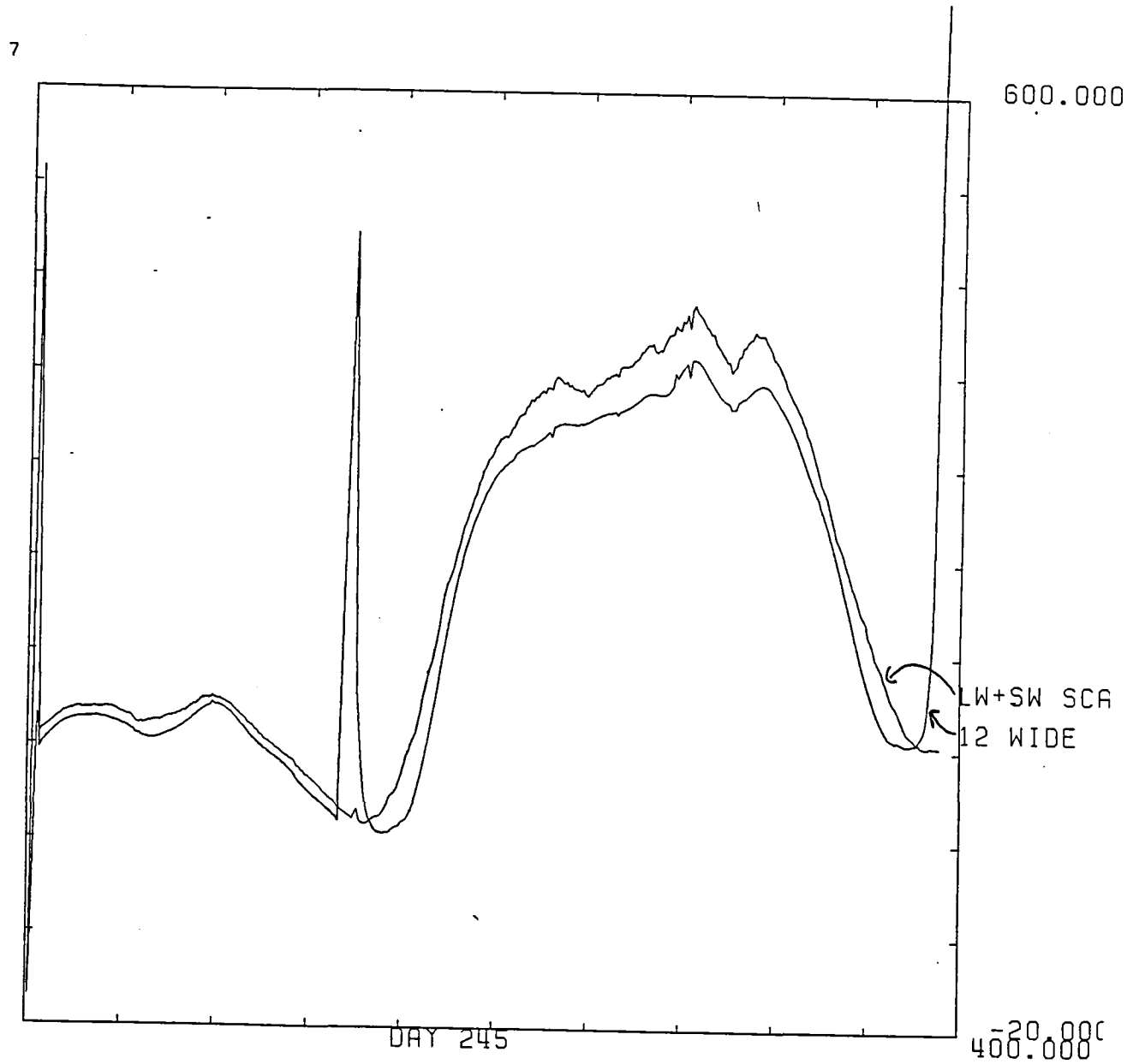

Figure 3a. Orbital composites for day 320

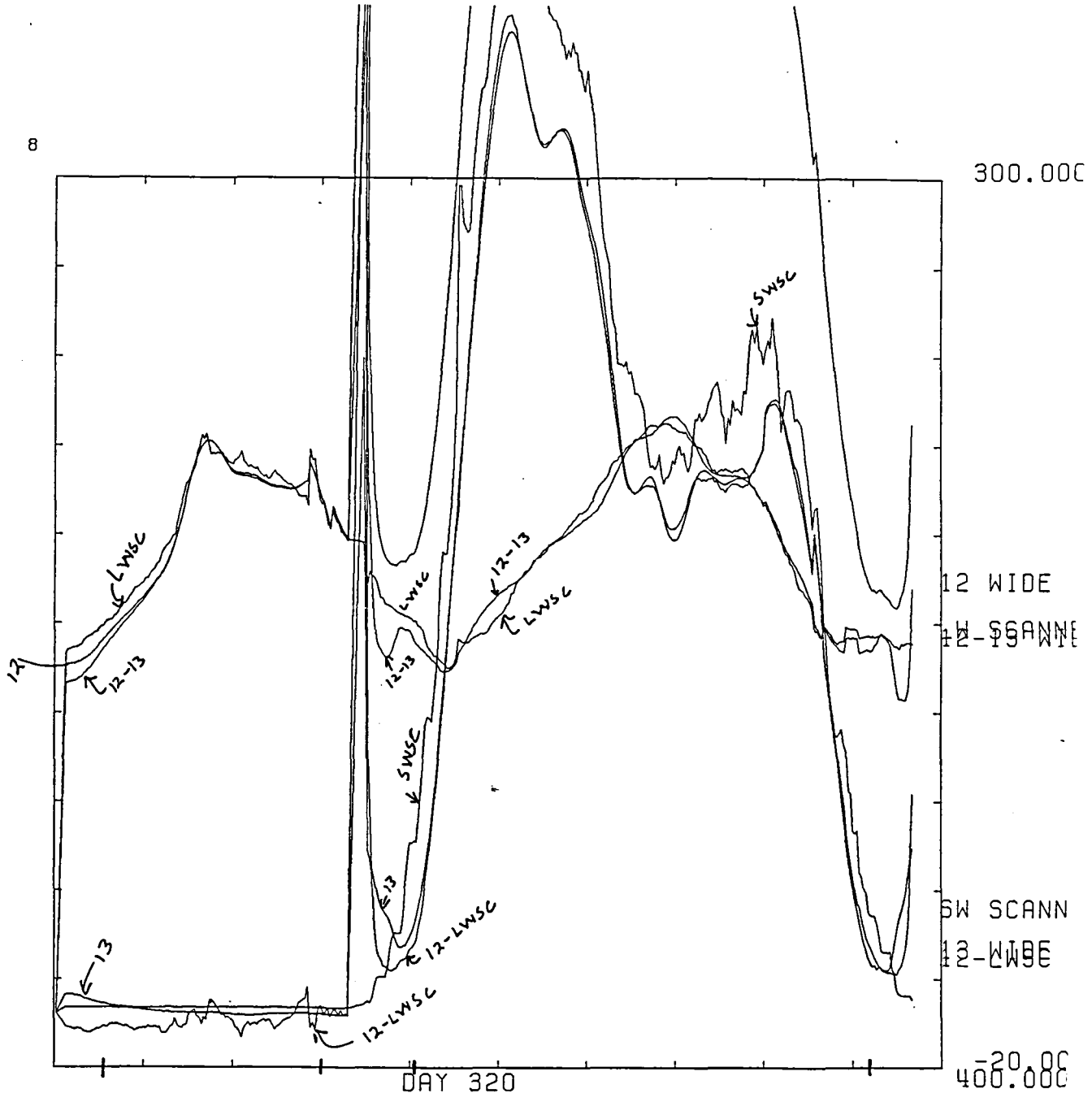

Figure 3b. Orbital composites for day 159

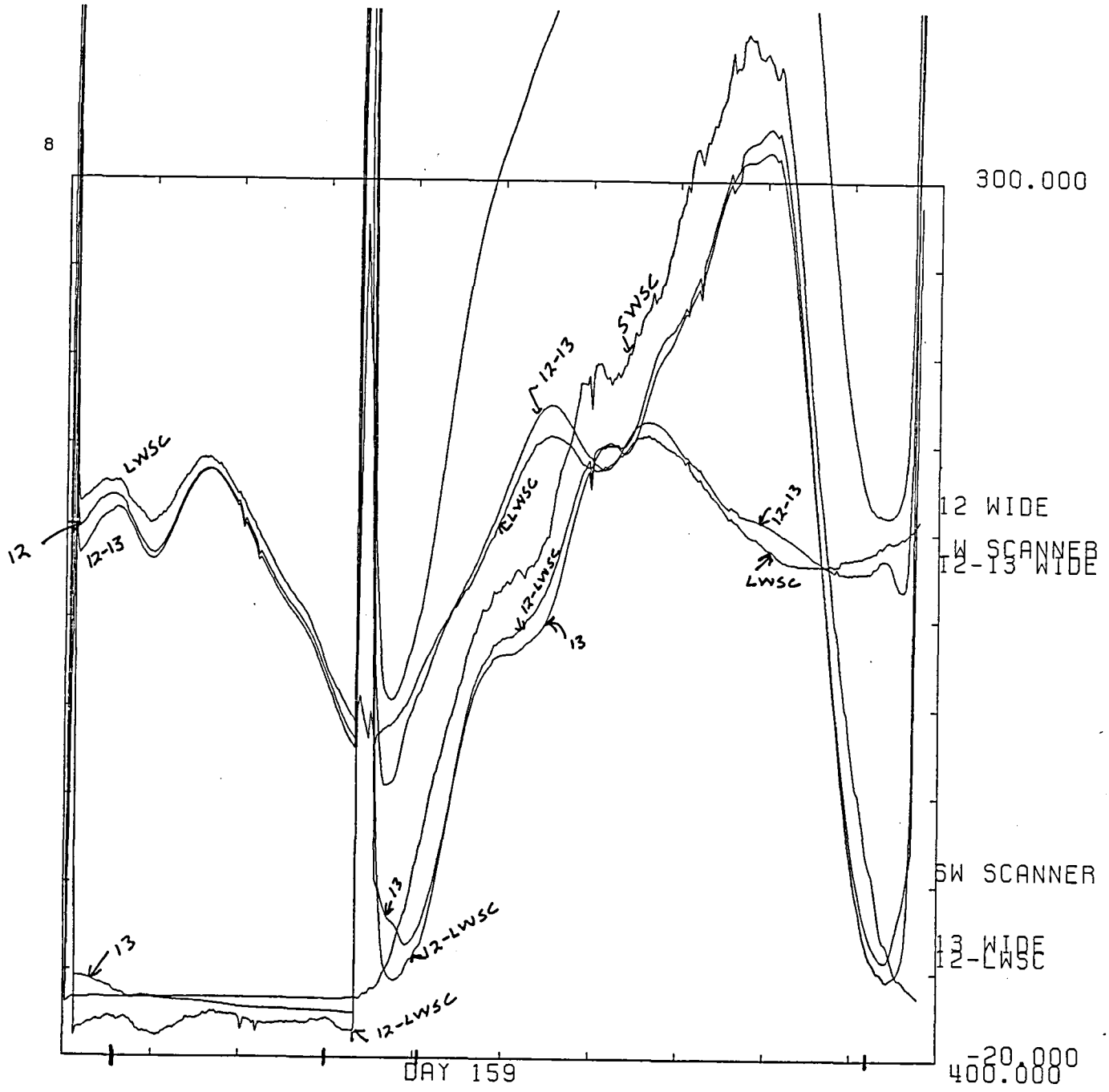

Figure 3c. Orbital composites for day 217

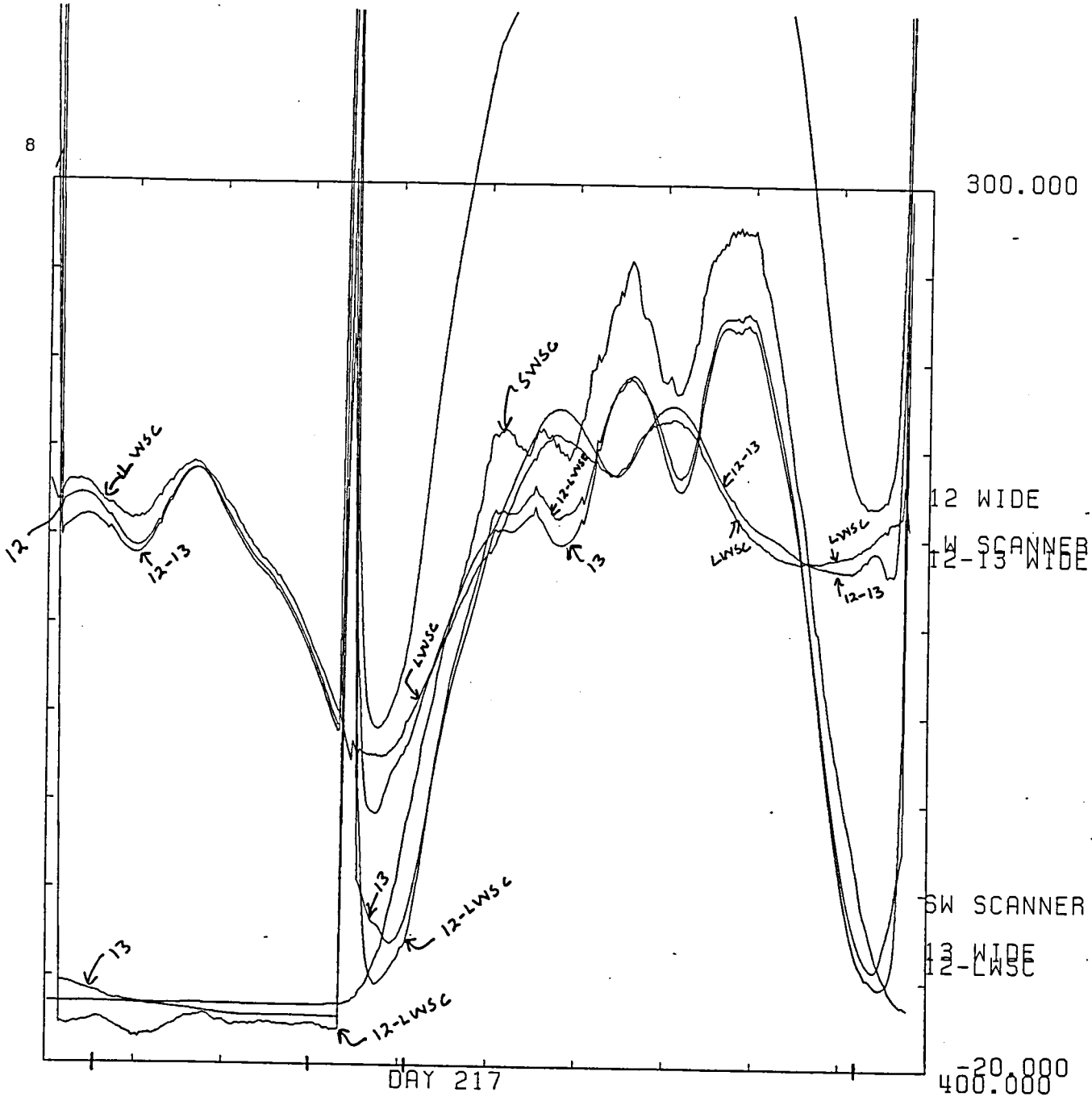

Figure 3d. Orbital composites for day 245

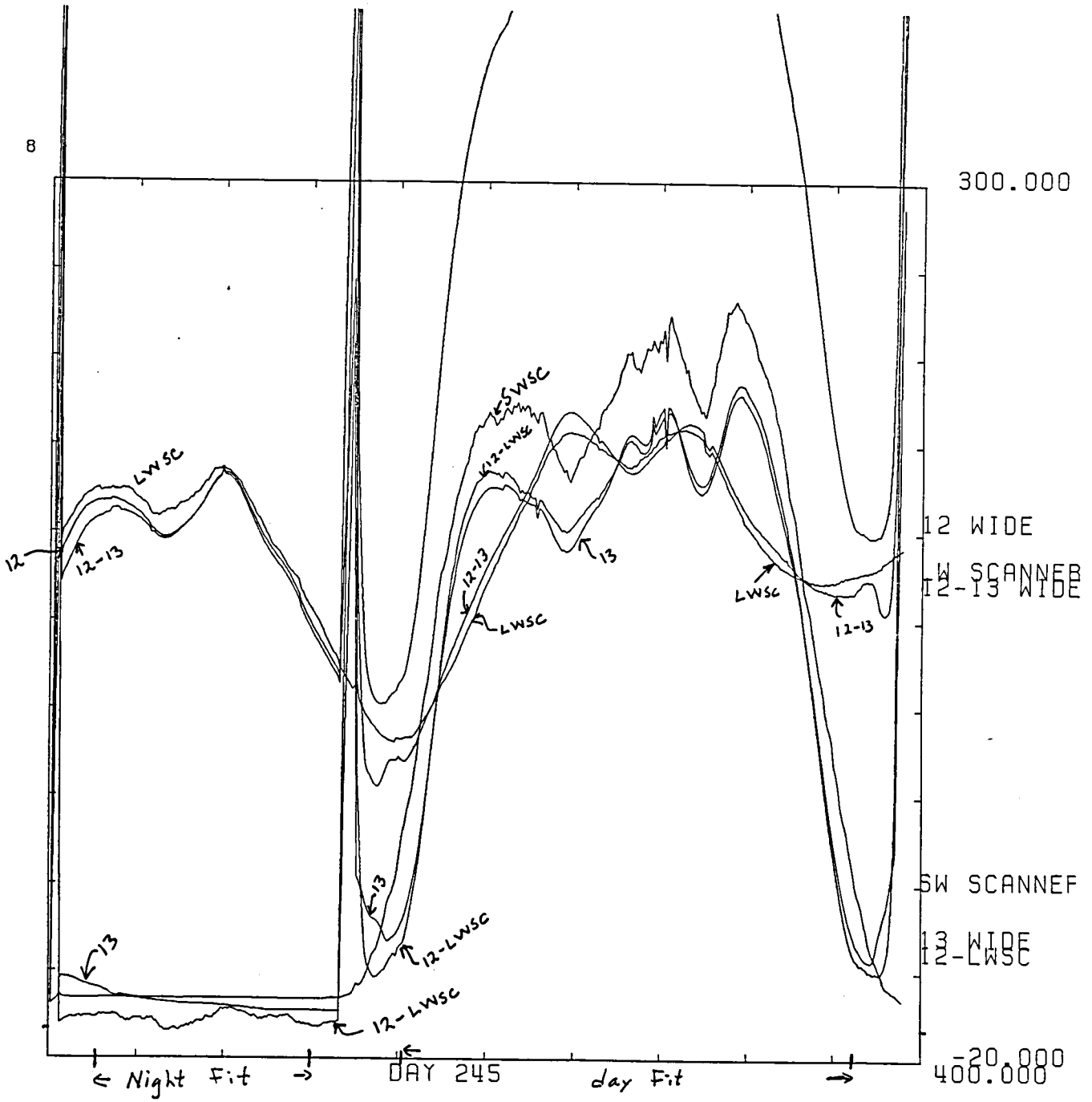

Figure 4 Scatter plots of 12 vs LWSC at night.

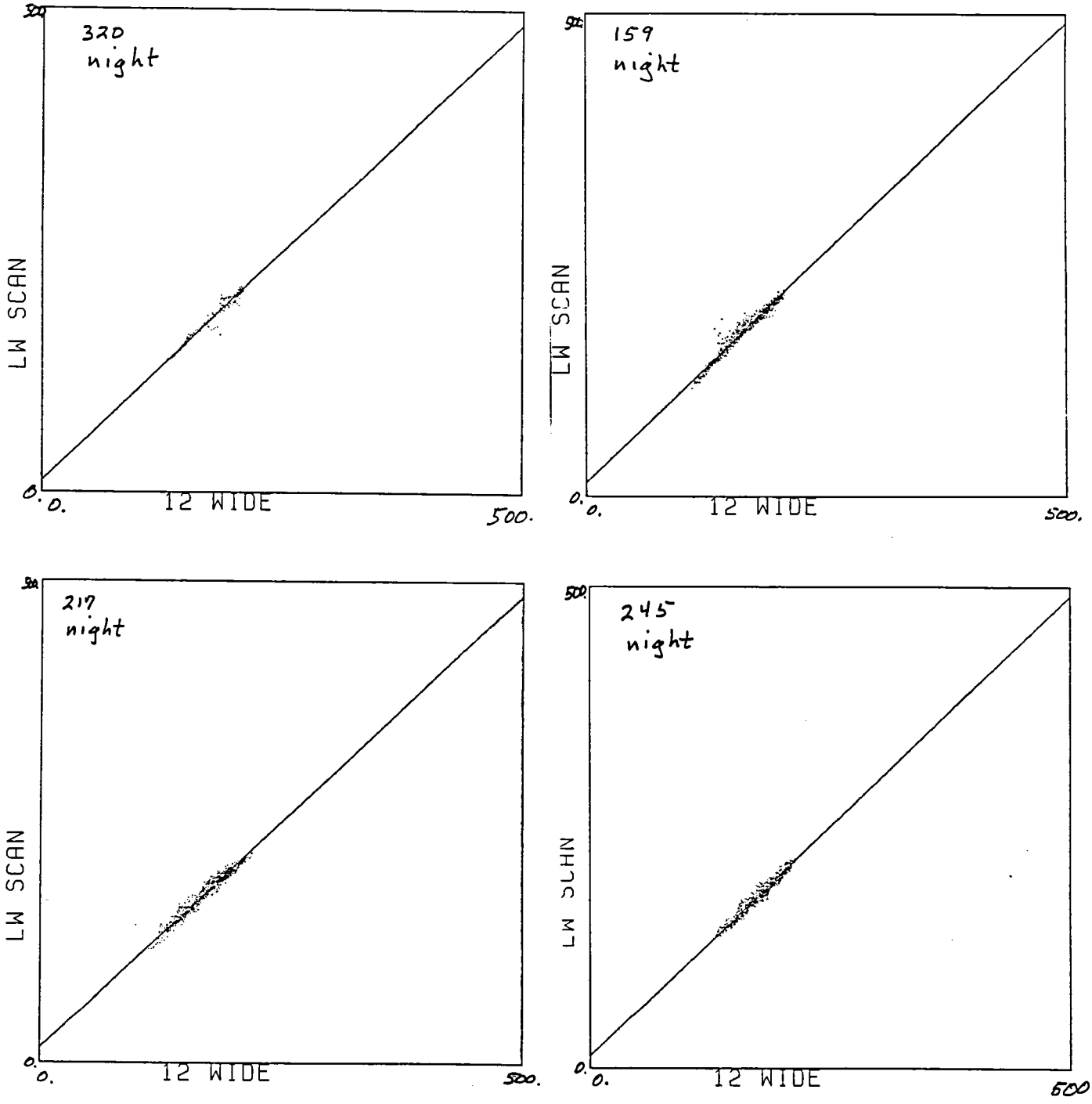

Figure 5 Scatter plots of 13 vs SWSC during day.

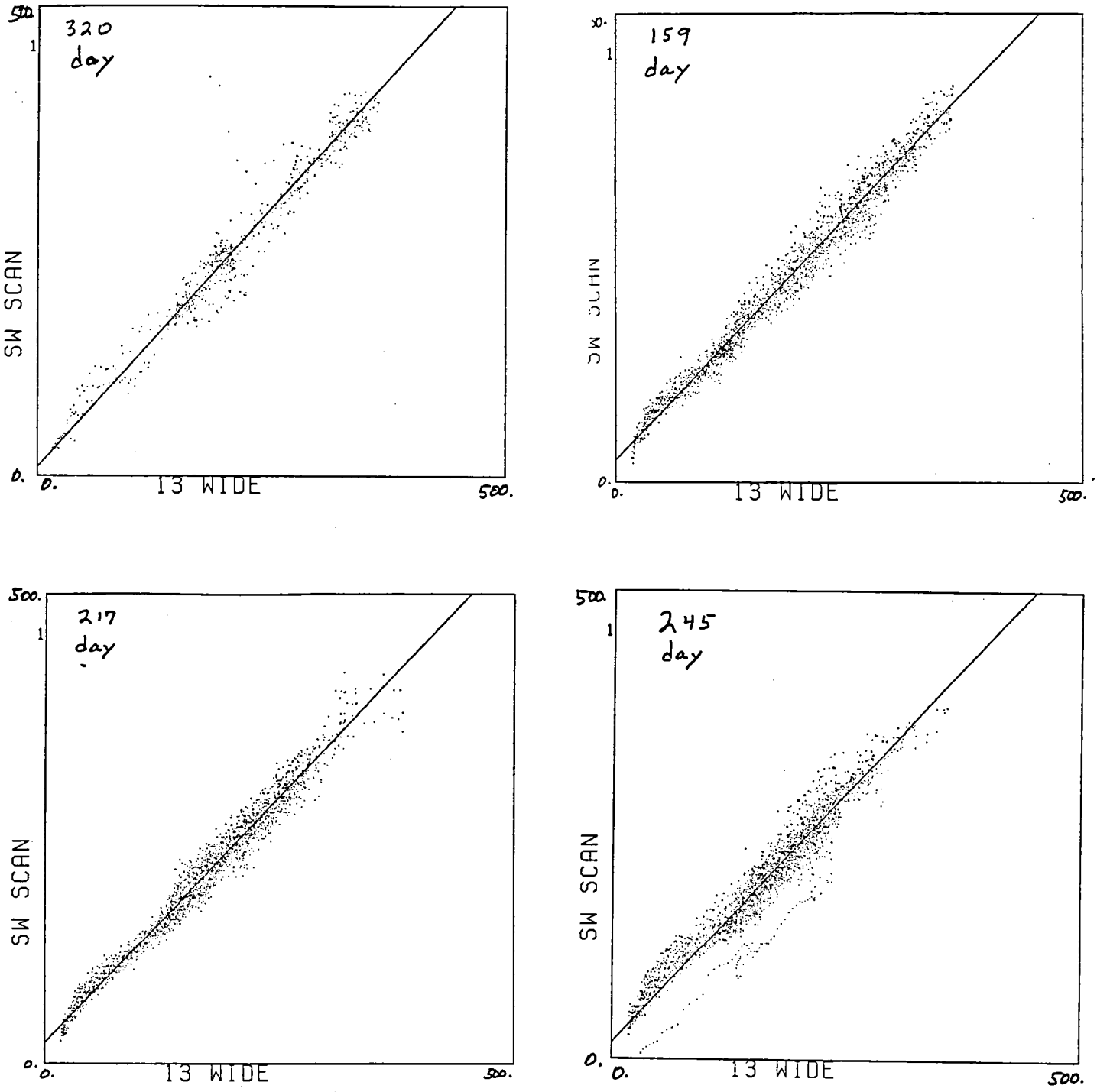

Figure 6 Scatter plots of 12-13 vs LWSC during day.

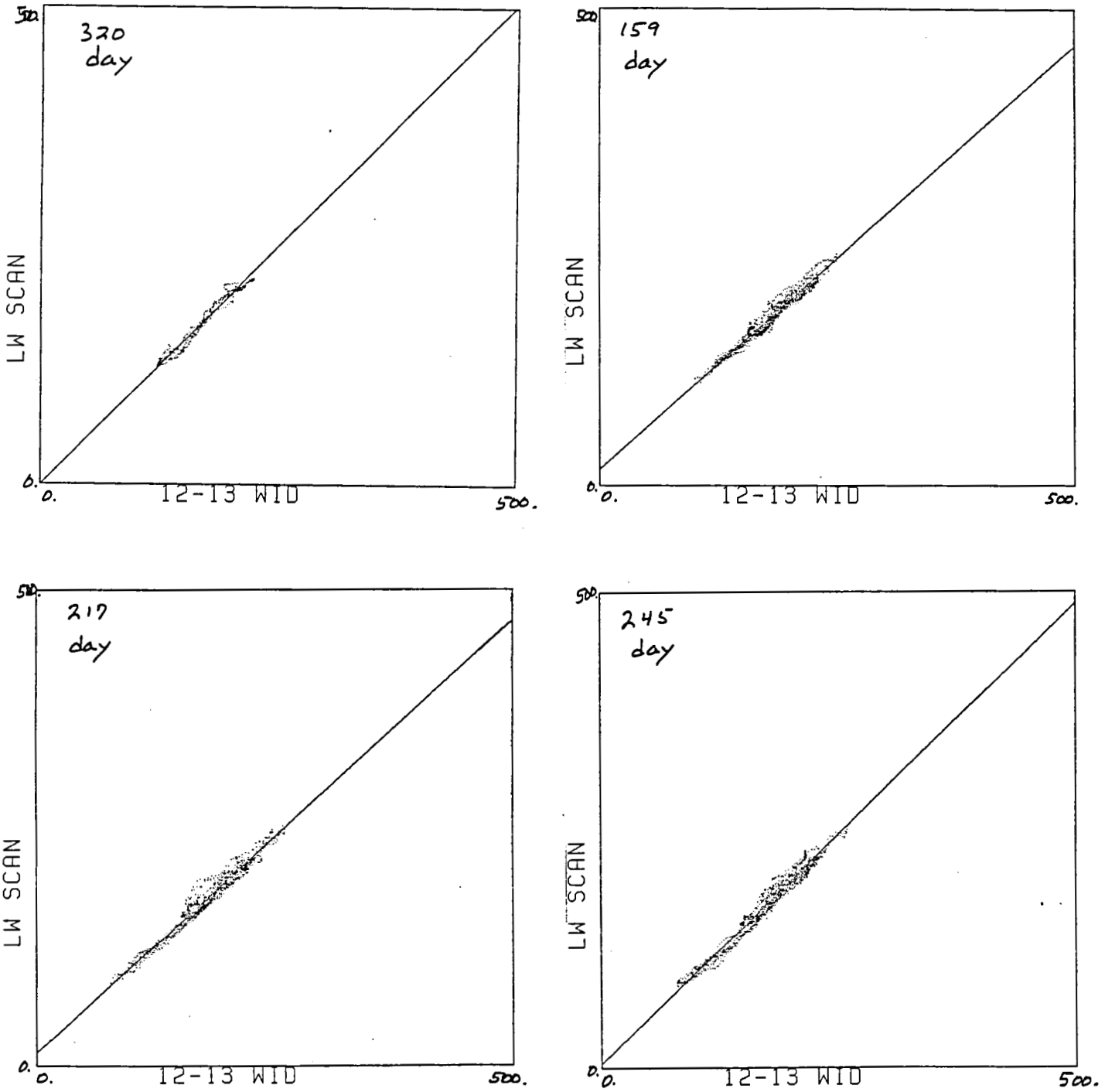

Figure 7 Scatter plots of 12-SWSC vs LWSC during day.

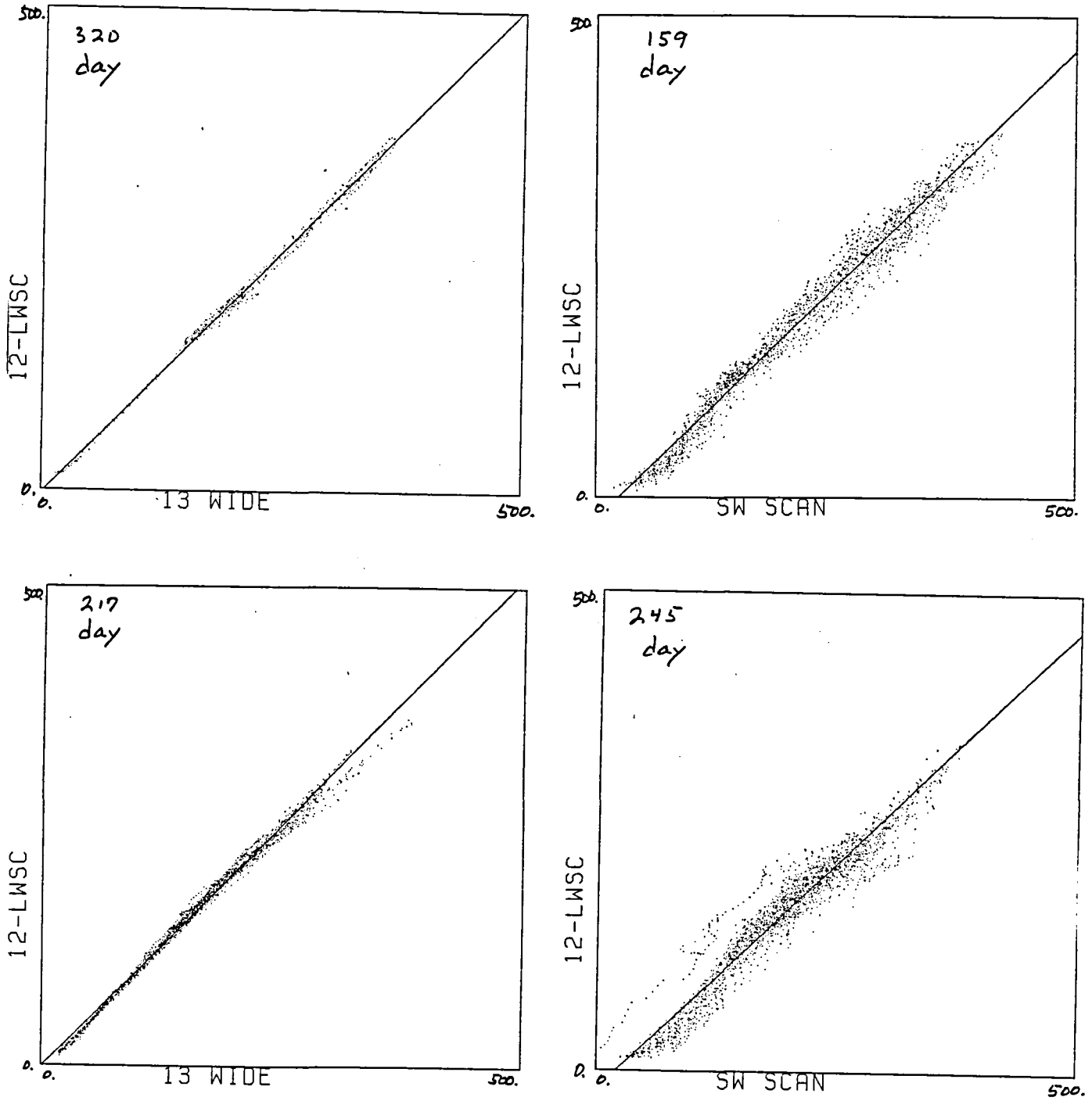

Figure 8 Composite differences: 13 - f(SWSC)

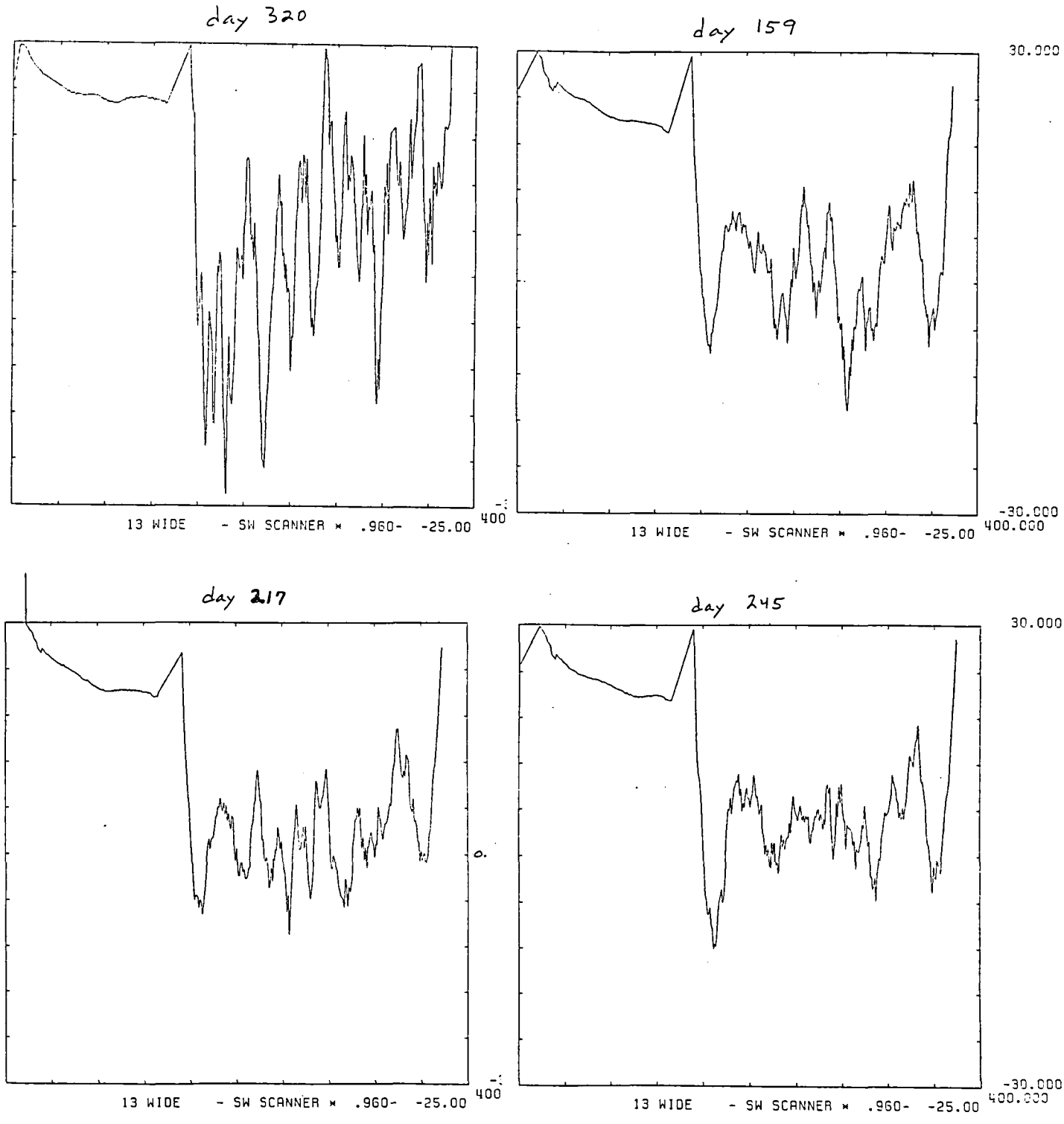

Figure 9 Composite differences: 13 - f(12-LWSC)

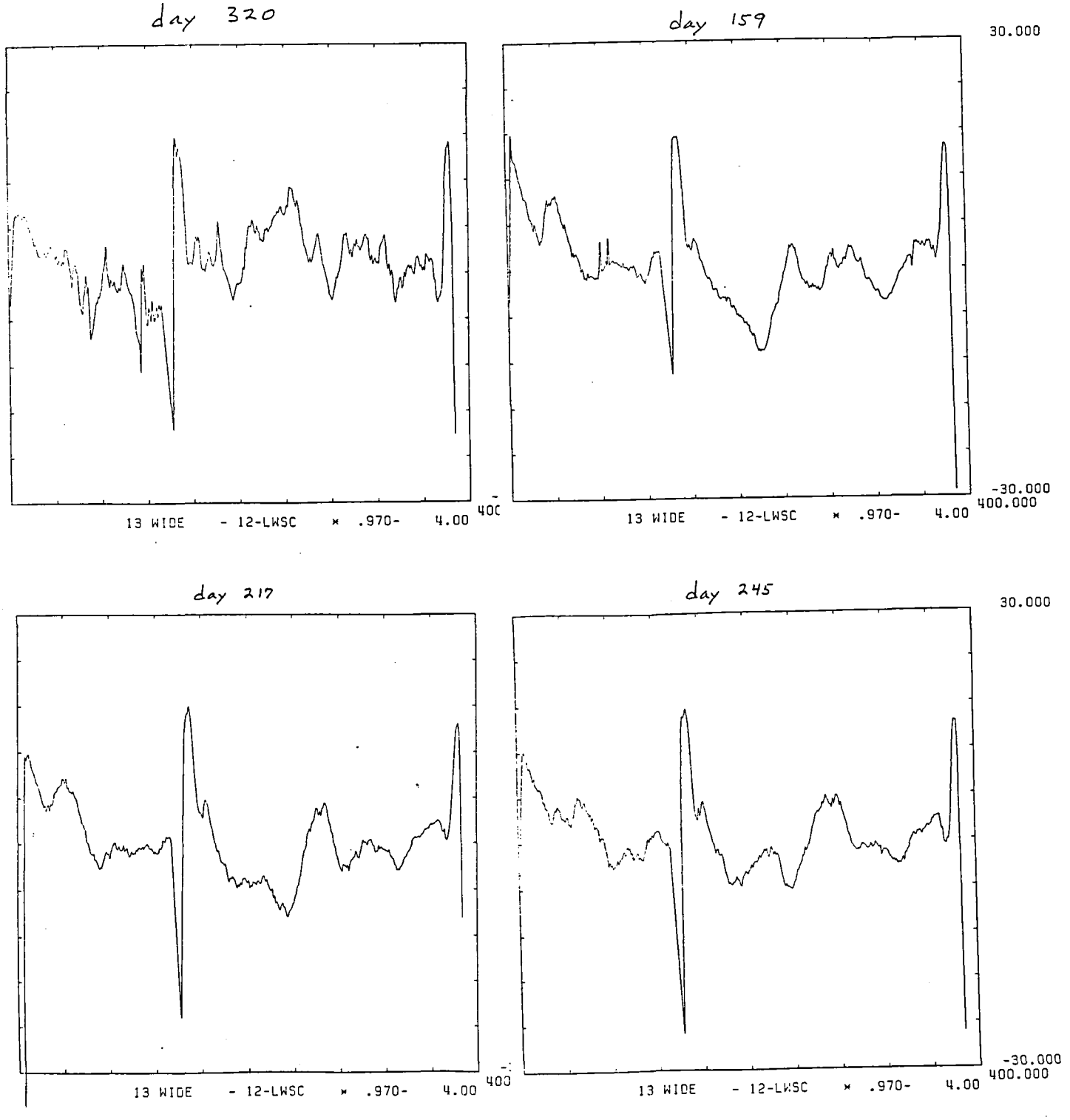

Figure 10 Composite temperature variations of shutters.

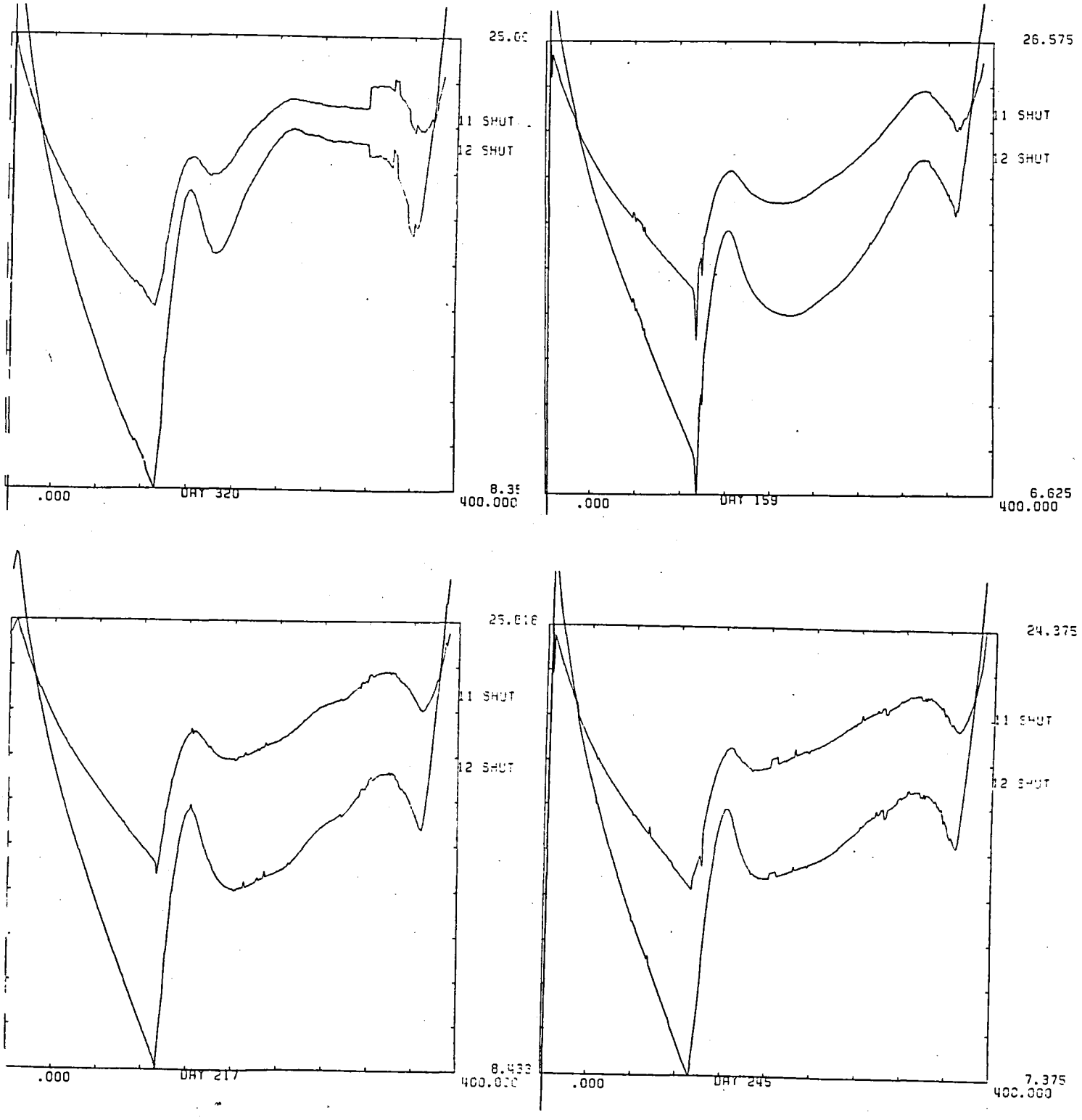

Figure 11 Composite temperature variations of various temperatures.

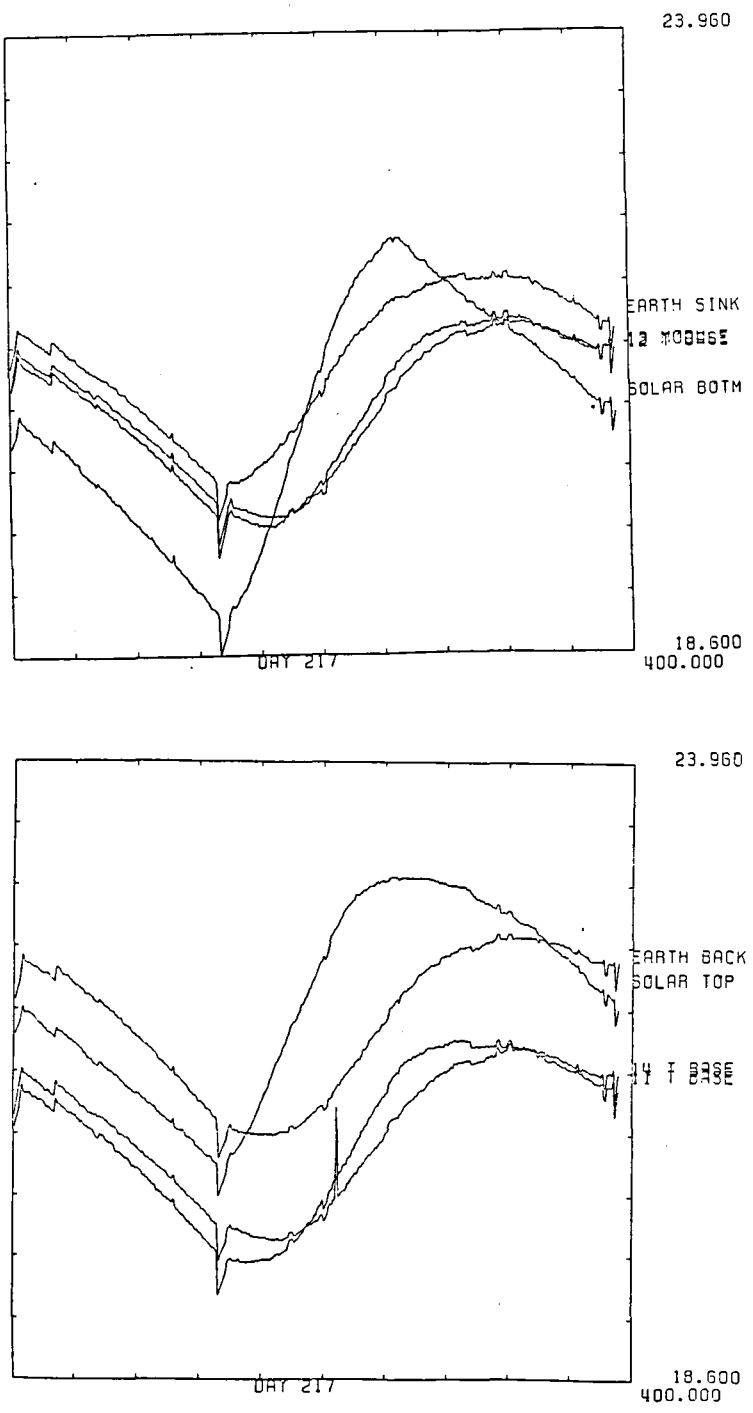

Table 1 TOTAL LEAST SQUARES FITS

b in W/m^2

Individaul Orbits		Composite		Date
LWSC= a (12) +b		Night		
a	b	a	b	
.946 (.027)	12.57 (.95)	.935 (.27)	14.54 (1.4)	320
.952 (.011)	14.82 (.16)	.975 (.023)	11.00 (1.1)	159
.939 (.011)	16.04 (.27)	.963 (.028)	11.74 (1.3)	217
.955 (.011)	13.22 (.15)	.945 (.030)	14.87 (1.5)	245
(12-LWSC = a (SWSC) + b		day		
a	b	a	b	
.922 (.021)	-12.77 (.65)	.941 (.023)	-17.27 (1.1)	320
.979 (.006)	-24.39 (.09)	.989 (.014)	-26.50 (0.6)	159
.974 (.008)	-22.71 (.09)	.999 (.014)	-27.77 (0.7)	217
.961 (.011)	-19.70 (.12)	1.004 (.017)	-34.29 (0.7)	245
SWSC = a (13) + b		day		
a	b	a	b	
1.100 (.022)	10.06 (.62)	1.082 (.024)	13.80 (1.0)	320
1.048 (.006)	23.57 (.08)	1.044 (.011)	24.26 (0.5)	159
1.052 (.007)	22.00 (.09)	1.042 (.012)	23.71 (0.6)	217
1.070 (.011)	17.54 (.11)	1.006 (.013)	28.05 (0.5)	245
(12 - LWSC) = a 13 + b		day		
a	b	a	b	
1.012 (.012)	-8.46 (.45)	1.018 (.05)	-4.26 (.22)	320
1.026 (.003)	-1.28 (.03)	1.032 (.006)	-2.51 (.24)	159
1.024 (.003)	-1.26 (.04)	1.041 (.008)	-4.08 (.29)	217
1.027 (.004)	-2.69 (.04)	1.042 (.011)	-5.18 (.28)	245
(LWSC = a (12-13) + b		day		
a	b	a	b	
1.007 (.016)	-0.65 (.32)	1.006 (.18)	-0.34 (.60)	320
.888 (.008)	16.85 (.10)	.889 (.03)	16.82 (.77)	159
.907 (.008)	14.05 (.08)	.921 (.02)	11.52 (.75)	217
.967 (.007)	4.08 (.07)	.973 (.02)	3.05 (.57)	245

The numbers in parenthesis are one sigma errors. There are many more points in the orbital data than in the composite so the fit errors are smaller.

APPENDIX II

FURTHER ANALYSIS OF DATA PRESENTED IN G.G. CAMPBELL AND T.H. VONDER HAAR REPORT - THE SHUTTER TEMPERATURE CONNECTION

The purpose of the Campbell/Vonder Haar study (see Appendix I) was to improve our understanding of the offset of the ERB WFOV channels, and the short wave WFOV Channel 13 in particular, during the day as a result of shortwave solar and/or earth flux heating. The tools were the scanner data integrated over equivalent fields of view, various temperatures and temperature gradients, and ground truth suggestions. One key assumption was that the long wave scanner data could be depended on due to it being a chopped radiometer and also because it has in-flight calibration provisions. It was hoped that Channel 12 data was well enough understood that it could be of use in analyzing Channel 13 data. These items are re-examined as the data in the report is analyzed and discussed.

Some general observations are in order before detailed analysis is considered. All of the wide field of view sensors (WFOV) should be suspected of having offsets. Further, these offsets may be different day to night and at the next level not constant during either day or night. On top of that, the differences day to night are not constant with the seasons or time of year.

One of the objectives of this effort has been to establish limits and/or definitions of these variations. Until fairly recently the offset problem was primarily associated with Channel 13. In actuality there is no basis for assuming that

the total channels, i.e., 11 and 12, have no offset. In fact there is a body of data which demands a different than zero offset assumption. Inter-comparison of 11 and 12 over a two-year period compiled by Fromm of RDS shows that, not only is there an offset difference between the two, but further the difference changes day to night. (See Figure 1.) To assume that Channel 12 has no offset and that 11, with its black painted baffles, in fact exhibits the offsets, at this point is risky.

Based on intercomparisons between Channel 12 and the integrated LW scanner (Table 1) at night, an average offset of -12.5 W/M^2 is indicated. The source of this offset may be: unaccounted for space loading, conversion from filtered to unfiltered radiance in the LW scanner data, or the temperature gradient in the earth flux assembly block or modules, or some combination of the above. one can argue that if it is due to anything but thermal gradients there should be no seasonal or varying com ponent. If it is thermally induced, then one can expect variations in offset due to the various heating inputs on an orbital or seasonal scale. One can further argue that if it is all thermally induced then its magnitude is about half of the Channel 13 effect (based on the nightime intercomparison) and thus its day to night differences might have half the magnitude of Channel 13.

The plan is to test various assumptions as to what Channel 12 is doing offset-wise and see what fits. Below we start out by assuming that, if Channel 12 has an offset, we assume it to be constant and get at least a first order look at what Channel 13 might be doing since its day to night offset is strongly suspect.

It turns out to be very instructive to study Channel 13 behavior by comparing it to (Channel 12-lw scanner). Figure 9 of Appendix (1) the attached report presents this as a difference vs. time for the 4 days analyzed. we need to keep in mind that the Channel 13 processing applicable to this data involves forcing Channel 13 to zero at midnight and applying a delayed 4% long wave scene correction. The raw offset before correction runs in the $22W/M^2$ to $25W/M^2$ range at night. A scanner plot of the same data is shown in Figure 7 of Appendix I for days 30 and 217. We concentrate on the difference vs. time plots. The night portion of the data is the left 1/3 of the plot. Shown in dashed lines are smoothed versions of this data revealing the well known Channel 13 decay after sunset of about 10 W/M^2. This says that most likely Channel 12 and the scanner do not exhibit a decay after the sun blip like 13, giving us the hope that transient effects on Channel 12 during the day may not be significant.

For day 320 the Channel 13 offset during the daytime period are on average about 3 to 4 W/M^2 less negative than at satelite midnight. this says, for example, that during southern hemisphere summer we are overestimating the short wave flux by that amount; again if one assumes that Channel 12's offset is constant.

The other 3 days exhibit varying amounts of offset during the daytime more negative than at satellite midnight. Day 159 goes more negative by about 6 W/M^2 over the southern latitudes. This means that without a more sophisticated offset correction technique we are underestimating short wave flux over southern latitudes by 6 W/M^2. Note, this is winter in the southern hemisphere and the earth flux assembly has much opportunity to lose heat near the South Pole. As we progress away from this

winter extreme through days 217 and 245, it is seen that this effect decreases. By day 245 the South Pacific underestimation would be only about 3 W/M^2 and the average over the day nearly zero. This suggests as we approach Southern Hemisphere summer and an illuminated antarctica that the earth flux assembly doesn't lose as much heat (i.e., reduced heat flux and thermal gradients) reducing the offset. We note that the offset variations we are talking about are in addition to the long wave dome heating corrections already being made.

We asked ourselves the question, "Is there any other manifestation of changes in this heat flow?" Careful examination of temperature data from the modules and earth flux assembly revealed no direct clues. However, one obtuse fact stuck out. The earth flux assembly temperature gave evidence of a rapid trend reversal when the satellite entered its day. Why? One could expect it to lag the actual modules due to their more direct exposure to the scene. Specifically the earth or scene side of the berylium block responds much earlier than the inside of the block which also serves to prove that the heating does not come from the instrument side of the earth block. See Figure 1 of this Appendix.

Examination of the physical arrangement suggested that the shutter system for Channel 12 might somehow be involved. It was noted that the super-insulation covering the earth flux assembly has a break or void around the shutter motors allowing for rather direct thermal coupling with surfaces heated by the sun. As a consequence, the shutter temperatures were looked at carefully. Figure 10 of Appendix I shows Channel 11 and Channel 12 shutter temperatures. The temperatures of the FOV limiting shutter for Channel 12 was not being monitored at this time. We note that the Channel 12 shutter, which is open, swings much

more widely in temperature than the Channel 11, one which is more closely coupled to the Channel 11 module since it is closed during the days in question. Effort was made during the design to decouple the shutters from the earth flux assembly heat sink by use of a vespel mounting block (vespel is a dimensionally stable low thermally conductive material). A wide swing in temperature is therefore not surprising. A loose thermal coupling fortunately served to accentuate differences in heating due to the sun and scene at different seasons. Note the considerably different signatures between day 320 and day 159 representing roughly winter and summer extremes.

It turns out that the pattern of Channel 13 - (12 LW scan) differences bears a remarkable resemblance to the Channel 12 shutter temperature. The dashed line represents the attempt at an overlay. What appears to come out is that a high correlation exists for about the first half of the day. Clearly, the shutter, which has a finish design, with a short wave absorptivity of 0.3, and long wave emissivity of 0.9 is strongly influenced by the sun as well as Antarctica. For our purposes, it is acting like a front surface radiometer which seems to predict to a large extent the offset variations of Channel 13 as the radiation environment changes the heat flows and offsets.

The correlation decreases as the day goes on and can be qualitatively explained as the whole earth flux assembly finally warming up and stabilizing the gradient through the sensors. The earth flux assembly temperature profile for day 217 is sketched in. In general, the data shows that the Channel 13 offset for the second half of the day is near the midnight value which presumably is forced to zero.

We now explore what happens if we allow Channel 12's offset to vary from night to day. If its variations are small compared to 13, then the numbers put forth in the previous discussion are probably good. If Channel 12 has similar variations to 13 but half the amplitude, then the real variations in channel 13 offset would be twice those indicated. An even worse possibility exists; that of Channel 12's offsets operating in opposition to those of Channel 13. This possibility must at least be considered although it is not likely that opposite behavior would operate over the same time scale.

There are at least three pieces of evidence that indicate Channels 12 and 13 do not track on a transient basis. First, as has already been mentioned, the transient exhibited by Channel 13 after sunset is not evident. Second, the 3-day signature in irradience levels so evident in Channel 13 data is not evident in Channel 12 data per studies by RDS (Ardunay). Most of the 3-day signature effect is explained by the 3-day on and 1-day off ERB duty cycle. Finally, during the SW heating tests performed by J. Swedberg it was clearly demonstrated that when the domes were removed from Channel 13, its transient behavior changed dramatically. In fact, its response in that state compared well with a Channel 12 module. We draw a tentative conclusion that the day to night variations of Channel 12's offset are insignificant.

An attempt to remove Channel 12 from the loop by comparing the integrated short wave scanner with Channel 13 yielded somewhat inconclusive results. The study did reveal that the short wave scan channels exhibit about a 25 W/M^2 positive offset. This offset exists relative to Channel 13 after Channel 13 has been midnight offset and LW scene corrected. The channel 13 errors over southern latitudes already mentioned might change this a

little but not much. The effect of this offset has been erroneously interpreted as approximately a 10% increase in sensitivity of the SW scan channels from pre-launch. While there is no known mechanism for a change in short wave scan channel sensitivity (given that the long wave channels which use the same kind of detectors are rock solid) there is an offset producing mechanism, that of scattered light. While it remains to be proven, it is evident that the effect of even a small out-of-field response would create an offset effect when much of the out of field scene is bright earth.

In any case, over the data set studied, there was too much structure remaining in the integrated scanner data to draw more then guarded conclusions. There is much more structure in the short wave scene than in the long wave scene so that identical integration techniques yield more noisy results in the short wave case. The only safe observation that can be made from the time plots of the difference is that indeed there is an offset of about +25 W/M^2 with an uncertainty of + 5 W/M^2. A much larger body of SW scan data needs to be considered before more definite conclusions can be reached.

The impact on angular models is the obvious area of possible concern by not accounting for the offset effect. Low light scene levels will be overestimated if the adjustment to SW scanner sensitivity is made.

Conclusions (Preliminary)

What is claimed as a result of the body of work represented by the Campbell/Vonder Haar Study effort is that a mechanism for variations in Channel 13 offset due to the scene has been identified which operates in addition to long wave dome heating. At this point, the seasonal effect over southern latitudes is the most pronounced. Orbit to orbit variations over the same latitudes are expected to be smaller due to the large ocean areas in the southern hemisphere. The data set used to date is too limited to make other than good estimates as to the range of the offset variations. Just being able to say that we are talking about a range of error for part of the daytime orbit in the $5W/M^2$ range is somewhat comforting. A larger data base will clearly not hurt. What this involves is using scan data taken in routines 3 and 4 employed on alternate days. A new integration routine is required.

CHANNEL TEMP PROFILE AVERAGING
APPROX 100 ORBITS

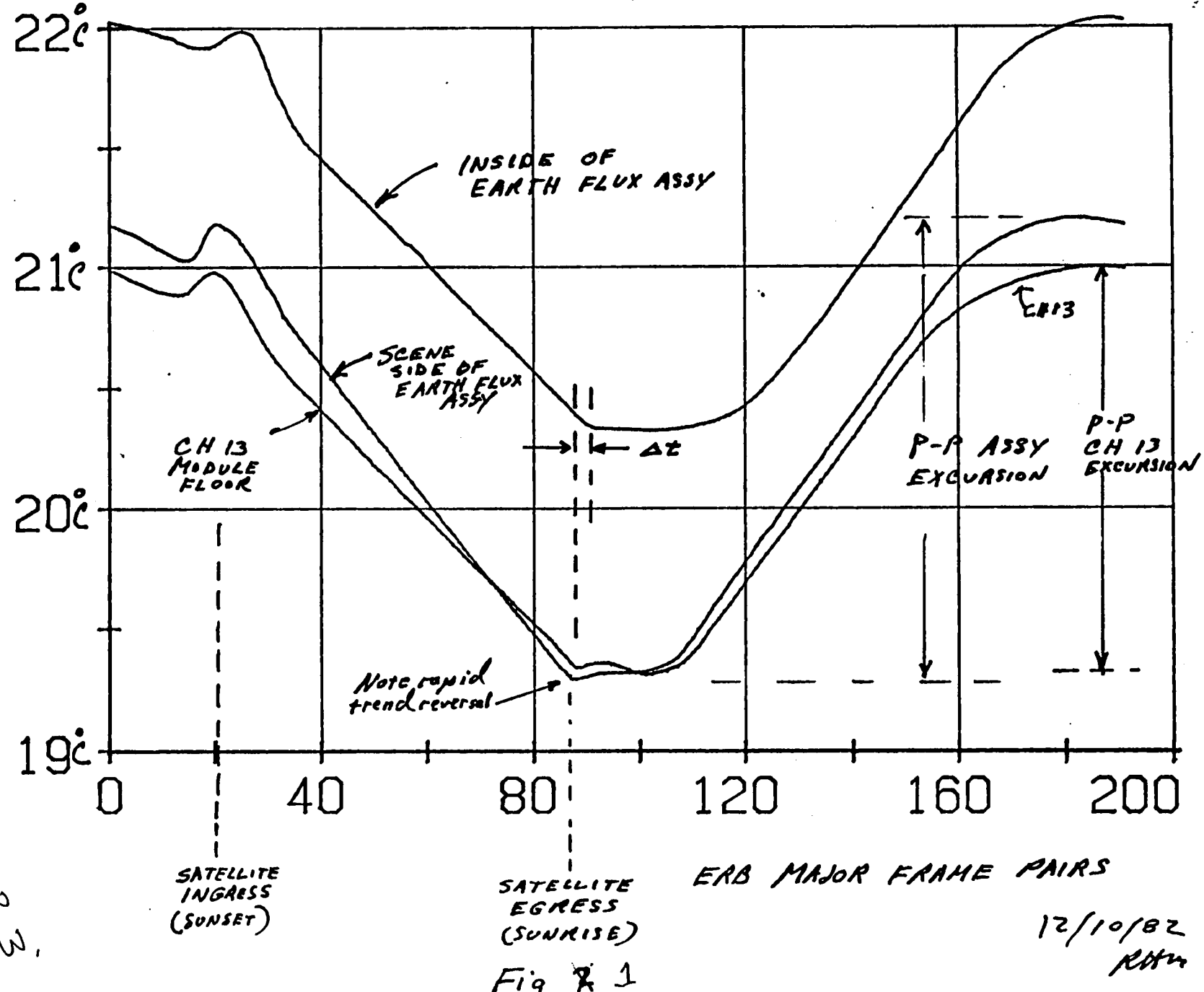

Remember fig 1, 2, 3.

12/10/82
RHH

Fig 1

Figure 9 Composite differences: 13 - f(12-LWSC)

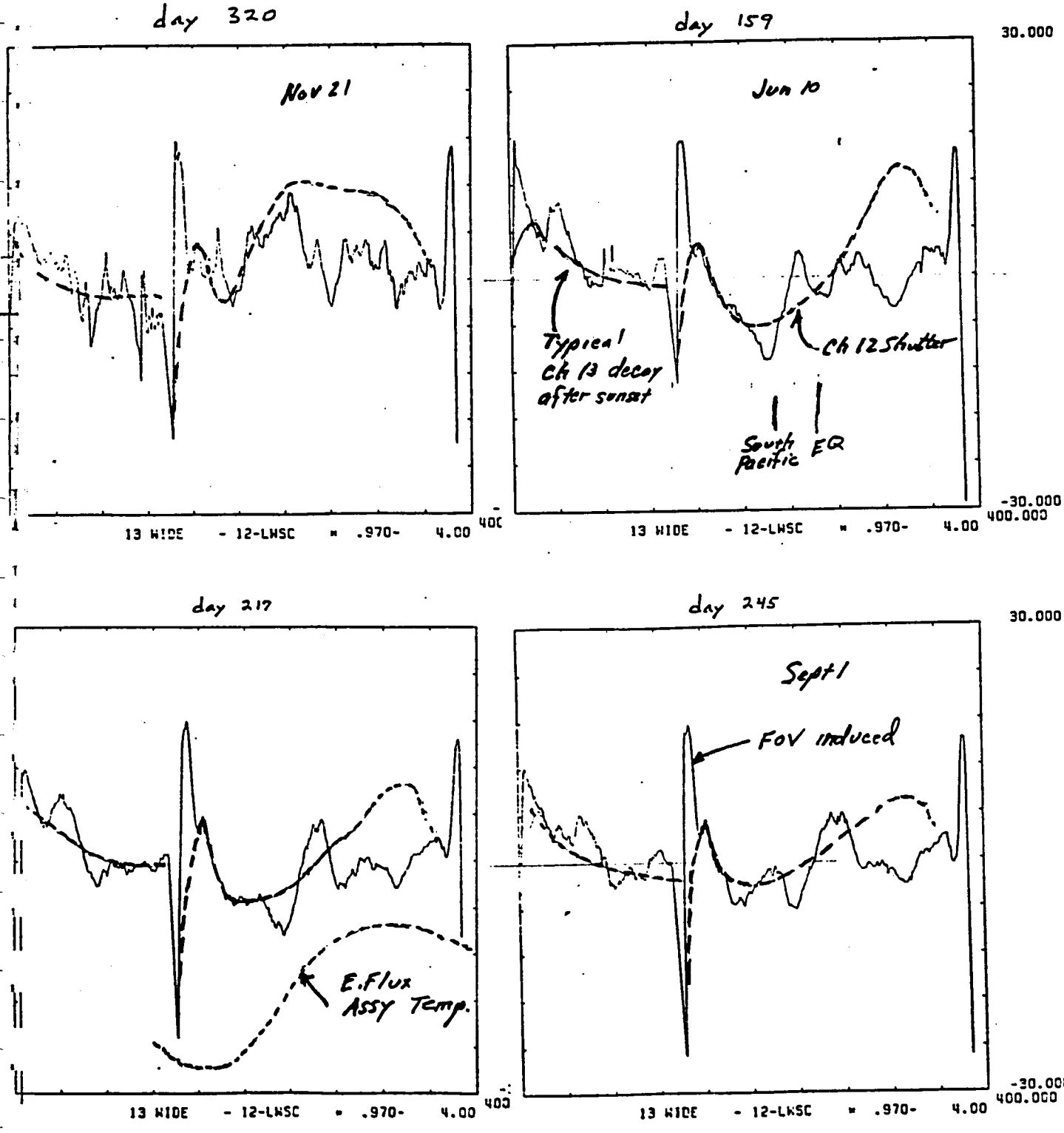

Δ ≈ 3.0/11.2

Sun → Sept

Figure 10 Composite temperature variations of shutters.

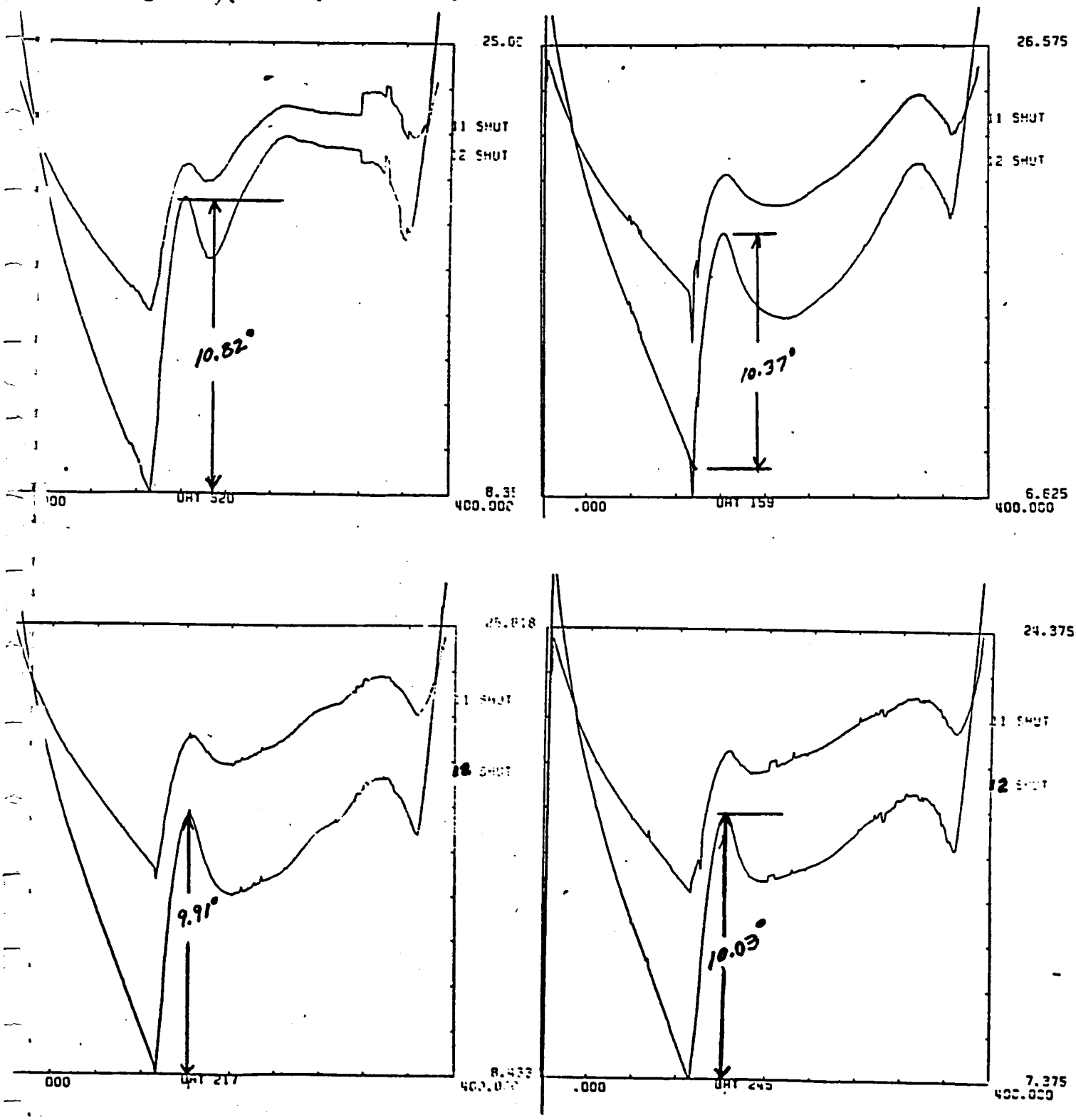

APPENDIX III

SUMMARY OF ACTIVITIES AND FINDINGS
RELATIVE TO NIMBUS ERB DATA
As Presented at the ERB NET Meeting, Feb. 14, 1984

BACKGROUND

At present it is felt that the physical explanation for varying offsets in the WFOV channels is a variation in the heat flow out of the earth flux assembly. These variations in heat flow are modulations on a dominant outflow of heat as evidenced by the fact that the extremities of the earth flux assembly are always the coldest part of the ERB observatory. The sensors were designed to minimize responses to thermal transients injected into the mounting points of the thermopiles by virtue of symmetrical front and back receivers. Since the surrounding aluminum body does not have infinite conductivity, a net heat flow out of or through the front of the module must in principle create a front to back receiver temperature difference. Therefore, even if the sensors are balanced in respect to transients, steady gradient induced offsets are still possible. It takes only a 10 milledegree back to front receiver temperature difference to produce a 20 W/M^2 equivalent offset in Ch 13.

It has been demonstrated that a great improvement in data consistency results when the effects of variations in heat flow due to the ERB operating duty cycle are removed. The simple expedient of forcing the offset of Ch 13 to zero at satellite midnight and interpolation between removes the 3 day duty cycle effect previously noted in Ch 13 data. It was recognized at the

outset of this procedure that if there was a significant modulation of heat flow through the earth flux assembly due to scene and sun heating, additional errors would probably exist. The problem of quantifying the effect had to be solved before any correction algorithm could be considered. The first suggestion that such an effect most likely existed was a seasonal variation in the difference between Ch 13 data and the"Pacific Ocean" calibration target area. Later it was shown that using the whole earth as a "reference target" a seasonal variation still exists. The conclusion was that even though not all variations could be conclusively shown to be instrumental rather than real, most of it was probably instrumental.

INVESTIGATIONS

1. The possibility of variations in the temperature gradient across the earth flux assembly block, if present, might be used for offset correction was investigated. The gradient would hopefully be function of heat flow through the earth flux assembly. It was known at the outset of the investigation that any gradient across the block, which is made of high thermally conductive berylium, would be small. No significant signature could be detected that correlated with known offset variations of Ch 13 at night for example. It was concluded that it may be possible to extract such information by averaging temperature from perhaps as many as 1000 orbits. This is computationally difficult at this stage. As it was, using daily averages of 12 or 13 orbits, no clear indications of structure were found. One fact that suggests that information is there comes from the observation that the day to night gradient across the block varies by at least 0.1°C. Refer to Fig.1. It is appropriate to point out that there is little confidence in the T

amplitude of about 1°C. The thermistor absolute calibration is not that dependable. This does not detract from the ability to detect change.

2. An empirical comparison of Ch 13 data with integrated SW scanner data was made to possibly reveal an orbital pattern of difference which could possibly relate to variations in heat flow over the orbit. The data for this comparison was compiled by Dr. Campbell of Metsat, Inc. and is reported in detail by him (see Appendix I).

   It was concluded that the data base was not sufficiently large to do effective smoothing of the spatial and time sampling involved in integrating the Mode 5 scan data. Only days in which the scanner was in Mode 5 were used. A more direct method suggested itself almost concurrently as described below.

3. Comparison of Ch 13 data with Ch 12 minus the integrated LW scanner as truth (instead of using the integrated SW scanner as above) yielded more indicative results. The form of the results is shown in Figure 2 for the four days initially studied and detail. The feature that attracted attention is that distinct orbital signature exist which vary in detail over the 4 days suggesting seasonal effects. We first observe that the nighttime pattern follows the decay characteristics after sunset just as seen from Ch 13 alone. This suggests that Ch 13 is erroneous rather then the LW scanner or Ch 12 at least at night.

   While there was some indication of a similar transient just after sunrise, the temperatures being closely monitored did not appear to yield a relationship. The temperatures here referred to were module and earth flux assembly temperatures.

4. A very strong characteristic or orbitally related structure was observed in heretofore ignored shutter temperatures and shutter to earth flux assembly temperature differences. It would appear fortunate that the shutters were thermally isolated from the rest of the assembly emphasizing any variations in the radiant environment on the front of the earth flux assembly. Simply noting the peak to peak variations in the shutter temperatures is quite a revelation (refer to Fig. 3). Over the course of the orbit the temperature of the shutter is both hotter and colder than the sensor modules. Further, it is evident that the sun impinging on the shutter around the times of the sun blip causes a rapid temperature rise. The finish of the shutter as well as the surrounding shroud or shield around the openings of the earth flux sensors is a paint designated D4D. It was selected to have a rather low absorptance in the visible; i.e., 0.3, and a high emissivity in the infrared; i.e., 0.9. This was intended to keep surfaces exposed to the sun from overheating, but for low mass items like the shutters and fiberglass shields around the earth flux assembly an absorptance of 0.3 results in rapid rise in temperature when $1370 W/M^2$ impinges on it. The suggestion is certainly that disturbances in the temperature gradients is substantial around the shutters. Since they are in close proximity to the modules, although fairly well isolated conductively, the temperature gradients in the modules appears to be altered to some extent. The question is to what extent!

Whether the shutters can only be considered indicators of what might be happening in the earth flux assembly and modules or whether the shutters act as significant sources or sinks is an unanswered question at this point in time.

The thermal paths from the shutters to the modules is quite complex and probably involves more radiative coupling than conductive coupling. It can be argued that attempts at thermally isolating the shutters were unsuccessful becasue of the radiative factor. Because of the low thermal mass of the shutters they quickly assume temperture differences where radiative coupling is established and the heat absorbed by the shutters is transmitted to the earth flux assembly anyway. At a solar incident angle near the sun blip of 60°, each shutter converts nearly a watt of short wave energy to heat, part of which will find its way to the block. Considering that the total heat into the block from the instrument electronics side is less than 10 watts, it is not surprising that sun and scene heating effects perturb any static offset. A much larger area of D4D painted fiberglass covers the sensor block except for the sensor openings themselves. On the sides of the earth flux assembly block, super insulation serves to insulate it from the covers. On the bottom or "scene" surface, however, the cover can communicate with the block directly by radiation. With an effective area on the order of 100 cm^2 a peak of nearly 5 watts is absorbed around the sun blip times. A temporary reversal of the heat flow in at least part of the assembly seems at least possible. In any case, there appears to be a strong relationship between Ch 13 offset and the shutter to module temperature difference. Fig. 4a, and 4b are plots of the above temperature difference vs. Ch 13 output at night, one for Nimbus 6 and one for Nimbus 7. A functional relationship is evident for both instruments. It may be approximated by two linear relationships, one where the shutter is colder than the modules and the other where it is warmer. It turns out that this division point is crossed each nighttime period. A preliminary check on

whether such a relationship holds in the daytime can be made from Fig. 5. Here the output of Ch 13 is plotted against orbit number during an instrument warm-up period. The Ch 13 reading is taken at the same time solar readings are taken each orbit. This is very near the minimum point in Ch 13 data after the sun blip. The shutter vs. module temperature difference is also plotted against orbit number. Again, a close relationship appears to exist. It represents a warm-up condition where Ch 13's offset at night is known to change.

Fig. 6 indicates the relationship vs. seasons that we have to work with. Days have been selected from all different seasons of the year. A large difference in the shutter temperature minus module temperature signature exist as 22a function of season. Comparing the summer and winter cases 6a and 6b first, as referenced in the northern hemisphere, we see that the shutter warms up rapidly and stays warm relative to the module all day due to the high Antarctic short wave flux. When Antarctica is dark, the shutter continues to cool very soon after the sun blip and stays colder than the modules for the entire daytime pass. At the equinox seasons it is seen there is little difference in shutter to module temperature. Further, it is seen that the midnight offset correction will result in about the right correction only for the equinox cases 6c abd 6d. The importance of a test on a residual earth flux assembly becomes obvious. An orbital type simulation was never performed so experimental confirmation of what appears to be happening in orbit should allow for more accurate algorithms.

The most direct evidence that the daytime behavior is something like the nighttime offset behavior comes from observing the Ch 13 flux minima around the sun blip. The minima following the sunrise blip is between 5 and 10W/M^2 more positive than the one preceeding the sunset sun blip. This is consistent with the temperature difference signatures in this regionas shown in Fig. 6. The nature of the signal minima can be seen in Figs. 10 and 12 of the main report while their locations on the temperature curves of Fig. 6 are denoted with an arrow. The extent to which the minimum are contaminated by actual scene variations is the only thing that clouds this argument quantitatively. It remains that the sunrise one is <u>always</u> more positive than the sunset one.

We need to be reminded that during thermal-vacuum testing and calibration activities of the flight instruments at Gulton, no significant offsets were observed. This was in large part due to the fact that there was no cold wall or plate to simulate space. A little reflection will suggest that such a cold plate would easily interfere with sensor stimulus equipment particularly in a small vacuum chamber. The offset of Ch 13 when not illuminated, for example, was always within a count or two of zero and was attributed to small electronic effects. Hindsight suggest that more careful analysis of the offset behavior of Ch 13 as the instrument mounting baseplate temperature was varied from the nominal 25° over the range of 10° to 40°C might have revealed the problem.

No simulation whatever was attempted of the short wave direct solar and reflected short wave impinging on the body of the instrument. It should be possible to set up tests

which even though they don't totally duplicate the environment are sufficiently close to indicate the existence of the effects. Figs. 6e and 6f are included to show that at the seasonal extremes there is a difference in the phase of the module heating curve due to the fact that the entire assembly heats up faster in southern hemisphere summer.

5. Channel 12 Offset Revisited

On the basis of the comparison of Ch 12 at night with the integrated LW scanner it is observed that one or the other must have an offset. Since the scanner is a chopped radiometer its offset can be argued to be zero because chopping occurs well toward the front of the optical train. Most importantly it occurs ahead of the spectral filters that might assume some temperature different from the detector due to scene or environment variations. It follows then that the most likely source of the offset is in Ch 12.

What is the source of the offset? The candidates are:

1. Thermal gradient through the earth flux assembly or module.

2. Deep space filling the FOV wings.

3. A combination of 1 and 2.

A confounding fact is that Ch 11 which has painted baffles has been shown by FOV measurements to no longer have wings beyond 121°. But Ch 11 still has an offset, albeit on the basis of comparisons with the integrated LW scanner at night different than Ch 12. Further, there is a day to

night difference in the Channel (11-12) offset on the basis of regression over the first two years of ERB operation as perpared by Fromm of RDS, Inc., see Fig. 7.

Another piece of data that must be reconciled is that in contrast to Ch 13, Ch 12 appears not to have a 3 day duty cycle signature. This suggests that variations in earth flux assembly heat flow do not produce variations in offset as appears to happen in Ch 13. This must mean either that there is not much flow out of Ch 12 or that what flow there is follows paths which do not produce offset.

The following explanation is offered:

1. Chs 11 and 12 have approximately equal offset but for entirely different reasons.

   1A. Ch 12's FOV wings account for nearly all of the offset required from the integratred LW nighttime intercomparison. Neither ERB duty cycle modulation or scene modulation is thus involved.

   1B. Ch 11 loses much more heat to the average cool earth than does Ch 12 because of the black painted baffles. Since the scene includes short wave, this flow is modulated on a day-night cycle.

2. Ch 13 loses much more heat to deep space and the scene than Ch 12 because among other factors the domes view factor of space is much higher. Further, the long wave emissivity of quartz is higher than polished aluminum.

   It would appear that the FOV wing problem of Ch 12 was traded for variable heat flow induced offsets when Ch 11's baffles were painted.

   As a consequence of this, the data reduction equations for Ch 11 and 12 should be modified to allow for the inclusion of these factors.

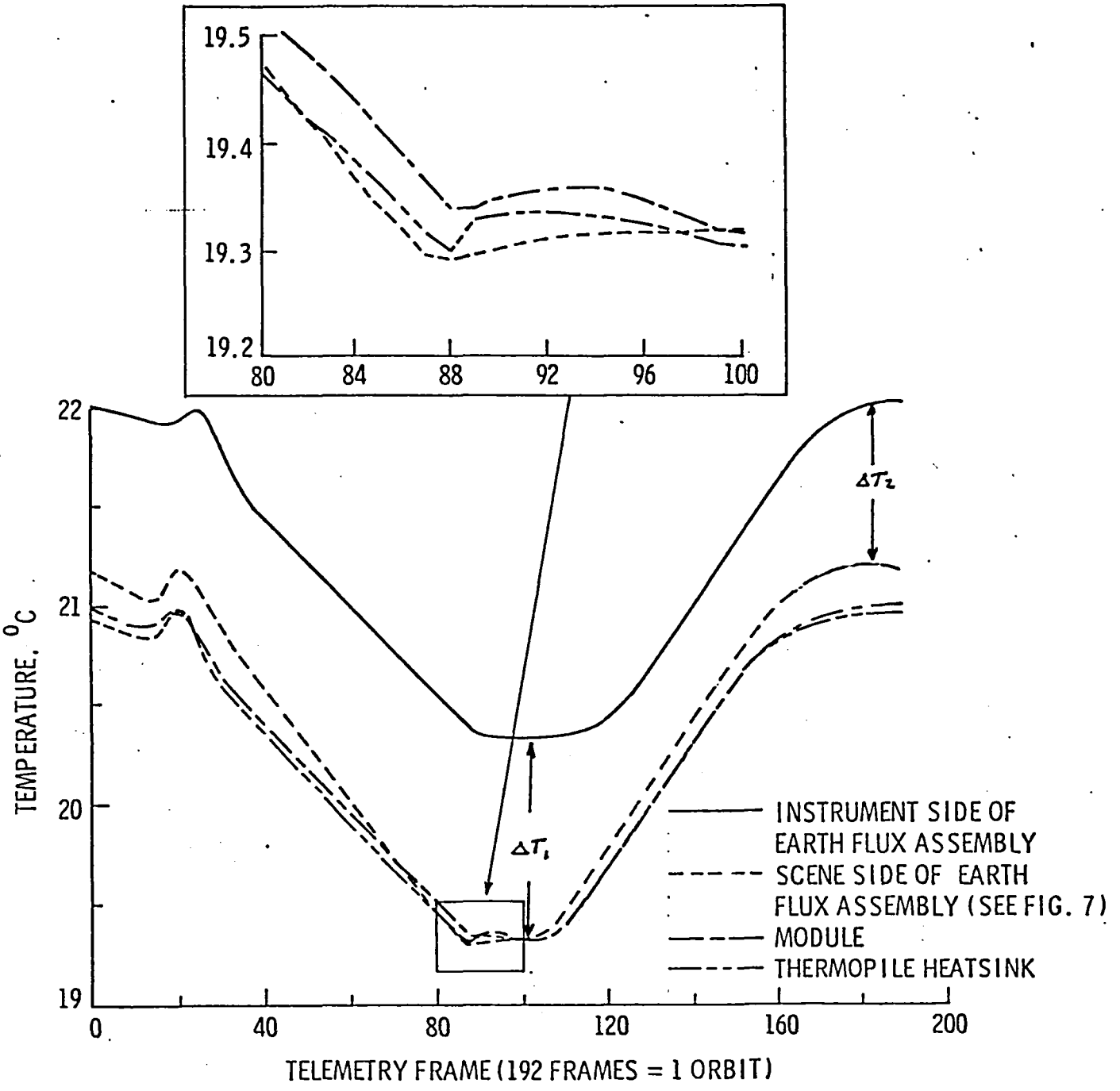

FIGURE 1 ERB CHANNEL 13 TEMPERATURE TRANSIENTS

Figure 2 Composite differences: 13 - f(12-LWSC)

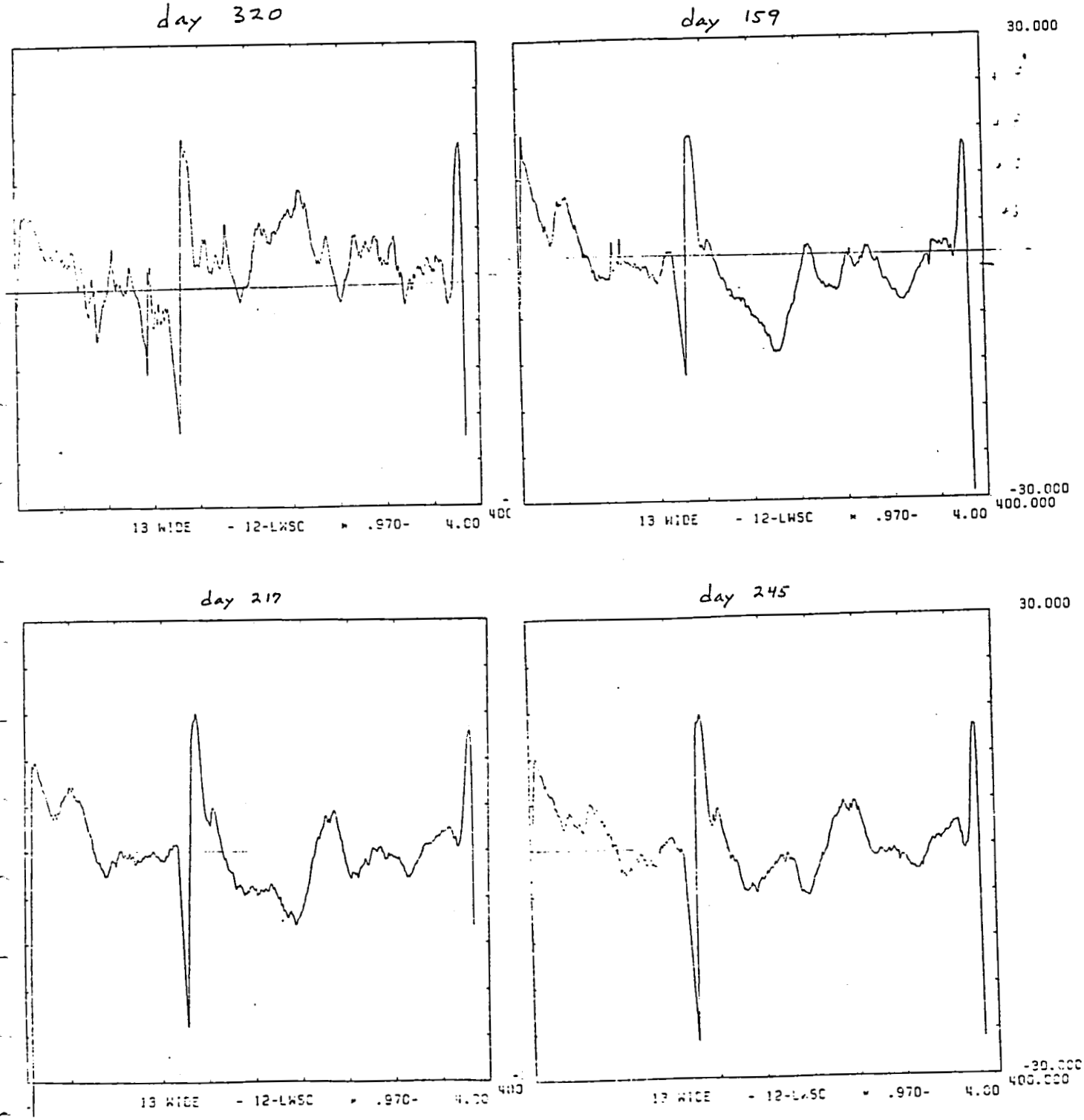

Figure 3 Composite temperature variations of shutters.

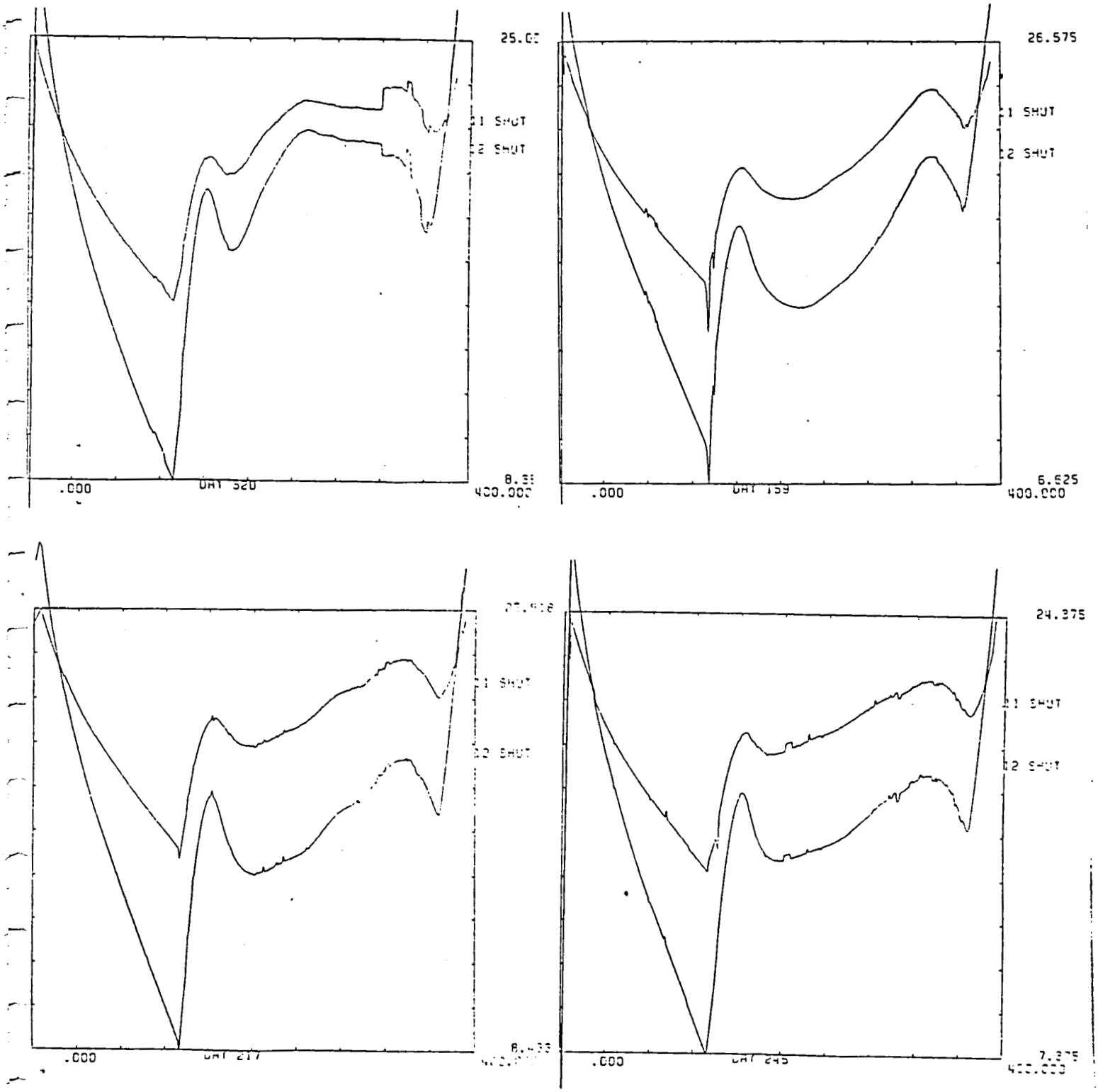

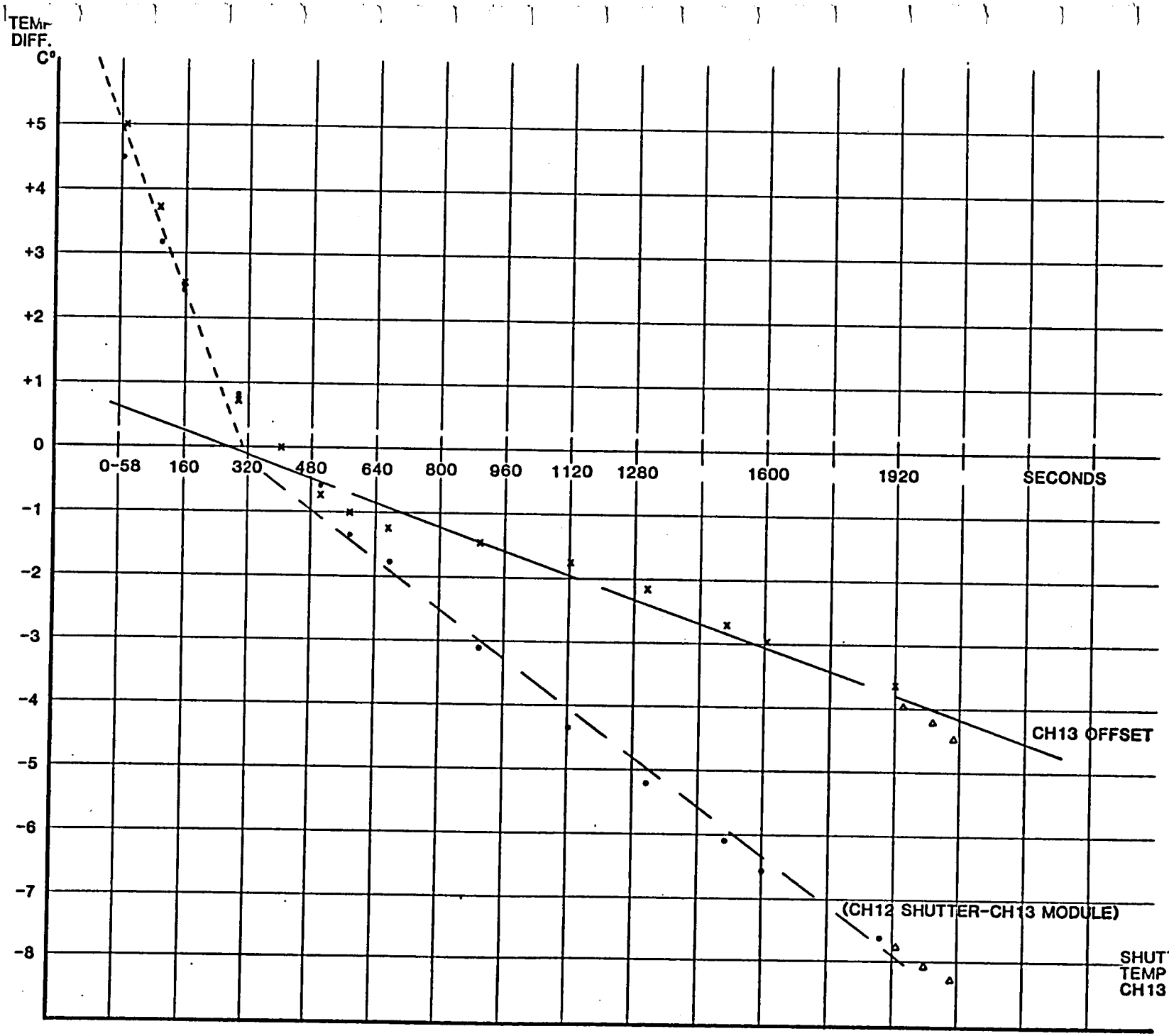

NIMBUS 7
DAY 68

SHUTTER TO MODULE
TEMP DIFFERENCES AND
CH13 OFFSETS AT NIGHT

FIGURE 4A

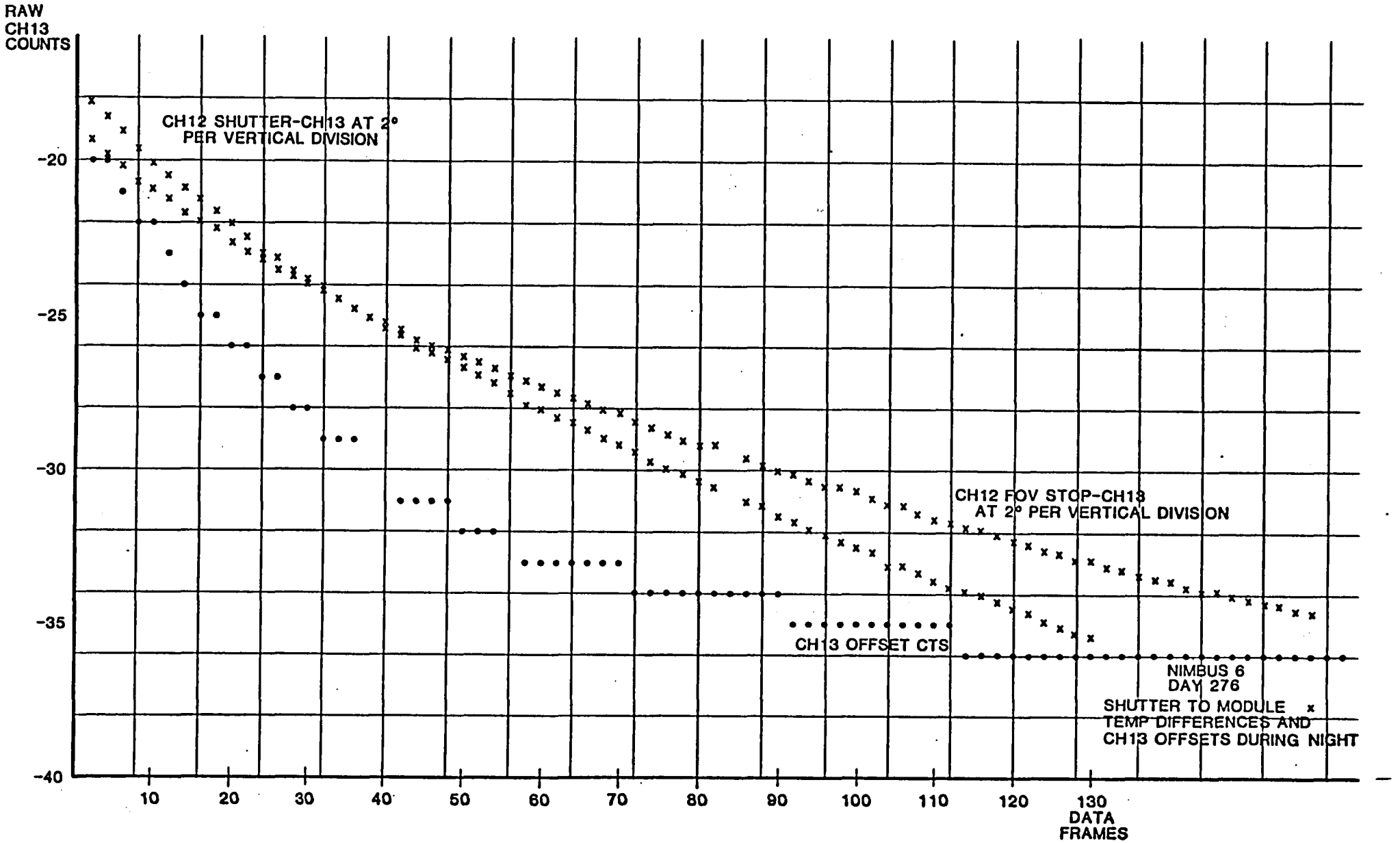
RAW
CH13
COUNTS
CH12 SHUTTER-CH13 AT 2°
PER VERTICAL DIVISION
-20
-25
-30
-35
-40
CH12 FOV STOP-CH13
AT 2° PER VERTICAL DIVISION
CH13 OFFSET CTS
NIMBUS 6
DAY 276
SHUTTER TO MODULE
TEMP DIFFERENCES AND
CH13 OFFSETS DURING NIGHT
10
20
30
40
50
60
70
80
90
100
110
120
130
DATA
FRAMES

FIGURE 4B

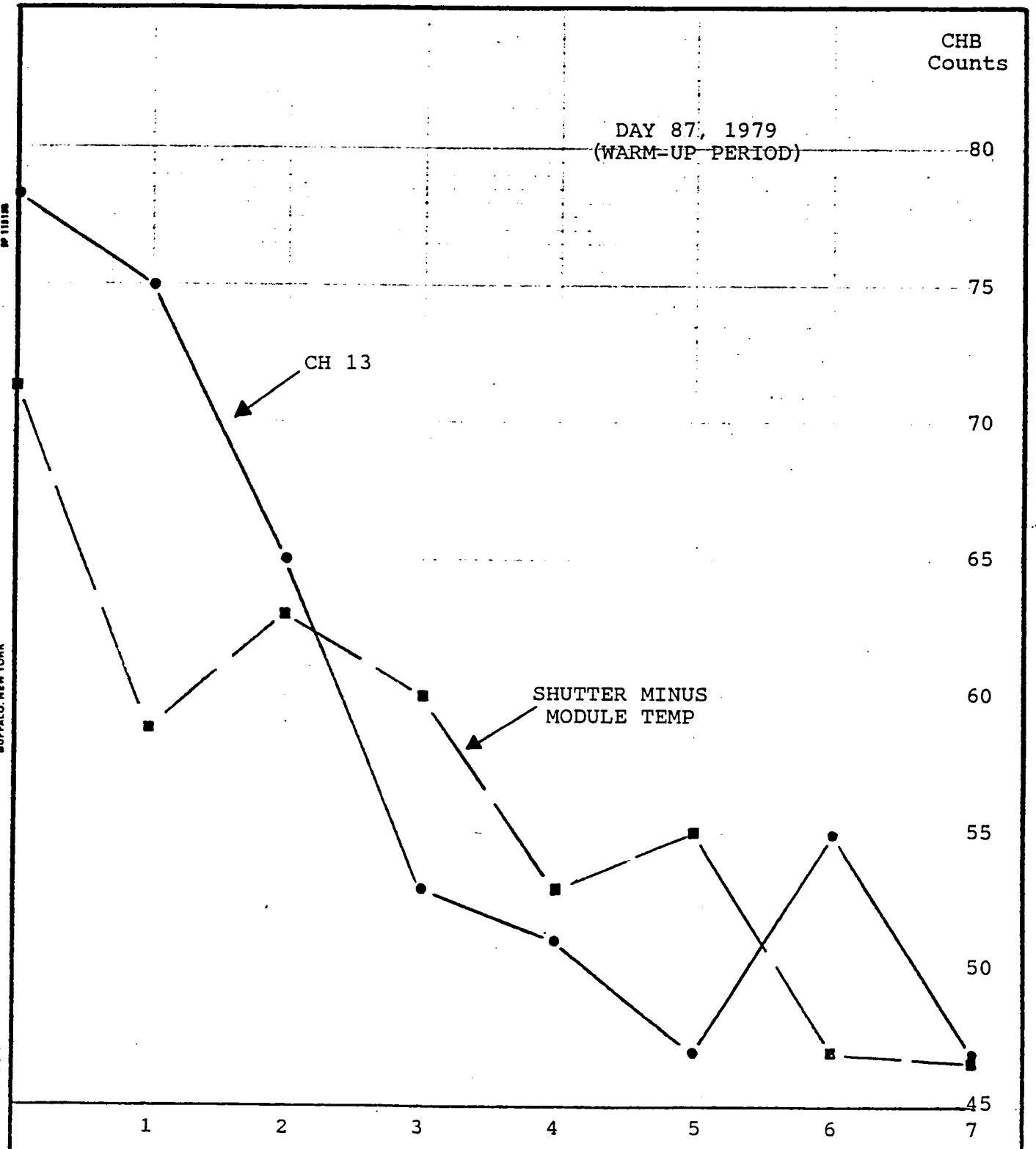

FIGURE 5

gulton DATA SYSTEMS DIVISION ALBUQUERQUE, NEW MEXICO	ISSUE	CODE IDENT NO 12574	SIZE A	DWG. SHEET

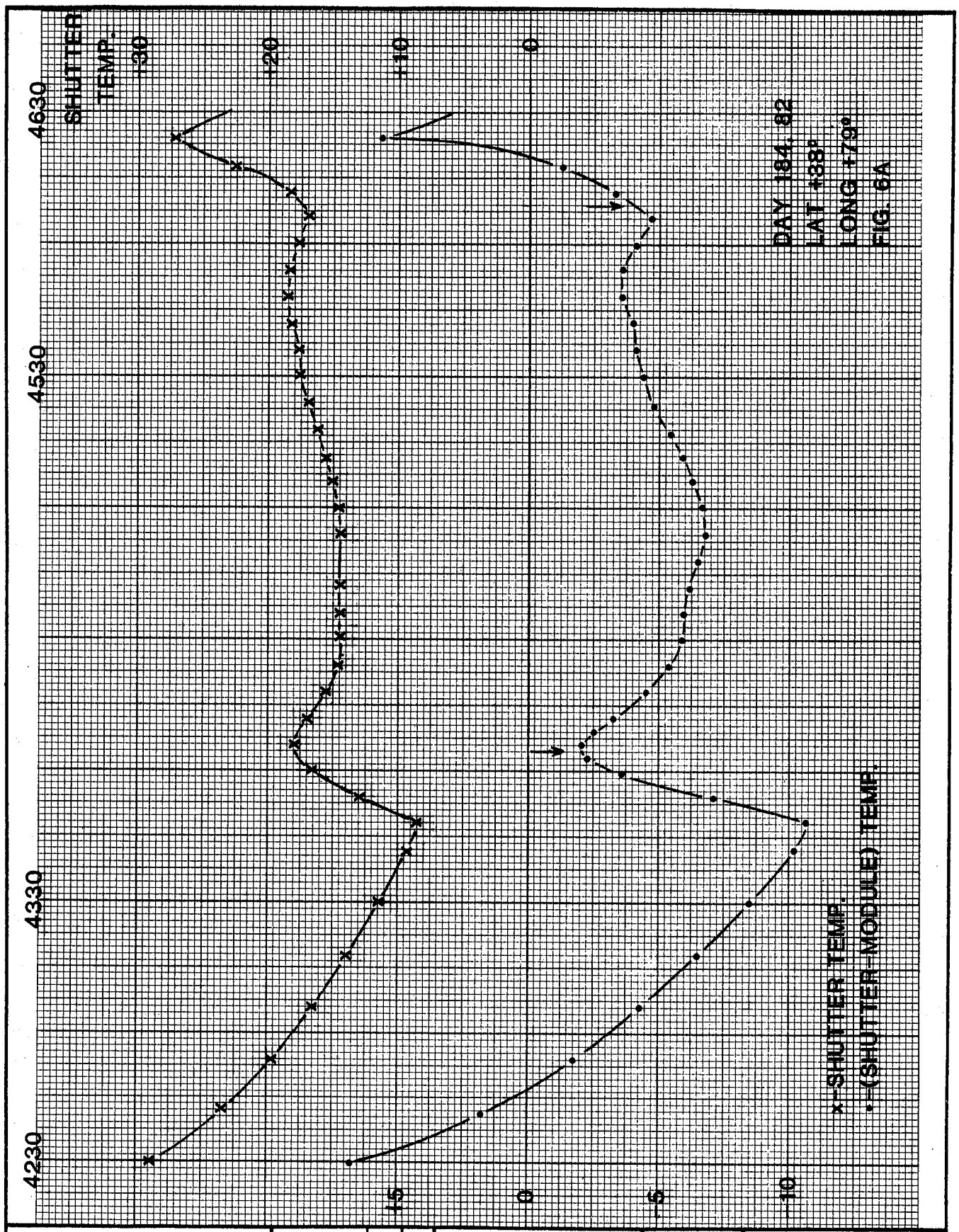

Gulton Industries Inc. DATA SYSTEMS DIVISION ALBUQUERQUE, NEW MEXICO	ISSUE	CODE IDENT. NO 12574	SIZE A	DWG. SHEET

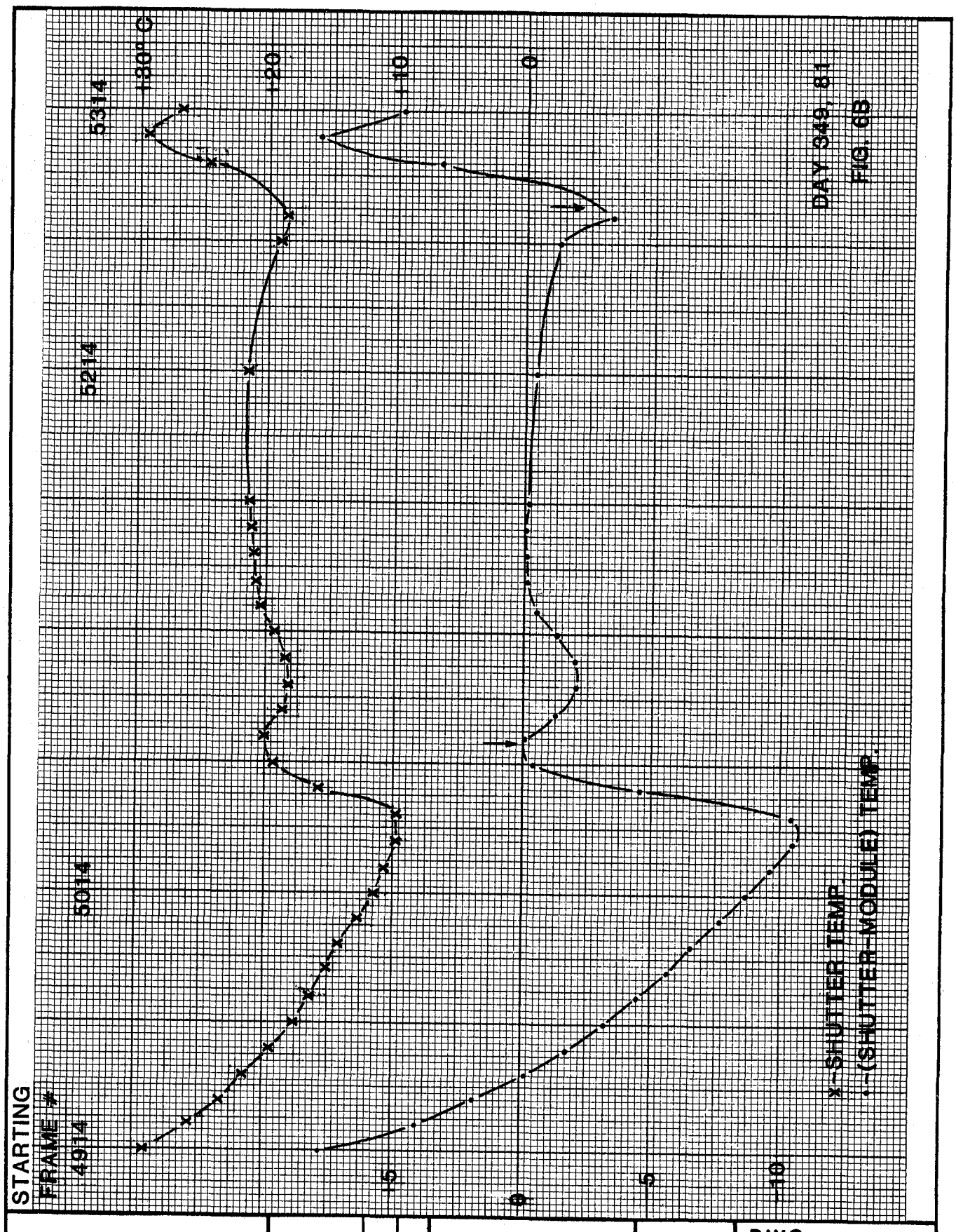

Gulton Industries Inc. DATA SYSTEMS DIVISION ALBUQUERQUE, NEW MEXICO	ISSUE	CODE IDENT. NO 12574	SIZE A	DWG. SHEET

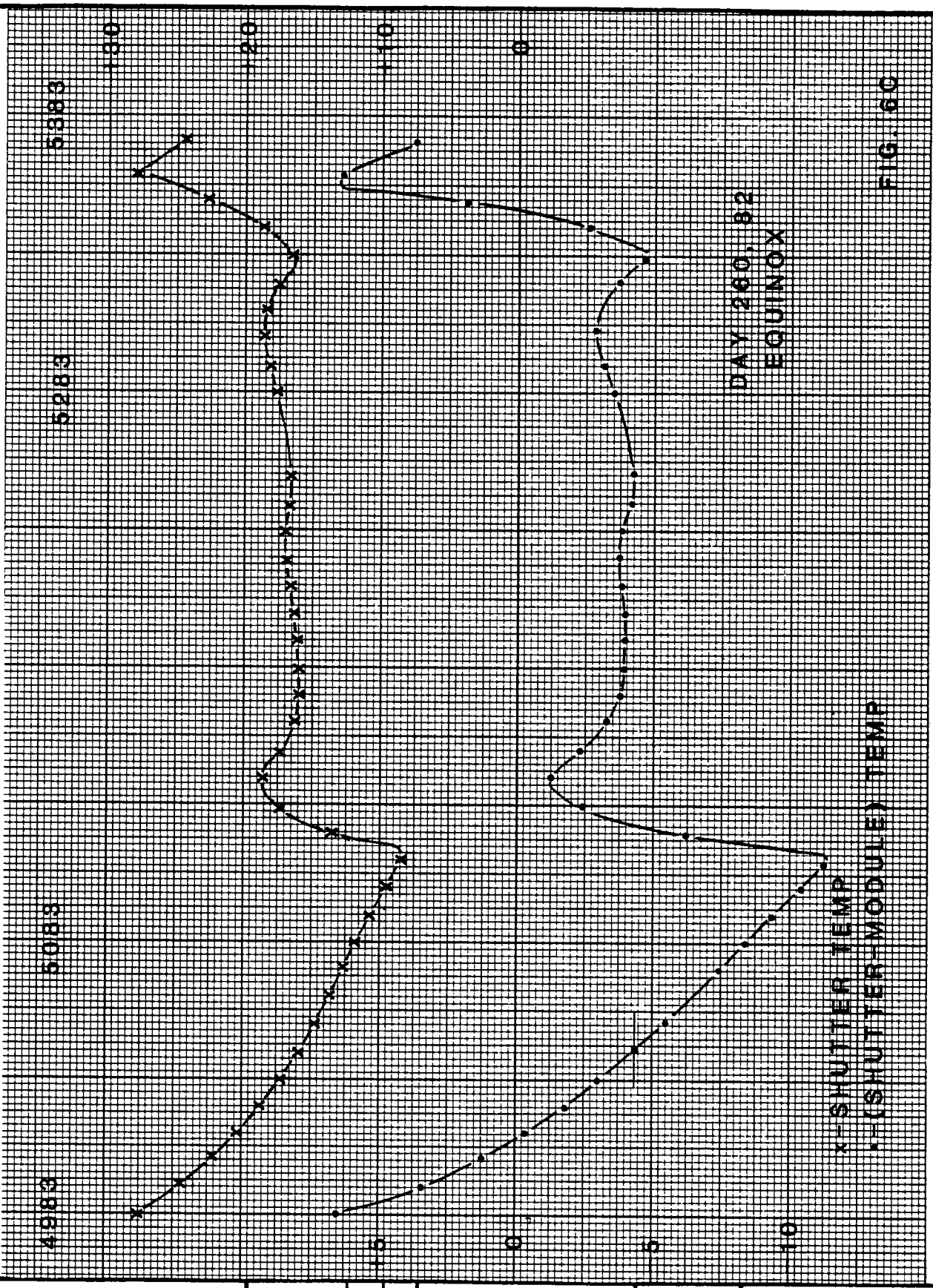

Gulton Industries Inc. DATA SYSTEMS DIVISION ALBUQUERQUE, NEW MEXICO	ISSUE	CODE IDENT. NO 12574	SIZE A	DWG. SHEET

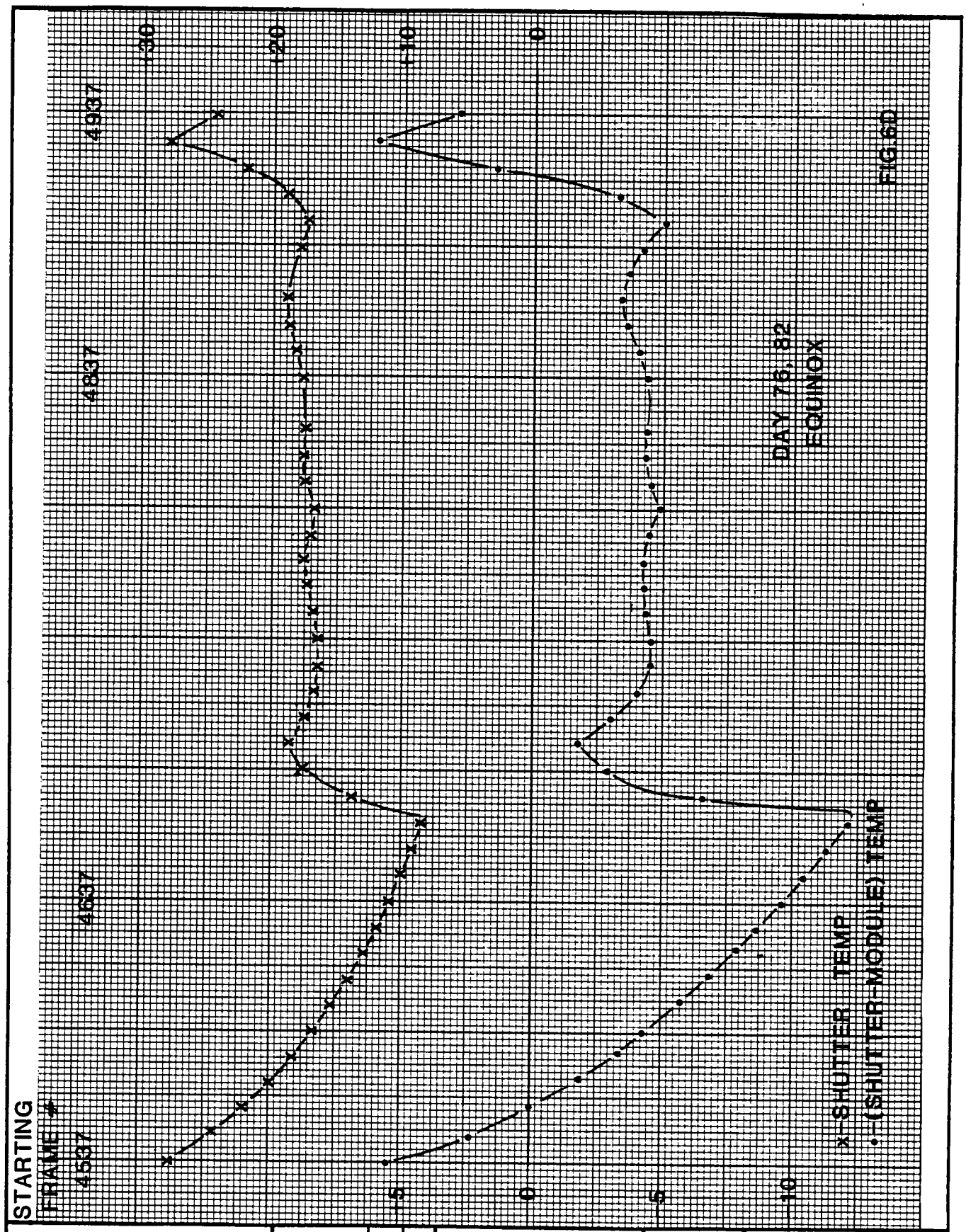

Gulton Industries Inc. DATA SYSTEMS DIVISION ALBUQUERQUE, NEW MEXICO	ISSUE	CODE IDENT. NO 12574	SIZE A	DWG. SHEET

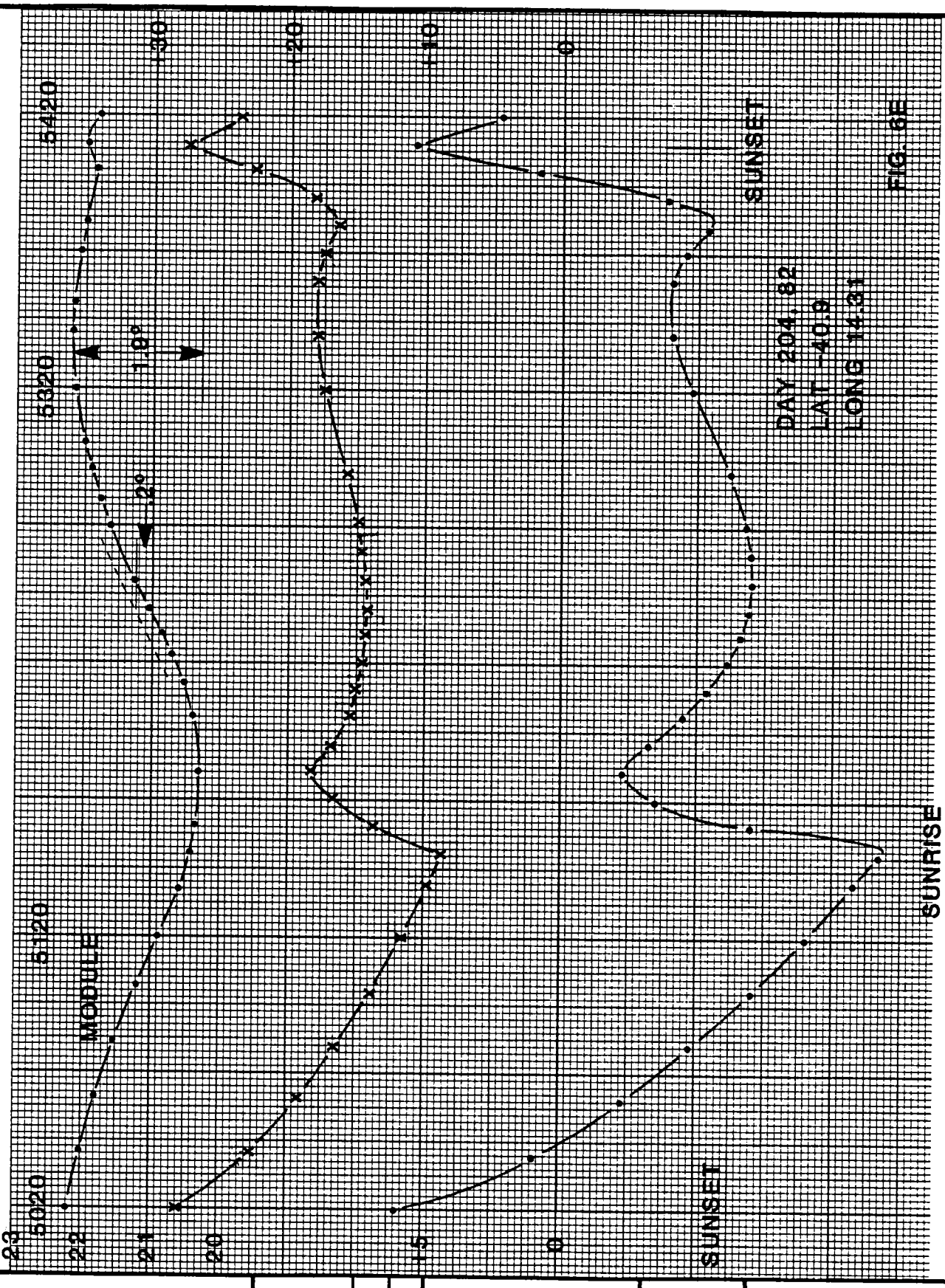

Gulton Industries Inc. DATA SYSTEMS DIVISION ALBUQUERQUE, NEW MEXICO	ISSUE	CODE IDENT. NO 12574	SIZE A	DWG. SHEET

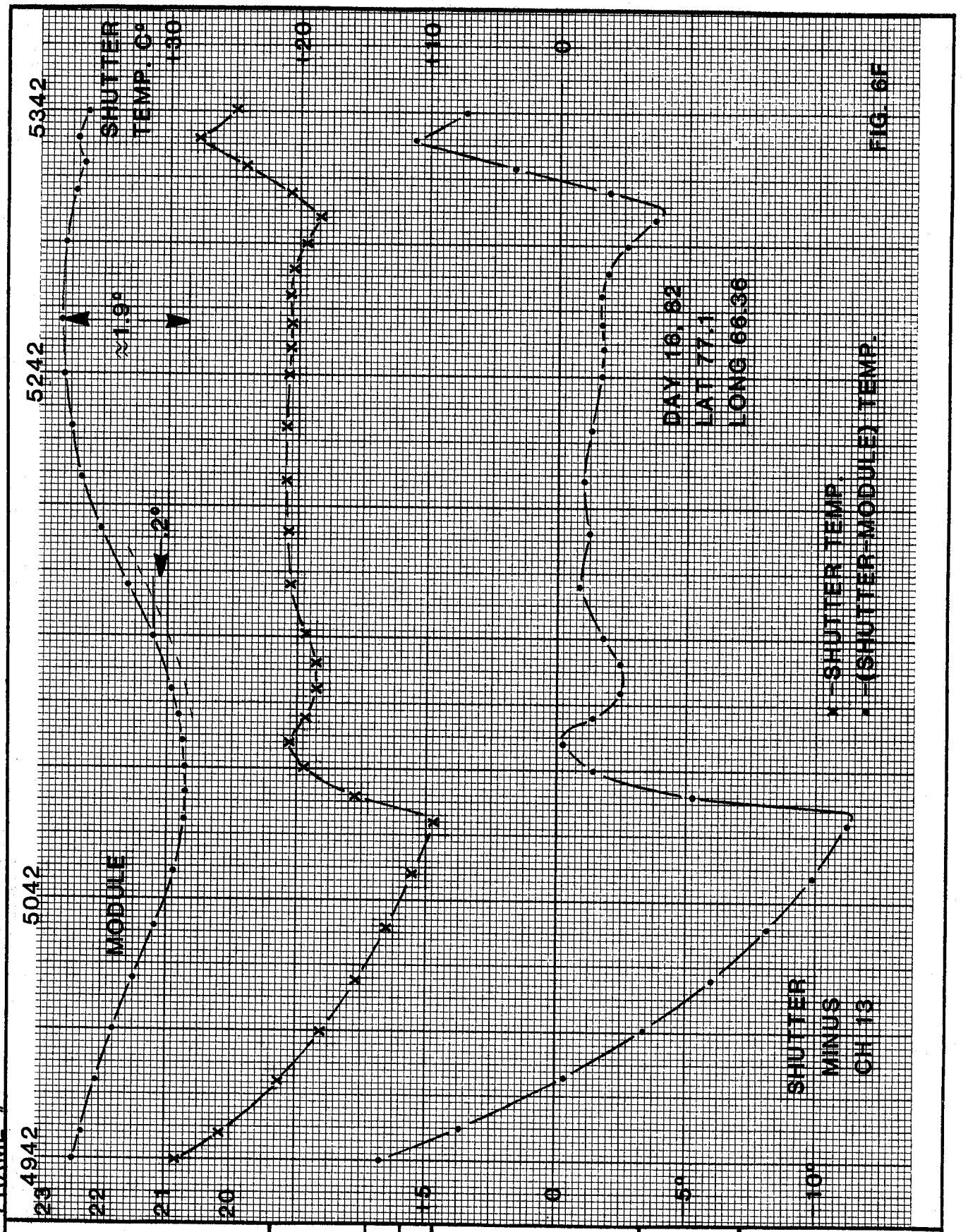

STARTING FRAME #

Gulton Industries Inc. DATA SYSTEMS DIVISION ALBUQUERQUE, NEW MEXICO	ISSUE	CODE IDENT. NO 12574	SIZE A
		DWG.	
		SHEET	

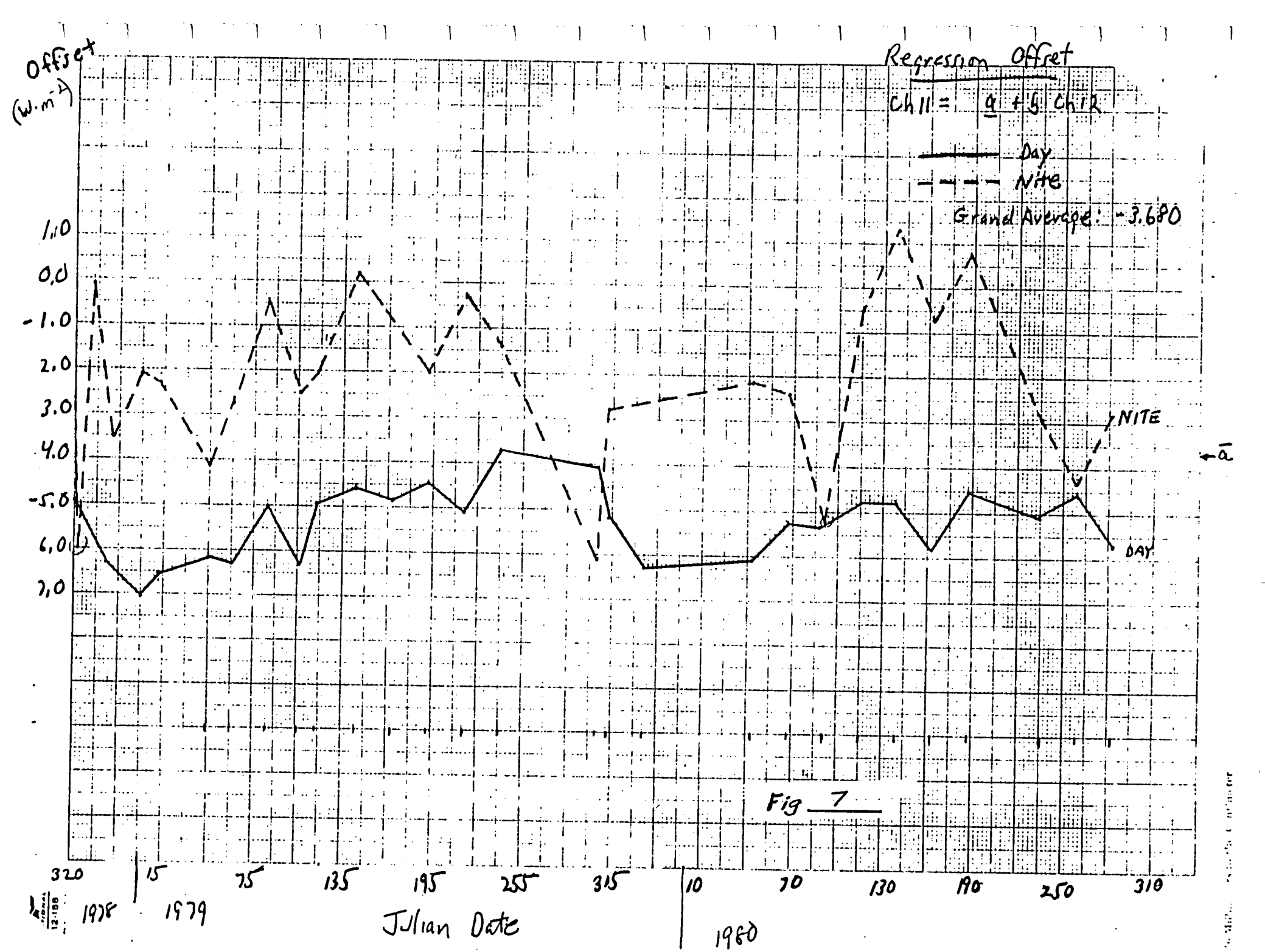
Offset
(W·m⁻²)
Regression Offset
Ch11 = a + b Ch12
Day
Nite
Grand Average: -3.680
1.0
0.0
-1.0
2.0
3.0
4.0
-5.0
6.0
7.0
NITE
DAY
ā
320
15
75
135
195
255
315
10
70
130
190
250
310
1978
1979
1980
Julian Date

Fig 7

1. Report No.	2. Government Accession No.	3. Recipient's Catalog No.
NASA CR-172318		

4. Title and Subtitle	5. Report Date
NIMBUS-EARTH RADIATION BUDGET INSTRUMENT ANALYSIS	6. Performing Organization Code

7. Author(s)	8. Performing Organization Report No.
R.H. MASCHHOFF	10. Work Unit No.

9. Performing Organization Name and Address	11. Contract or Grant No.
DATA SYSTEMS DIV. GULTON INDUSTRIES P.O. Box 3027 Albuquerque, N.M., 87190	NAS1-16468

12. Sponsoring Agency Name and Address	13. Type of Report and Period Covered
National Aeronautics and Space Administration Washington, DC 20546	Contractor Report
	14. Sponsoring Agency Code

15. Supplementary Notes

Langley Technical Monitor: A. Jalink, Jr.

16. Abstract Studies were conducted on the WFOV-Earth Flux Channels of the Nimbus ERB instrument with the objective of improving the understanding and/or confidence in the data collected by it. The studies involved laboratory tests on flight space earth flux subassemblies followed by a set of in flight verification procedures to see if the laboratory derived correction factors produced consistent results. Intercomparisons between the WFOV data and integrated scanner data as well as other "truth" were used in these verification procedures. The main source of errors were found to be temperature and temperature gradient related offsets. The findings have led to construction of a model for the short wave WFOV channel which use instrument temperatures and temperature differences to predict or establish offsets which need to be applied to data reduction alogrithms for maximum final data product accuracy. It is expected that models for the other sensors can be constructed using similar procedures. The final modelling procedures are being carried out under contract with GSFC and are beyond the scope of this effort.

17. Key Words (Suggested by Author(s))	18. Distribution Statement
Radiometers, Radiation Budget	Unclassified - Unlimited

19. Security Classif. (of this report)	20. Security Classif. (of this page)	21. No. of Pages	22. Price
Unclassified	Unclassified		